Title
Identification and Characterization of the Earliest Stages of Human Lymphoid Commitment

Author
Kohn, Lisa Ann

Publication Date
2013

Peer reviewed|Thesis/dissertation

.

UNIVERSITY OF CALIFORNIA
Los Angeles

Identification and Characterization of the Earliest Stages of Human Lymphoid Commitment

A dissertation submitted in partial satisfaction of the

Requirements for the degree Doctor of Philosophy

in Cellular and Molecular Pathology

By
Lisa Ann Kohn

2013

ABSTRACT OF THE DISSERTATION

Identification and Characterization of the Earliest Stages of Human Lymphoid Commitment

by

Lisa Ann Kohn

Doctor of Philosophy in

Cellular and Molecular Pathology

UNIVERSITY OF CALIFORNIA, Los Angeles, 2013

Professor Gay M. Crooks, Chair

Hematopoiesis is the process of differentiation from hematopoietic stem cells (HSC) into mature blood cells. Once a multi-potent stem cell has been influenced by intrinsic (transcription factors) or extrinsic (cytokines and micro-environmental) factors, it undergoes a loss of lineage potential and become committed to a cell lineage or lineages. Differentiation from multipotent HSC into functional T, B, or Natural Killer (NK) cells consists of passage through intermediate progenitor stages prior to becoming a mature lymphoid cell.

This thesis examines the process of lymphoid differentiation using several different aproaches. The majority of my research has focused on the identification of a functionally and molecularly distinct stage of early human hematopoietic commitment. This stage of commitment corresponds to the loss of erythroid and megakaryocytic potential while maintaining the capacity to generate all cells of the lymphoid lineage and the monocytic/macrophage cells of the myeloid lineage, going against the model of hematopoiesis that the earliest lineage decision bifurcates lymphoid potential and myeloid-erythroid potential. These progenitors are distinctive from all previously identified human lymphoid-committed progenitors, in that this population lacks the cell surface antigen CD10 and therefore does not have a bias toward B cell potential and minimal T and NK cell potential. These cells are functionally analogous to a population of cells described in mouse, the Lymphoid-primed Multi-Potent Progenitor (LMPP), and both the mouse LMPP and our novel human LMPP are strong candidates to be thymic seeding cells.

In the second part of my work, we applied the identification of the human LMPP progenitor

population in normal BM to the clinically relevant question how the lack of IL2RG signaling affects the regulation of the lymphoid commitment. In humans with X-linked Severe Combined Immune Deficiency (X-SCID) a null mutation of the *IL2RG* gene results in an inability to differentiate or function in response to multiple lymphoid cytokines resulting in an absence of peripheral T and NK cells, and present but functionally impaired B cells. In contrast, mice lacking IL2RG signaling are fully unable to develop B cells, with deficits in the early stage of B cell commitment. The in-progress studies described in this thesis demonstrate that the earliest stages of B lymphoid development are unaffected by defects in IL2RG signaling in these human patients. These results demonstrate the critical differences between lymphopoiesis in mice and humans, and the importance of overcoming experimental hurdles in order to directly investigate human lymphoid commitment.

The third part was of my work was done in collaboration with others, examinig factors that influenced thymic entry in a murine transplant model. Differentiation of progenitors into T lymphoid cells is a multi-step process in which T cell precursors receive critical extrinsic signals in the thymus to undergo the beginning stages of thymocyte development. In comparison to adults, neonatal mice have stronger thymocyte proliferation and vascular endothelial growth factor (VEGF) dependent angiogenesis in the thymus. Neonatal mice undergo more rapid thymic reconstitution than adults post-transplantation, even when BM engraftment is minimal and in the absence of pre-transplantation radiation. We show that inhibition of VEGF prior to transplantation prevents rapid thymic reconstitution in neonates, but has no effect on thymic reconstitution in adults. These data suggest that the early radiation-independent thymic reconstitution in the neonatal host is mediated by VEGF, and reveals a novel pathway that might be targeted to improve immune reconstitution post-transplantation.

To summarize, the body of this thesis examines the stages of lymphoid differentiation in several contexts: normal human hematopoiesis, dysfunctional human hematopoiesis, and murine thymic reconstitution post-HSCT. Taken together, description of a human LMPP progenitor phenotype opens up the possibility for future study molecular regulation of the first stages of lymphoid commitment in normal and aberrant human hematopoiesis.

The Dissertation for Lisa Ann Kohn is approved

Steven Bensinger

Kenneth Dorshkind

Christel Uittenbogaart

Gay M Crooks, Chair

UNIVERSITY OF CALIFORNIA, Los Angeles
2013

Dedication

This dissertation is dedicated to Don, Sheryl, Scott and Bee.
Thank you for all of the love and support you have given me.

Table of Contents

ACKNOWLEDGMENTS

I would like to thank my mentor, Dr. Gay M. Crooks, for providing me with invaluable, once in a lifetime mentorship. Her brilliant scientific guidance and co-existent clinical expertise has been an inspiration to me, both in the laboratory and in my broader career. Dr. Crooks is consistently and exceptionally generous with her time. The laboratory community that Dr. Crooks fosters is extraordinarily collaborative and interactive, and simply the best place to work, ever.

I would like to thank my thesis committee, Dr. Steve Bensinger, Dr. Ken Dorshkind, and Dr. Christel Uittenbogaart for expert advice in many aspects of my work. I would also like to thank Dr. Uittenbogaart for mentorship she has provided me beginning in my years as a medical student.

I thank Qian-Lin Hao and Dr. Crooks for pioneering of the studies that are featured in Chapter 2. I thank Dr. Raj Sasidharan, Shundi Ge, Yuhua "Judy" Zhu Y, Dr. Chintan Parekh, Dr. Hanna Mikkola for their important contributions to this manuscript.

I would like to thank Dr. Crooks for leading the work featured in Chapter 3, and to the physcian-scientists at UCLA and Childrens Hospital Los Angeles, Drs. Satiro De Oliveira, Neena Kapoor, Ami Shah, Hisham Abdel-Azim, and Donald Kohn, for procuring patient samples and for experimental advice.

I thank Dr. Andrew Cuddihy, Dr. Batul Suturwala, and Dr. Crooks for leading the work featured in Chapter 4, and to thank Shundi Ge, Julie Jang, Jacob Andrade for contributing to this manuscript.

I thank all of the members of the Crooks lab I have worked with during my time here; for their technical expertise, thought provoking questions, critical scientific analysis, and ongoing international potlucks. Special thanks to Judy Zhu, who trained me to be meticulous in every note I write and experiment I do, and always made sure I was well fed. Thanks to Shundi Ge, whose expertise and generosity has been a critical component to the work shown here. To Arineh Sahaghian, Rebecca Chan, and Sania Zadia, I say thank you to the many hours and many LS columns you gave. To physician-scientists Christopher Seet, Batul Suturwala, and Chintan Parekh, I thank you for teaching me both the physician's and the scientist's points of view. To William Kim and Julia Chin: you are wonderful, intelligent, convivial and entertaining graduate students, and I look forward to reading your upcoming publications. I wish Christopher Seet and Salemiz Sandoval good luck in every endeavor in lab and with their families; it has been an honor to work with each of you on this project. I thank Brooke LaTour and Mirko Corselli for making sure I was always sufficiently caffeinated; your scientific advice and personal friendships have been invaluable and I miss you both. It has been a wonderful place to do research, and I can only thank the people for making it so.

I thank Jessica Scholes, Felicia Cordrea, and the Broad Flow Cytomtery Core for technical expertise, always being kind, and being above and beyond accommodating, even when I bring seven independent rainbow colored sort panels and 28 tubes to sort into.

I thank Brenda Mueller, Doug Smoot, and Susie Esquivel for ongoing administrative support and for preventing many potential panic attacks. Thank you to the staff at Profeta for keeping me caffeinated.

Chapter 2 is reproduced with permission from Nature Immunology. Chapter 4 is reproduced with permission from Biology of Blood and Marrow Transplant.

I thank the UCLA Medical Scientist Training Program for funding from 2007-2010 on the T32 GM008042, and for the fantastic and inspiring leadership of Dr. Steve Smale and Dr. Kelsey Martin. I thank Dr. Crooks' National Institute of Health's (NIH) PO1 AI072686 for funding from 2009-2011, and National Heart Lung and Blood Institute at NIH Ruth L. Kirschstein National Research Service Awards for Individual Predoctoral MD/PhD Fellowship 1F30HL110458-01A1 for funding me from 2012-2015.

Vita: **Lisa Kohn**

EDUCATION

08/2007 to 05/2015	David Geffen School of Medicine at UCLA, Los Angeles, California Medical Scientist Training Program M.D., 2015 (expected) Ph.D. in 2013 (expected)
08/2001 to 05/2005	University of California at Berkeley Major Molecular Cell Biology, Emphasis Immunology Minor Theater, Dance and Performance Studies Bachelor of Arts with Honors

HONORS AND AWARDS

12/2012 - Present	Fellowship 1F30HL110458-01A1 National Heart Lung and Blood Institute at NIH Ruth L. Kirschstein National Research Service Awards for Individual Predoctoral MD/PhD Fellows (F30)
8/2012	ISEH Travel Grants for Students & Post-Doctoral Fellows 41st Annual Meeting of the International Society of Experimental Hematology, Amsterdam, Netherlands, Aug. 2012

RESEARCH EXPERIENCE

06/2009 to Present	Graduate Student University of California at Los Angeles Thesis Laboratory: Gay Crooks, M.D., Professor Dept. Cellular and Molecular Pathology Project: Characterizing Human Lymphoid Progenitors in Bone Marrow
06/2008 to 08/2008	Graduate Student Rotation University of California at Los Angeles Laboratory: Benhur Lee, M.D., Professor, Dept. of Microbiology, Immunology, and Molecular Genetics Project: Creation of a bi-functional CD4/CCR5 receptor for HIV fusion and infection on erythrocytes Project: HIV Infection of NOD/SCID mice reconstituted with Human CD34+ cells and Human Thymus and Liver
07/2005 to 07/2007	Staff Research Associate II University of California at San Francisco Laboratory: Alexander Johnson, Ph.D., Professor, Dept. of Microbiology and Immunology Project: Generation of large scale homozygous knock out library in *Candida albicans* to screen for virulence factors
08/2004 to 05/2005	Undergraduate Research Assistant University California at Berkeley Laboratory: Steven Lindow, Ph.D., Professor, Dept. of Plant and Microbial Biology

	Project: Examine interaction and competition of bacteria and environmental fungi on a plant surface
06/2004 to 08/2004	Summer Research Intern Childrens Hospital Los Angeles University of Southern California Keck School of Medicine Laboratory: Gay Crooks, M.D., Associate Professor, Dept. of Pediatrics at USC Keck School of Medicine Project: Role of Transcription Factor p63 in Bone Marrow Epithelial Progenitors

PUBLICATIONS

1. **Kohn LA,** Hao Q-L, Sasidharan R, Ge S, Zhu Y, Parekh C, Mikkola HKA, Crooks GM. Lymphoid Priming in Human Bone Marrow Begins Prior to CD10 Expression with Up-Regulation of L-selectin. *Nature Immunology* 2012 Oct;13(10):963-71. doi: 10.1038/ni.2405. Epub 2012 Sep 2. PMID: 22941246

2. Cuddihy A, Suterwala B, Ge S, **Kohn LA,** Jung J, Andrade J, Wang X, Crooks GM. Rapid thymic reconstitution following bone marrow transplantation in neonatal mice is VEGF-dependent. *Biology of Blood and Marrow Transplant.* 2012 May;18(5):683-9. Epub 2012 Jan 25. PMID: 22281302 [PubMed - in process] PMCID: PMC3334422 [Available on 2013/5/1]

3. Noble SM, French S, **Kohn LA,** Chen V, Johnson AD. Systematic screens of a *Candida albicans* homozygous deletion library decouple morphogenetic switching and pathogenicity. *Nature Genetics* 42, 590-598 June 2010 PMCID: PMC2893244

Talks

1. **Kohn LA,** Hao Q-L, Sasidharan R, Ge S, Zhu Y, Parekh C, Mikkola HKA, Crooks GM. Identification and Characterization of a CD10- Multi-Lymphoid Progenitor in Human Bone Marrow. Presented at 41st Annual Meeting of the International Society of Experimental Hematology in Amsterdam, Netherlands, August 2012.

2. **Kohn L,** Chikere K, Hong P, Lee B, Red Blood Cell Viral Trap Journal of Investigative Medicine Vol 57, Number 1, Jan 2009 Presented at 37th Annual Western Student Medical Research Forum in Carmel, California, January 2009.

Posters

1. **Kohn LA,** Hao Q-L, Sasidharan R, Ge S, Zhu Y, Parekh C, Mikkola HKA, Crooks GM. Lymphoid Priming in Human Bone Marrow Begins Prior to CD10 Expression with Up-Regulation of L-selectin. Presented at the 52nd Annual Mid-Winter Conference of Immunologists in Asilomar, California, January 2013.

2. **Kohn LA,** Hao Q-L, Sasidharan R, Ge S, Zhu Y, Parekh C, Mikkola HKA, Crooks GM. Identification and Characterization of a CD10- Multi-Lymphoid Progenitor in Human Bone Marrow. Presented at 41st Annual Meeting of the International Society of Experimental Hematology in Amsterdam, Netherlands, August 2012.

3. **Kohn LA,** Hao Q-L, Sasidharan R, Ge S, Zhu Y, Parekh C, Mikkola HKA, Crooks GM. Defining the Earliest Stages of Lymphoid Commitment in Human Bone Marrow. Presented at 8th Annual Stem Cell Symposium in Los Angeles, California, February 2012.

Chapter 1

Introduction

Hematopoietic Lineage Commitment

Hematopoiesis is the process of differentiation from a hematopoietic stem cell (HSC) into mature blood cells. An HSC has the capacity to become every type of blood cell, and to divide into two identical stem cells (self-renewal) or to divide into a stem and more differentiated progenitor (asymmetrical division). The stepwise process of differentiation from multipotent HSC into functional T, B, or Natural Killer (NK) cells consists of passage through many intermediate progenitor stages prior to becoming mature lymphoid cells.

A major goal of developmental biology is to elucidate the mechanisms that underlie the transition from full multi-potency into committed, restricted lineage potential. Lineage commitment occurs due to both cell-extrinsic and cell-intrinsic events. Cell-extrinsic factors include cytokines and other micro-environmental stimuli provided by direct cell-to-cell contacts. Cell-intrinsic factors include changes in gene expression as mediated by transcription factors.

The appropriate bone marrow micro-environmental stimuli are critical to the earliest stages of lymphoid commitment in post-natal life. In order to continue their differentiation into T lymphocytes, bone marrow derived progenitors must migrate to the cortico-medullary junction of the thymus.[1,2] Once in the thymus, they undergo development mediated by signals from the Notch ligands, Delta-like ligand 1 and 4,[3-6] within distinct physiologic compartments[7] which makes T lineage differentiation highly dependent on micro-environmental extrinisic factors.[8]

The binding of cytokines to receptors on hematopoietic cells is a major extrinsic mechanism that influences lineage commitment. Amongst the most critical cytokine

receptors in lymphopoiesis, the common gamma chain (γc, encoded by the *IL2RG* gene), is a common signaling chain shared between the interleukin receptors IL-2, IL-4, IL-7, IL-9, IL-15 and IL-21.[9-14] After γc dimerizes with one of the above listed receptor units, its signaling is mediated by the hematopoietic specific tyrosine kinase Janus-activated kinase 3 (JAK3)-signal transducer and activator of transcription (STAT) pathway.[15,16]

Emphasizing the importance of the γc-associated cytokine receptors in normal hematopoietic differentiation, humans with nonsense mutations in *IL2RG*,[17] *IL7R*α[18,19] or down stream signal transducer *JAK3*[20] have Severe Combined Immune Deficiency (SCID) characterized by reduced or absent T cells,[14] because early thymocyte development is critically dependent on IL-7.[21] Meanwhile, mice that lack γc signaling (either *IL2RG*[22,23] and *JAK3*[24-26] null mice) are unable to develop either T or B cells. The lack of murine B cell development has been specifically attributed to deficient IL7 signaling, as both IL7Rα null[27,28] and IL7 null[29] mice are also unable to develop B or T cells, and B cell development is arrested at the pre-proB stage.

Cell intrinsic transcriptional regulation is controlled by sequentially expressed transcription factors that are critical to cell lineage commitment.[30] Early B cell differentiation is controlled by a network of transcription factors that includes E2A, EBF, and PAX5.[31-34]

Once a multi-potent stem cell has been influenced by intrinsic or extrinsic factors, it undergoes a loss of lineage potential and become committed to a cell lineage or lineages. These cells that are considered "lineage restricted" will be the subject of the next section of this thesis.

Modeling Hematopoiesis: The Dichotomous Split and Progenitors

Early models of hematopoietic cell development assumed strictly dichotomous pathways of lineage commitment.[35] Common Myeloid Progenitor (CMP) are progenitors with capacity to generate myeloid, erythroid, or megakaryocytic cells, but not lymphoid cells,[36,37] while Common Lymphoid Progenitor (CLP) are progenitors with capacity to generate B, T and NK lymphoid cells.[35,38] These progenitor cell types can be distinguished from each other and isolated as viable cells through the use of immunophenotypes that characterize the cells based on differential expression of cell surface proteins.

CLP and CMP were believed to be mutually exclusive in their differentiation capacity; the differentiation from an HSC into either progenitor represented a bifurcation in hematopoietic lineage commitment. In this model, all lymphopoiesis would originate exclusively from a CLP, and an individual CLP would have the ability to differentiate into all lymphoid cell types. In contrast, all myeloid, erythroid and megakaryocytic lineages would be generated from CMP.

Revisions to the Model: Small Tweaks and Fundamental Challenges

Advances in technological assays and thorough study have brought two revisions to the model of dichotomous lineage commitment. The first revision questions the specific immunophenotype initially associated with the human CLP.[39] The second revision fundamentally questions the concept of dichotomous lineage commitment, as recent evidence demonstrates a gradual loss of lineage potential that can occur via multiple alternative pathways.[40-45] In the next few pages, I will unpack the evidence that exists supporting the multiple alternative pathways available for progenitor differentiation and then I will expound upon the evolution of specific immunophenotypes for classifying

progenitors. First I will describe the specific murine populations with lympho-myeloid capacity, and then explain analogous populations isolated from human hematopoietic sources

Murine studies

Much elegant data has been generated in mouse studies to both support and challenge the classic idea that the lymphoid and the myelo-erythroid pathways emerge separately from a multipotent progenitor stage[35,42,45,46] Murine CLPs have been immuno-phenotypically defined as lineage marker negative (Lin^-) Sca-1^{lo} c-kit^{lo} IL7Rα^+ cells from bone marrow.[35]

The concept of dichotomous lineage commitment has evolved into models of gradual loss of lineage potential that can occur via multiple alternative pathways. Ample evidence has been gathered in the study of murine hematopoiesis demonstrating cells that have retained capacity for lymphoid and myeloid differentiation, but do not have erythroid or megakaryocytic potential.. Rather than invalidating the concepts of CMP and CLP, this additional evidence adds to the extensive tree of hematopoietic development.

Progenitors have been isolated from various murine sources that have myeloid and partial lymphoid potential. Murine fetal liver[40] and BM $CD45R^-CD19^+$ [41] progenitors have demonstrable clonal B and macrophage potential. Progenitor cells have been isolated from the thymus that can generate T, NK, and dendritic lymphoid cells and myeloid cells (but have lost B cell capacity).[47,48]

The earliest multipotent progenitor in murine BM that has lost erythroid-megakaryocytic potential has been termed the Lymphoid-primed Multipotent Progenitor

(LMPP)[42]. In contrast to murine CLPs, which are defined by IL-7rα expression within the c-Kit^{lo}Lin^{-}Sca-1^{lo} population[35], LMPPs are isolated from more primitive c-Kit^{+}Lin^{-}Sca-1^{+} cells by **c**ell surface expression of Flt3[42]. The 'lymphoid-primed' LMPPs in mouse bone marrow retain full lymphoid and some myeloid potential but have lost erythro-megakaryocytic potential, whereas CLPs represent a more mature, lymphoid-restricted progenitor population.

The development of T cells is a multi-step process in which progenitors migrate from the BM to the thymus by the use of specific homing molecules and chemokine receptors. In the thymus, T cell precursors receive multiple signals in order to undergo the beginning stages of thymocyte development. Therefore, for a BM progenitor to become a thymocyte, it must both express receptors involved in thymic homing and migration, and have the intrinsic capacity to differentiate into a T cell once in the thymic microenvironment.

Controversy about the phenotypic identity and lineage potential of precursors that seed the mouse thymus has continued for over a decade. It seems likely that more than one type of bone marrow progenitor may be able to seed the thymus and establish thymopoiesis.[47-52] The phenotypic properties, global gene-expression profiles and *in vivo* and *in vitro* lineage potential indicate that murine early thymic progenitors (ETPs) (thymic Lin^{-} CD4^{-}CD8α^{-}CD25^{-}c-Kit^{hi}) resemble LMPPs (BM c-Kit^{+}Lin^{-}Sca-1^{+}Flt3^{+}) in many of these aspects.[50] Another population of mouse bone marrow progenitors that efficiently and rapidly reconstitute the mouse thymus after transplantation is the c-Kit^{+}Lin^{-}Sca-1^{+}CD62L^{+} RAG-1^{-} progenitor population that is found in both mouse bone marrow and mouse thymus.[51]

Ligands that are expressed in the vasculature of the cortico-medullary junction of human thymus, where homing occurs, are likely mediators of homing. In mice, homing appears to be dependent on the interaction of P-selectin on the thymic endothelium with the receptor P-selectin glycoprotein ligand 1 (PSGL-1) on the surface of the BM derived progenitors.[53] Murine studies have demonstrated that the CC chemokine receptors (CCR) 7 and 9 are also critical for the process of thymopoiesis; mice deficient for both receptors have severely reduced numbers of early T cells in the thymus.[54]

Human Studies

Most studies of the earliest progenitor stages in human hematopoiesis have used neonatal umbilical cord blood as the source of hematopoietic cells. However, because substantial differences between progenitors from UCB and BM are known to exist in terms of immunophenotype[55-57] and proliferative capacity,[58-61] to understand how lymphopoiesis is regulated during steady-state adult hematopoiesis it is necessary to directly study hematopoietic stem cells and progenitors from postnatal human BM[57,62].

Since 1995, human adult and fetal bone marrow (BM) lymphoid differentiation has been assumed to begin with the expression of the cell surface antigen CD10 (aka common acute lymphoblastic leukemia antigen or membrane metallo-endopeptidase) on $CD34^+$ cells[38,63]. These $CD34^+Lin^-CD10^+CD45RA^+CD38^+$ CLPs (henceforth referred to only as $CD10^+$) can give rise to cells of all lymphoid lineages (T, B, and NK cells) and lack significant erythroid or myeloid potential. The description of the $CD10^+$ CLP was the first direct evidence supporting the previously hypothetical concept of a CLP.

Since its first description, there have been many technological advances in immuno-phenotyping, molecular characterization, and functional output that have allowed a more

in-depth examination of the original $CD10^+$ population. Subsequent work has shown that $CD10^{hi}$ expression on progenitors is associated with a strong bias toward B cell potential and minimal T and natural killer (NK) cell potential[39,59]. Attempts to hone in on a CLP that is less bound to the B lineage have further fractionated the $CD10^+$ population. $CD10^+$ cells that lack expression of CD24 are more evenly able to differentiate into all lymphoid cell types and are the precursors to the $CD10^+CD24^+$ population. However, $CD10^+CD24^-$ progenitors have molecular evidence of B cell commitment with expression of *PAX5, EBF1* and *VPREB*[59]. A more recently identified $CD34^+CD10^+CD38^{neg\text{-}lo}$ population, termed Multi-lymphoid Progenitor (MLP), has been shown to have full lymphoid potential, but nonetheless expresses the B cell associated genes *PAX5* and *CD79A*.[64] Notably, the strategy for the isolation of these MLP included cells with intermediate expression of CD38, which is a greater CD38 expression than that in the most primitive HSC fraction. Both of these refinements of the original CLP phenotype continue to utilize CD10 expression as the primary marker of lymphoid commitment.

The reliance on CD10 expression as a marker of lymphoid commitment in human BM hematopoietic progenitors has meant that states of differentiation could be compared only between various progenitors committed predominantly to the B cell lineage. **Therefore, to understand the progenitor hierarchy of human lymphoid commitment, we hypothesized that a stage of lymphoid priming exists that precedes B lymphoid commitment, either prior to or independent of CD10 expression.** This hypothesis was the basis for the research paper included in **Chapter 2** of this thesis.

In order to find alternative markers of lymphoid commitment to evaluate in human BM, we looked to information gained from other hematopoietic sources, including human

umbilical cord blood (UCB) and murine bone marrow. Within UCB, the earliest lymphoid committed cells were identified as $CD34^+$ $CD38^-$ $CD7^+$ (henceforth referred to as $CD7^+$ CLPs), irrespective of CD10 expression.[65] These progenitors also co-expressed CD45RA and HLA-DR, but expressed neither B cell associated transcription factor PAX5 nor the murine CLP marker IL7Rα. Later work confirmed that the UCB $CD7^+$ CLP was less B-lineage biased than the UCB $CD10^+$ CLP.[66] From this work in UCB, the $CD7^+$ population was a promising candidate to study in BM for full lymphoid potential and restriction to generate other lineages. However, because substantial differences between progenitors from UCB and BM are known to exist in terms of immunophenotype and function, we could not take for granted that functional capacity, surface immunophenotype and transcriptional profiles of the progenitor populations will be consistent amongst hematopoietic sources.[55-57] Indeed, other groups have shown that a subset of BM CD34+ cells express CD7, but that it is a lower percentage than amongst UCB CD34+ cells.[39,64]

The naive-cell marker CD45RA has been shown to be expressed on various human lymphoid progenitors, including the human BM $CD10^+$ CLP[38], UCB CD7+ CLP [65,67] and granulocyte-macrophage progenitors (GMP) in BM and UCB[37]. Indeed, as early as 1995 Galy et al stated that $CD34^+$ Lin^- $CD45RA^+$ cells have great capacity to generate T and NK cells, regardless of CD10 expression,[68] Therefore, we decided to screen progenitor populations for the presence of CD45RA, to see if it is correlated with lymphoid restriction in BM progenitor cells.

We also considered cell surface markers that had been proven useful to discriminate murine populations with different capacities to differentiate into lymphocytes. L-selectin (CD62L) is expressed on mature lymphocytes and mediates

homing to peripheral lymphoid organs[69]. Recent studies have reported that up-regulation of CD62L expression on $Lin^{-}c\text{-}Kit^{+}Sca1^{+}$ (LSK) murine BM cells correlates with loss of erythroid and megakaryocyte potential.[70] These $CD62L^{+}$ LSK cells have a high expression of FLT3 and efficiently engraft the thymus[51,70,71].

Assays

Much of the ability to discriminate more finely between populations of progenitors is due to the improvements in the separation of cell populations. The development of multi-color flow cytometry facilitates complex 6-10 parameter cell sorting strategies, permitting isolation of increasingly specific populations of cells in a single step. In addition, multi-color flow cytometry allows more complex analysis of individual cells, and so cells can be more thoroughly identified by what they do and do not express. As an example, in T cell differentiation conditions, a cell can be interrogated for CD45 (pan-leukocyte), CD4 (monocyte or T cell), CD8 (T cell or NK cell), CD3 (pan-T cell, though often less upregulated in *in vitro* conditions), CD14 (monocyte), and TCRαβ (T cell), so that through the use of multiple markers it can be stated with more confidence that a cell is or is not a T cell.

In Vivo Lineage Potential

In order to assess the lineage differentiation potential of HSC and progenitors, the cells must receive the proper signals for differentiation. One attempt to model the signaling of physiologic hematopoiesis utilizes transplantation of cells into irradiated and/or immune deficient mice. Transplantation of human hematopoietic cells into irradiated immune-deficient Non-Obese Diabetic/Severe Combined Immune-Deficient/ γc-/- (NSG) mice can produce human engraftment,[72] determined by the percentage of cells

positive for human CD45 and Human Leukocyte Antigen in the mouse BM, spleen, and peripheral blood. Irradiation of recipient mice facilitates engraftment and proliferation in the BM. This cross-species model emulates post-transplant immune reconstitution in human patients, but is also used as surrogate for physiologic lineage potential. In these xenogeneic transplants, lineage skewing and difficulty in homing may limit the capacity to fully estimate a cell's natural *in vivo* potential.[56]

Recent studies demonstrated human engraftment from transplanted limiting dilutions (as few as a single cell) of HSCs isolated from UCB[73]. These experiments used intra-femoral transplantation into sub-lethally irradiated NSG recipients. Transplantation of human cells directly into the murine bone marrow cavity may reduce peripheral loss of HSC and progenitors that are unable to home to BM.[74,75] In order to detect engraftment from such limited numbers of cells, extensive time (20 weeks) was required for sufficient self-renewal.

A key characteristic that separates HSC from progenitors is that progenitors lack the capacity to self-renew. Therefore, in contrast to xenogeneic transplantation studies that utilize HSC, progenitors would not be expected to continuously expand in number or persist long-term after transplantation, making transplantation assays more difficult. The original paper describing the $CD10^+$ CLP[38] did not demonstrate engraftment of either BM or UCB progenitors.

Subsequent work has provided data regarding transplanted progenitors isolated from UCB, but no transplant data from progenitors isolated from human BM has been reported.[59,64] This is likely due to inherent lower proliferative capacity of stem and progenitors from BM relative to UCB[58-61]. Even utilizing relatively more proliferative

UCB progenitors as a cell source, the engraftment levels for $CD38^{dim/lo}CD10+$ Multi-Lymphoid Progenitors (MLP) was very low (ranged from <0.01% to 0.05%) and was detected only short term (at 2 weeks).[64]

Transplantation of human hematopoietic stem and progenitor cells into neonatal (but not adult) NSG mice can provide the thymic reconstitution necessary to produce human T cells.[76] However, xenogeneic transplantation models may have limitations for T cell potential if species-specific interactions are required for homing and/or differentiation of BM progenitor populations. A study examining non-renewing human MLP progenitors did not observe T cell development because, in the authors' words, "MLPs generated only a transient graft in the injected femur and T cell development requires long-term engraftment."[64]

What unique characteristics make neonatal thymi more receptive to engraftment than adult thymi? In comparison to adults, neonatal mice have strong thymocyte proliferation and postnatal vascular endothelial growth factor (VEGF) dependent angiogenesis in the thymus,[77] which may allow the neonatal thymus to be a more hospitable environment for donor T cell production than adult thymus. VEGF dependent angiogenesis ceases beyond the first week of postnatal life, and blocking VEGF during this period reduces both vascular density and thymocyte numbers.[77] **Therefore, we hypothesized that the same VEGF-mediated mechanisms that contribute to robust thymopoiesis during normal neonatal development allow the neonatal thymus to provide a more receptive pattern of thymic reconstitution after BM transplantation than adult thymi.** These questions were the basis for the research paper included in **Chapter 4** of this thesis.

In Vitro Lineage Potential

An alternative method to reproduce many signaling and regulatory aspects of physiologic hematopoiesis utilizes *in vitro* growth of human cells co-cultured on adherent stromal cell lines. These *in vitro* cultures can be used to assess either maintenance of the original phenotype, or differentiation into a specific cell type. S17 is a murine stromal cell that acts as an *in vitro* microenvironment to both support differentiation into B cells and support long term culture without the use of additional growth factors.[78-80] The murine clonal stromal cell line "MS5," created in 1989,[81] supports proliferation and differentiation of human stem and progenitors cells.[82] The murine clonal stromal cell line "OP-9" was derived from macrophage colony-stimulating factor (M-CSF) null mice, and supports human lymphopoeisis.[83] One downside to the use of the OP9 cell line is that it has a tendency to differentiate into adipocytes,[84] which is sub-optimal to support hematopoiesis. Each of these cell lines can support myeloid development and B and NK lymphoid development, but they do not provide the proper signals to support T lymphoid development.

A drawback to the use of stromal cells is that the physiological relevance of lineage potential demonstrated using stromal assays continues to be debated.[42,46,52,85,86] Richie-Erlich et al. noted in 2011 that mouse IL-7Ra^{+} CLPs, despite their complete lack of either colony forming unit (CFU) activity or *in vivo* myeloid potential, can generate myeloid cells in stromal co-cultures, which suggests that myeloid differentiation may be an alternative pathway found in certain *in vitro* conditions.[85] Residual myeloid and dendritic potential has been reported for many lymphoid-committed progenitors that have no myeloid capacity in other readouts.[38,64,65,85] This has been postulated to be due to

supra-physiologic levels of cytokines. Nonetheless, it is clear that the capacity for myeloid differentiation *in vitro* progressively wanes as lymphoid commitment proceeds and that this residual, mostly monocytic, potential is retained after erythroid potential is lost.

T Cell Lineage Potential

After arriving in the thymus, hematopoietic progenitor cells undergo T cell receptor genomic rearrangement followed by positive and negative selection in distinct physiologic compartments within the thymus. This process has been challenging to model *in vitro* because of the complexity of signals required to induce T cell maturation within the thymus. In 2002, Zúñiga-Pflücker developed a murine BM stromal line that ectopically expresses the Notch ligand Delta-like Ligand 1 (OP9-DLL1) and has the capacity to induce differentiation of murine and human hematopoietic progenitors into T cells.[5,6] Similar to the reduced expansion capacity of human BM cells in xenogeneic transplantation, BM HSC and progenitors exhibit lower proliferative capacity and slower differentiation kinetics relative to UCB in the OP9-DL1 culture system.[61]

Experimental restrictions make it difficult to definitively prove the identity of the bone marrow precursors that normally seed the human thymus. Inherent proliferative limitations already discussed make it highly unlikely that BM engraftment and thymic migration will be seen from lymphoid progenitor cells in the existing xenogeneic transplant models. Speculation regarding the identity of the progenitors that seed the human thymus have relied on two major methods 1) Detection of cells in BM and the thymus that share a similar immunophenotype and molecular phenotype or 2) Expression of one component of a ligand-receptor pair whose cognate binding partner is detected in

the thymus (especially at the thymic entry point, the cortico-medullary junction.) The $CD10^{+}CD24^{-}$ population in bone marrow probably represents a lymphoid progenitor that seeds the human thymus, given the finding of a similar immunophenotypic subset among human thymocytes.[59]

Clonal Lineage Potential

To prove that a progenitor has true multi-lineage capacity, clonal studies must be performed to show multiple cell types arise from a single cell. Sorting of single cells is facilitated using the automatic cell deposition unit (ACDU) on Becton Dickinson flow cytometry sorters. Many studies have demonstrated B/NK development from a single cell, or T-myeloid from a single cell. However, existing stromal lines have difficulty assessing multi-potentiality, as B and T cell development have mutually exclusive activation of molecular pathways, including Notch signaling.[3,4,87] Recent studies using inducible Notch ligands have attempted to generate both B and T lymphoid cells from a single initiating cell, but have not been able to generate greater than 0.5% B cells using this system.[88]

An alternative assay to detect hematopoietic differentiation from an individual cell is the colony-forming unit (CFU) assay. HSC or progenitor cells are plated in a semi-solid methylcellulose medium with cytokines that promote myeloid and erythroid differentiation. Hematopoietic colonies generated from a single initiating cell can be identified and the number of clonogenic initiating cells enumerated as CFU-C. These colonies may consist of a single cell type, or some combination of granulocytes, monocytes, or erythroid cells. It could be argued that the CFU assay is a more stringent *in vitro* assay than the stromal co-cultures, as it detects only clonogenic myeloid and/or erythroid progenitors and is well correlated with *in vivo* readouts[85]. A major drawback of

this assay is that it does not support the growth of lymphoid cells, and so cannot be used to assess clonal lymphoid output.

Gene Expression Analysis

Quantitative Reverse Transcriptase Polymerase Chain Reaction (qRT-PCR) has been the gold standard for assessing RNA transcript levels for individual genes of interest, but evaluation of overall gene expression signature amongst progenitor cell types is made possible by the use of either whole genome microarray or RNA-Sequencing (RNA-Seq). Each of these techniques creates a large dataset that is representative of the gene expression of an analyzed population of cells. Unsupervised Principal Component Analysis (PCA) can reduce the overall complexity of the large datasets generated by whole genome analysis, by representing each set of data as point on a map so that more similar datasets are closer on the map. Unsupervised hierarchical clustering can also create an overall assessment of global similarity between sets of data.[89] Global gene expression amongst 38 hematopoietic populations has revealed some transcription factors are expressed predominantly in a single lineage, while others increase gradually along differentiation.[90] This extensive work by Novershtern et al. did not include any progenitors representing stages between HSC and the CD34+CD10+CD19+ B cell progenitor, demonstrating the gap in knowledge of the earliest stages of lymphoid commitment.

All current methods to separate lymphoid restricted progenitors from other types of progenitors isolate populations of cells. Examination of CD10+ progenitors has revealed great functional heterogeneity within the population, in which some cells retain full lymphoid potential while other cells are more committed to the B cell lineage[59].

Murine CLPs have been demonstrated to be a population that is both functionally and molecularly heterogeneous, composed of mixture of cells with relatively restricted lineage potential.[91]

Single cell qRT-PCR analysis can determine the expression of specific genes related to stem cell maintenance and lymphoid differentiation, and uncover previously undetectable heterogeneous gene expression. The Fluidigm BioMark Real-Time PCR system can perform single cell gene expression analyses using microfluidics[92]. This allows resolution of subpopulations of seemingly homogenous lymphoid progenitors , based on the extent to which lymphoid associated transcript levels and novel surface markers can be correlated.

Clinical Relevance

Lymphoid Deficiencies and Lymphoid Recovery post BMT

In addition to allowing the study of regulation of early human hematopoiesis, the identification of cells in the early stages of lymphoid commitment has several potential clinical uses. Quantitating lymphoid progenitors may provide a useful assay to assess the inherent lymphoid potential of a BM or mobilized peripheral blood (MPB) transplant unit. In addition, these progenitors may provide an alternative to HSC or mature cells for manipulation and use in cell therapies such as in tumor immunotherapy.

Hematopoietic Stem Cell Transplant (HSCT) has developed over 50 years to become a valuable therapy to treat hematologic disorders and malignancies including aplastic anemia, immunodeficiencies, and leukemias. A combination of irradiation and chemotherapy is required for pre-transplantation conditioning, in order to facilitate engraftment of the transplanted cells. However, when infants with SCID receive HSCT,

pre-transplantation conditioning is not required for lymphoid reconstitution,[93-95] and T cell reconstitution is particularly robust for newborns.[96-98] This permissive engraftment suggests that, similarly to findings in the mouse explored in **Chapter 4,** the human neonatal thymus is more permissive to engraft donor cells, possible as a consequence of the neonatal VEGF dependent angiogenesis.[77]

In addition to its clinical utility, HSCT has also provided an opportunity to observe the process of human post-natal hematopoiesis. One of the limitations of HSCT is slow recovery of immune function due to delayed development of lymphoid cells, especially T cells. After transplantation, thymic reconstitution with *de novo* production of T cells is delayed by at least 3 months and T cell numbers often never return to normal levels.[99] Delayed recovery of T cells leaves patients at risk for severe infections and malignant disease, and patients without lymphocyte recovery 2 months after HSCT are less likely to survive long-term.[100]Identification and characterization of progenitors in the human BM with strong T cell capacity is therefore translationally relevant to understanding the problem of delayed immune reconstitution post HSCT. In summary, increased knowledge of the progenitor hierarchy of human lymphoid commitment, through the discovery of a stage of lymphoid priming prior to B lymphoid commitment, is essential for the development of diagnostic and therapeutic advances in lymphoid differentiation and thymic reconstitution in clinical settings. .

Severe Combined Immune Deficiency

Severe Combined Immune Deficiency (SCID) disease is a genetic syndrome characterized by a profound or absolute deficiency in functional T lymphoid cells, and depending on the specific mutation, B and Natural Killer (NK) cell production may be

also affected. Multiple genetic defects can cause this syndrome. The most common form of SCID, X-SCID, is caused by a null mutation of the *IL2RG* gene, that results in a complex phenotype characterized by an inability to differentiate or function in response to multiple lymphoid cytokines.[101] In humans, this deficiency in γc results in an absence of peripheral T and NK cells, and present but functionally impaired B cells.[14,102] Disruption of the gene encoding JAK3 leads to JAK3-SCID, an autosomal recessive form of SCID with an otherwise identical clinical phenotype to X-SCID.[20,103]

Although humans with mutations in *IL2RG* or *JAK3* have normal numbers of circulating B cells, mice lacking γc signaling are fully unable to develop B cells, arresting at the pre-proB stage.[17,22-26] This is due to deficient IL7 signaling, as IL7 and IL7Rα null mice are also unable to develop B or T cells.[28,29] Human patients with IL7Rα defects have a normal number of B cells, unlike *IL7Rα* null mice,[18] but similar to patients with defects in IL2RG or JAK3.

A potential explanation for circulating B cells found in patients with SCID is that the cells are of the B-1 cell population, a population of spontaneously IgM secreting B cells of fetal origin that arise from a distinct hematopoietic progenitor.[104,105] Recent developments have identified a potential B1 population in human UCB and peripheral blood (though human BM was not examined.)[106]

All stages of hematopoiesis, from early progenitors to many categories of mature lymphoid cells, have been examined in mice that are null for *IL2RG, IL7Rα, or IL7R*.[107] However, examination of hematopoietic progenitors in humans with SCID is more difficult, as it requires an invasive bone marrow draw. Despite the experimental hurdles, it is important to directly investigate mechanisms of human lymphoid commitment,

especially because cytokine deficiencies result in different phenotypes in humans and mice.

The studies described in **Chapter 2** increased our understanding of the hierarchy of human lymphoid progenitors in normal bone marrow. Using the knowledge gained from those studies, we sought to examine the stages of lymphoid lineage commitment, specifically B lineage commitment, in patients with SCID. Because SCID patients have normal numbers of circulating B cells, **we hypothesized that the earliest stages of B lymphoid development will be unaffected in these patients, and that we would be able to detect both B1 and non-B1 mature populations.** These hypotheses were the basis for in-progress research presented in **Chapter 3** of this thesis.

The body of this thesis examines the process of lymphoid differentiation in several contexts: normal human hematopoiesis, dysfunctional human hematopoiesis, and murine thymic reconstitution post-HSCT. The majority of my research has focused on the identification of a functionally and molecularly distinct stage of early human hematopoietic commitment. These cells are functionally analogous to a population of cells described in mouse, the Lymphoid-primed Multi-Potent Progenitor (LMPP), and both the mouse LMPP and our novel human LMPP are strong candidates to be thymic seeding cells. The identification an LMPP in human BM will be an important tool to the future study molecular regulation of the first stages of lymphoid commitment in human hematopoiesis.

References

1. Zlotoff, D.A. & Bhandoola, A. Hematopoietic progenitor migration to the adult thymus. *Ann N Y Acad Sci* **1217**, 122-138 (2011).
2. Aguila, H.L.*, et al.* From stem cells to lymphocytes: biology and transplantation. *Immunol Rev* **157**, 13-40 (1997).
3. Wilson, A., MacDonald, H.R. & Radtke, F. Notch 1-deficient common lymphoid precursors adopt a B cell fate in the thymus. *J Exp Med* **194**, 1003-1012 (2001).
4. Besseyrias, V.*, et al.* Hierarchy of Notch-Delta interactions promoting T cell lineage commitment and maturation. *J Exp Med* **204**, 331-343 (2007).
5. Schmitt, T.M. & Zuniga-Pflucker, J.C. Induction of T cell development from hematopoietic progenitor cells by delta-like-1 in vitro. *Immunity* **17**, 749-756 (2002).
6. La Motte-Mohs, R.N., Herer, E. & Zuniga-Pflucker, J.C. Induction of T-cell development from human cord blood hematopoietic stem cells by Delta-like 1 in vitro. *Blood* **105**, 1431-1439 (2005).
7. Lind, E.F., Prockop, S.E., Porritt, H.E. & Petrie, H.T. Mapping precursor movement through the postnatal thymus reveals specific microenvironments supporting defined stages of early lymphoid development. *J Exp Med* **194**, 127-134 (2001).
8. Heinzel, K., Benz, C., Martins, V.C., Haidl, I.D. & Bleul, C.C. Bone marrow-derived hemopoietic precursors commit to the T cell lineage only after arrival in the thymic microenvironment. *J Immunol* **178**, 858-868 (2007).
9. Russell, S.M.*, et al.* Interleukin-2 receptor gamma chain: a functional component of the interleukin-4 receptor. *Science* **262**, 1880-1883 (1993).
10. Noguchi, M.*, et al.* Interleukin-2 receptor gamma chain: a functional component of the interleukin-7 receptor. *Science* **262**, 1877-1880 (1993).
11. Kondo, M.*, et al.* Sharing of the interleukin-2 (IL-2) receptor gamma chain between receptors for IL-2 and IL-4. *Science* **262**, 1874-1877 (1993).
12. Kimura, Y.*, et al.* Sharing of the IL-2 receptor gamma chain with the functional IL-9 receptor complex. *Int Immunol* **7**, 115-120 (1995).
13. Asao, H.*, et al.* Cutting edge: the common gamma-chain is an indispensable subunit of the IL-21 receptor complex. *J Immunol* **167**, 1-5 (2001).
14. Leonard, W.J. Cytokines and immunodeficiency diseases. *Nat Rev Immunol* **1**, 200-208 (2001).
15. Witthuhn, B.A.*, et al.* Involvement of the Jak-3 Janus kinase in signalling by interleukins 2 and 4 in lymphoid and myeloid cells. *Nature* **370**, 153-157 (1994).
16. Johnston, J.A.*, et al.* Phosphorylation and activation of the Jak-3 Janus kinase in response to interleukin-2. *Nature* **370**, 151-153 (1994).
17. Sugamura, K.*, et al.* The interleukin-2 receptor gamma chain: its role in the multiple cytokine receptor complexes and T cell development in XSCID. *Annu Rev Immunol* **14**, 179-205 (1996).

18. Puel, A., Ziegler, S.F., Buckley, R.H. & Leonard, W.J. Defective IL7R expression in T(-)B(+)NK(+) severe combined immunodeficiency. *Nat Genet* **20**, 394-397 (1998).
19. Roifman, C.M., Zhang, J., Chitayat, D. & Sharfe, N. A partial deficiency of interleukin-7R alpha is sufficient to abrogate T-cell development and cause severe combined immunodeficiency. *Blood* **96**, 2803-2807 (2000).
20. Russell, S.M.*, et al.* Mutation of Jak3 in a patient with SCID: essential role of Jak3 in lymphoid development. *Science* **270**, 797-800 (1995).
21. Plum, J., De Smedt, M., Leclercq, G., Verhasselt, B. & Vandekerckhove, B. Interleukin-7 is a critical growth factor in early human T-cell development. *Blood* **88**, 4239-4245 (1996).
22. DiSanto, J.P., Muller, W., Guy-Grand, D., Fischer, A. & Rajewsky, K. Lymphoid development in mice with a targeted deletion of the interleukin 2 receptor gamma chain. *Proc Natl Acad Sci U S A* **92**, 377-381 (1995).
23. Cao, X.*, et al.* Defective lymphoid development in mice lacking expression of the common cytokine receptor gamma chain. *Immunity* **2**, 223-238 (1995).
24. Thomis, D.C., Gurniak, C.B., Tivol, E., Sharpe, A.H. & Berg, L.J. Defects in B lymphocyte maturation and T lymphocyte activation in mice lacking Jak3. *Science* **270**, 794-797 (1995).
25. Park, S.Y.*, et al.* Developmental defects of lymphoid cells in Jak3 kinase-deficient mice. *Immunity* **3**, 771-782 (1995).
26. Nosaka, T.*, et al.* Defective lymphoid development in mice lacking Jak3. *Science* **270**, 800-802 (1995).
27. Kikuchi, K., Lai, A.Y., Hsu, C.L. & Kondo, M. IL-7 receptor signaling is necessary for stage transition in adult B cell development through up-regulation of EBF. *J Exp Med* **201**, 1197-1203 (2005).
28. Peschon, J.J.*, et al.* Early lymphocyte expansion is severely impaired in interleukin 7 receptor-deficient mice. *J Exp Med* **180**, 1955-1960 (1994).
29. von Freeden-Jeffry, U.*, et al.* Lymphopenia in interleukin (IL)-7 gene-deleted mice identifies IL-7 as a nonredundant cytokine. *J Exp Med* **181**, 1519-1526 (1995).
30. Iwasaki, H. & Akashi, K. Hematopoietic developmental pathways: on cellular basis. *Oncogene* **26**, 6687-6696 (2007).
31. Matthias, P. & Rolink, A.G. Transcriptional networks in developing and mature B cells. *Nat Rev Immunol* **5**, 497-508 (2005).
32. Hagman, J. & Lukin, K. Transcription factors drive B cell development. *Curr Opin Immunol* **18**, 127-134 (2006).
33. Singh, H. & Pongubala, J.M. Gene regulatory networks and the determination of lymphoid cell fates. *Curr Opin Immunol* **18**, 116-120 (2006).
34. Busslinger, M. Transcriptional control of early B cell development. *Annu Rev Immunol* **22**, 55-79 (2004).
35. Kondo, M., Weissman, I.L. & Akashi, K. Identification of clonogenic common lymphoid progenitors in mouse bone marrow. *Cell* **91**, 661-672 (1997).
36. Akashi, K., Traver, D., Miyamoto, T. & Weissman, I.L. A clonogenic common myeloid progenitor that gives rise to all myeloid lineages. *Nature* **404**, 193-197 (2000).

37. Manz, M.G., Miyamoto, T., Akashi, K. & Weissman, I.L. Prospective isolation of human clonogenic common myeloid progenitors. *Proc Natl Acad Sci U S A* **99**, 11872-11877 (2002).
38. Galy, A., Travis, M., Cen, D. & Chen, B. Human T, B, natural killer, and dendritic cells arise from a common bone marrow progenitor cell subset. *Immunity* **3**, 459-473 (1995).
39. Ichii, M.*, et al.* The density of CD10 corresponds to commitment and progression in the human B lymphoid lineage. *PLoS One* **5**, e12954 (2010).
40. Cumano, A., Paige, C.J., Iscove, N.N. & Brady, G. Bipotential precursors of B cells and macrophages in murine fetal liver. *Nature* **356**, 612-615 (1992).
41. Montecino-Rodriguez, E., Leathers, H. & Dorshkind, K. Bipotential B-macrophage progenitors are present in adult bone marrow. *Nat Immunol* **2**, 83-88 (2001).
42. Adolfsson, J.*, et al.* Identification of Flt3+ lympho-myeloid stem cells lacking erythro-megakaryocytic potential a revised road map for adult blood lineage commitment. *Cell* **121**, 295-306 (2005).
43. Luc, S., Buza-Vidas, N. & Jacobsen, S.E.W. Biological and Molecular Evidence for Existence of Lymphoid-Primed Multipotent Progenitors. *Ann. N.Y. Acad. Sci* (2007).
44. Luc, S., Buza-Vidas, N. & Jacobsen, S.E. Delineating the cellular pathways of hematopoietic lineage commitment. *Semin Immunol* **20**, 213-220 (2008).
45. Luc, S.*, et al.* Down-regulation of Mpl marks the transition to lymphoid-primed multipotent progenitors with gradual loss of granulocyte-monocyte potential. *Blood* **111**, 3424-3434 (2008).
46. Forsberg, E.C., Serwold, T., Kogan, S., Weissman, I.L. & Passegue, E. New evidence supporting megakaryocyte-erythrocyte potential of flk2/flt3+ multipotent hematopoietic progenitors. *Cell* **126**, 415-426 (2006).
47. Wada, H.*, et al.* Adult T-cell progenitors retain myeloid potential. *Nature* **452**, 768-772 (2008).
48. Bell, J.J. & Bhandoola, A. The earliest thymic progenitors for T cells possess myeloid lineage potential. *Nature* **452**, 764-767 (2008).
49. Ceredig, R. Fates and potentials of thymus-seeding progenitors. *Nat Immunol* **13**, 309-310 (2012).
50. Luc, S.*, et al.* The earliest thymic T cell progenitors sustain B cell and myeloid lineage potential. *Nat Immunol* **13**, 412-419 (2012).
51. Perry, S.S., Welner, R.S., Kouro, T., Kincade, P.W. & Sun, X.H. Primitive lymphoid progenitors in bone marrow with T lineage reconstituting potential. *J Immunol* **177**, 2880-2887 (2006).
52. Schlenner, S.M. & Rodewald, H.R. Early T cell development and the pitfalls of potential. *Trends Immunol* **31**, 303-310 (2010).
53. Rossi, F.M.*, et al.* Recruitment of adult thymic progenitors is regulated by P-selectin and its ligand PSGL-1. *Nat Immunol* **6**, 626-634 (2005).
54. Krueger, A., Willenzon, S., Lyszkiewicz, M., Kremmer, E. & Forster, R. CC chemokine receptor 7 and 9 double-deficient hematopoietic progenitors are severely impaired in seeding the adult thymus. *Blood* **115**, 1906-1912 (2010).

55. Rossi, M.I., *et al.* B lymphopoiesis is active throughout human life, but there are developmental age-related changes. *Blood* **101**, 576-584 (2003).
56. Payne, K.J. & Crooks, G.M. Immune-cell lineage commitment: translation from mice to humans. *Immunity* **26**, 674-677 (2007).
57. Mold, J.E., *et al.* Fetal and adult hematopoietic stem cells give rise to distinct T cell lineages in humans. *Science* **330**, 1695-1699 (2010).
58. Hao, Q.L., Shah, A.J., Thiemann, F.T., Smogorzewska, E.M. & Crooks, G.M. A functional comparison of CD34 + CD38- cells in cord blood and bone marrow. *Blood* **86**, 3745-3753 (1995).
59. Six, E.M., *et al.* A human postnatal lymphoid progenitor capable of circulating and seeding the thymus. *J Exp Med* **204**, 3085-3093 (2007).
60. Arakawa-Hoyt, J., *et al.* The number and generative capacity of human B lymphocyte progenitors, measured in vitro and in vivo, is higher in umbilical cord blood than in adult or pediatric bone marrow. *Bone Marrow Transplant* **24**, 1167-1176 (1999).
61. De Smedt, M., *et al.* T-lymphoid differentiation potential measured in vitro is higher in CD34+CD38-/lo hematopoietic stem cells from umbilical cord blood than from bone marrow and is an intrinsic property of the cells. *Haematologica* **96**, 646-654 (2011).
62. Leavy, O. Haematopoiesis: Baby tolerance. *Nat Rev Immunol* **11**, 78 (2011).
63. Lanza, R.P. *Handbook of stem cells*, (Elsevier Academic, Boston, MA, 2004).
64. Doulatov, S., *et al.* Revised map of the human progenitor hierarchy shows the origin of macrophages and dendritic cells in early lymphoid development. *Nat Immunol* **11**, 585-593 (2010).
65. Hao, Q.L., *et al.* Identification of a novel, human multilymphoid progenitor in cord blood. *Blood* **97**, 3683-3690 (2001).
66. Haddad, R., *et al.* Molecular characterization of early human T/NK and B-lymphoid progenitor cells in umbilical cord blood. *Blood* **104**, 3918-3926 (2004).
67. Storms, R.W., Goodell, M.A., Fisher, A., Mulligan, R.C. & Smith, C. Hoechst dye efflux reveals a novel CD7(+)CD34(-) lymphoid progenitor in human umbilical cord blood. *Blood* **96**, 2125-2133 (2000).
68. Galy, A.H., *et al.* Generation of T cells from cytokine-mobilized peripheral blood and adult bone marrow CD34+ cells. *Blood* **84**, 104-110 (1994).
69. Rosen, S.D. Ligands for L-selectin: homing, inflammation, and beyond. *Annu Rev Immunol* **22**, 129-156 (2004).
70. Perry, S.S., *et al.* L-selectin defines a bone marrow analog to the thymic early T-lineage progenitor. *Blood* **103**, 2990-2996 (2004).
71. Cho, S. & Spangrude, G.J. Enrichment of functionally distinct mouse hematopoietic progenitor cell populations using CD62L. *J Immunol* **187**, 5203-5210 (2011).
72. Ito, M., *et al.* NOD/SCID/gamma(c)(null) mouse: an excellent recipient mouse model for engraftment of human cells. *Blood* **100**, 3175-3182 (2002).
73. Notta, F., *et al.* Isolation of single human hematopoietic stem cells capable of long-term multilineage engraftment. *Science* **333**, 218-221 (2011).

74. McKenzie, J.L., Gan, O.I., Doedens, M. & Dick, J.E. Human short-term repopulating stem cells are efficiently detected following intrafemoral transplantation into NOD/SCID recipients depleted of CD122+ cells. *Blood* **106**, 1259-1261 (2005).
75. Mazurier, F., Doedens, M., Gan, O.I. & Dick, J.E. Rapid myeloerythroid repopulation after intrafemoral transplantation of NOD-SCID mice reveals a new class of human stem cells. *Nat Med* **9**, 959-963 (2003).
76. Ishikawa, F., Saito, Y., Yoshida, S., Harada, M. & Shultz, L.D. The differentiative and regenerative properties of human hematopoietic stem/progenitor cells in NOD-SCID/IL2rgamma(null) mice. *Curr Top Microbiol Immunol* **324**, 87-94 (2008).
77. Cuddihy, A.R.*, et al.* VEGF-mediated cross-talk within the neonatal murine thymus. *Blood* **113**, 2723-2731 (2009).
78. Rawlings, D.J., Quan, S.G., Kato, R.M. & Witte, O.N. Long-term culture system for selective growth of human B-cell progenitors. *Proc Natl Acad Sci U S A* **92**, 1570-1574 (1995).
79. Rawlings, D.J.*, et al.* Differentiation of human CD34+CD38- cord blood stem cells into B cell progenitors in vitro. *Exp Hematol* **25**, 66-72 (1997).
80. Fluckiger, A.C.*, et al.* In vitro reconstitution of human B-cell ontogeny: from CD34(+) multipotent progenitors to Ig-secreting cells. *Blood* **92**, 4509-4520 (1998).
81. Itoh, K.*, et al.* Reproducible establishment of hemopoietic supportive stromal cell lines from murine bone marrow. *Exp Hematol* **17**, 145-153 (1989).
82. Issaad, C., Croisille, L., Katz, A., Vainchenker, W. & Coulombel, L. A murine stromal cell line allows the proliferation of very primitive human CD34++/CD38- progenitor cells in long-term cultures and semisolid assays. *Blood* **81**, 2916-2924 (1993).
83. Feugier, P.*, et al.* Osteopetrotic mouse stroma with thrombopoietin, c-kit ligand, and flk-2 ligand supports long-term mobilized CD34+ hematopoiesis in vitro. *Stem Cells Dev* **14**, 505-516 (2005).
84. Wolins, N.E.*, et al.* OP9 mouse stromal cells rapidly differentiate into adipocytes: characterization of a useful new model of adipogenesis. *J Lipid Res* **47**, 450-460 (2006).
85. Richie Ehrlich, L.I., Serwold, T. & Weissman, I.L. In vitro assays misrepresent in vivo lineage potentials of murine lymphoid progenitors. *Blood* **117**, 2618-2624 (2011).
86. Crooks, G.M. Lineage assays: which pathway to take? *Blood* **117**, 2560 (2011).
87. Pui, J.C.*, et al.* Notch1 expression in early lymphopoiesis influences B versus T lineage determination. *Immunity* **11**, 299-308 (1999).
88. Calvo, J., BenYoucef, A., Baijer, J., Rouyez, M.C. & Pflumio, F. Assessment of human multi-potent hematopoietic stem/progenitor cell potential using a single in vitro screening system. *PLoS One* **7**, e50495 (2012).
89. de Hoon, M.J., Imoto, S., Nolan, J. & Miyano, S. Open source clustering software. *Bioinformatics* **20**, 1453-1454 (2004).
90. Novershtern, N.*, et al.* Densely interconnected transcriptional circuits control cell states in human hematopoiesis. *Cell* **144**, 296-309 (2011).

91. Mansson, R.*, et al.* Molecular evidence for hierarchical transcriptional lineage priming in fetal and adult stem cells and multipotent progenitors. *Immunity* **26**, 407-419 (2007).
92. Warren, L., Bryder, D., Weissman, I.L. & Quake, S.R. Transcription factor profiling in individual hematopoietic progenitors by digital RT-PCR. *Proc Natl Acad Sci U S A* **103**, 17807-17812 (2006).
93. Eyrich, M.*, et al.* Onset of thymic recovery and plateau of thymic output are differentially regulated after stem cell transplantation in children. *Biol Blood Marrow Transplant* **11**, 194-205 (2005).
94. Hakim, F.T.*, et al.* Age-dependent incidence, time course, and consequences of thymic renewal in adults. *J Clin Invest* **115**, 930-939 (2005).
95. Mackall, C.L.*, et al.* Age, thymopoiesis, and CD4+ T-lymphocyte regeneration after intensive chemotherapy. *N Engl J Med* **332**, 143-149 (1995).
96. Myers, L.A., Patel, D.D., Puck, J.M. & Buckley, R.H. Hematopoietic stem cell transplantation for severe combined immunodeficiency in the neonatal period leads to superior thymic output and improved survival. *Blood* **99**, 872-878 (2002).
97. Buckley, R.H. Molecular defects in human severe combined immunodeficiency and approaches to immune reconstitution. *Annu Rev Immunol* **22**, 625-655 (2004).
98. Krenger, W., Blazar, B.R. & Hollander, G.A. Thymic T-cell development in allogeneic stem cell transplantation. *Blood* **117**, 6768-6776 (2011).
99. Parkman, R. & Weinberg, K.I. Immunological reconstitution following bone marrow transplantation. *Immunol Rev* **157**, 73-78 (1997).
100. Ciurea, S.O.*, et al.* Lymphocyte recovery predicts outcomes in cord blood and T cell-depleted haploidentical stem cell transplantation. *Biol Blood Marrow Transplant* **17**, 1169-1175 (2011).
101. Noguchi, M.*, et al.* Interleukin-2 receptor gamma chain mutation results in X-linked severe combined immunodeficiency in humans. *Cell* **73**, 147-157 (1993).
102. Buckley, R.H. Primary immunodeficiency diseases due to defects in lymphocytes. *N Engl J Med* **343**, 1313-1324 (2000).
103. Macchi, P.*, et al.* Mutations of Jak-3 gene in patients with autosomal severe combined immune deficiency (SCID). *Nature* **377**, 65-68 (1995).
104. Montecino-Rodriguez, E., Leathers, H. & Dorshkind, K. Identification of a B-1 B cell-specified progenitor. *Nat Immunol* **7**, 293-301 (2006).
105. Dorshkind, K. & Montecino-Rodriguez, E. Fetal B-cell lymphopoiesis and the emergence of B-1-cell potential. *Nat Rev Immunol* **7**, 213-219 (2007).
106. Griffin, D.O., Holodick, N.E. & Rothstein, T.L. Human B1 cells in umbilical cord and adult peripheral blood express the novel phenotype CD20+ CD27+ CD43+ CD70. *J Exp Med* **208**, 67-80 (2011).
107. Kikuchi, K., Kasai, H., Watanabe, A., Lai, A.Y. & Kondo, M. IL-7 specifies B cell fate at the common lymphoid progenitor to pre-proB transition stage by maintaining early B cell factor expression. *J Immunol* **181**, 383-392 (2008).

Chapter 2

Lymphoid Priming in Human Bone Marrow Begins Before Expression of CD10 with Upregulation of L-selectin.

Chapter 2 presents research on the earliest stages of lymphoid commitment in human bone marrow. We identified a $CD34^{+}Lin^{-}CD10^{-}$ progenitor subpopulation in human BM with high expression of CD62L that was devoid of clonogenic myeloid or erythroid potential. These cells generated B cells, NK cells and T cells as well as monocytic and dendritic cells, were able to rapidly engraft immunodeficient mice, and may be capable of seeding the thymus.

Lisa Ann Kohn designed, performed, collected, and analyzed experiments and wrote the paper.

Nature Immunology, 2012

Lymphoid priming in human bone marrow begins before expression of CD10 with upregulation of L-selectin

Lisa A Kohn[1], Qian-Lin Hao[2], Rajkumar Sasidharan[3], Chintan Parekh[4], Shundi Ge[1], Yuhua Zhu[1], Hanna K A Mikkola[3,5] & Gay M Crooks[1,4,5]

[1]Department of Pathology & Laboratory Medicine, *University of California*, *Los Angeles*, *California*, *USA. [2]Division of Research Immunology & Bone Marrow Transplantation*, *Children's Hospital Los Angeles*, *Los Angeles*, *California*, *USA. [3]Department of Molecular*, *Cell and Developmental Biology*, *University of California*, *Los Angeles*, *Los Angeles*, *California*, *USA. [4]Department of Pediatrics*, David Geffen School of Medicine, *University of California*, *Los Angeles*, *Los Angeles*, *California*, *USA. [5]Eli and Edythe Broad Center for Regenerative Medicine and Stem Cell Research*, *University of California, Los Angeles*, *Los Angeles*, *California*, *USA. Correspondence should be addressed to G.M.C. (gcrooks@mednet.ucla.edu).*

Received 21 February; accepted 24 July; published online 2 September 2012;

doi:10.1038/ni.2405

Expression of the cell surface antigen CD10 has long been used to define human lymphoid commitment. We report a unique lymphoid-primed population in human bone marrow that was generated from hematopoietic stem cells (HSCs) before the onset of the expression of CD10 and commitment to the B cell lineage. We identified this subset by high expression of the homing molecule L-selectin (CD62L). $CD10^{-}CD62L^{hi}$ progenitors had full lymphoid and monocytic potential but lacked erythroid potential. Gene-expression profiling placed the $CD10^{-}CD62L^{hi}$ population at an intermediate stage of differentiation between HSCs

and lineage-negative (Lin^-) $CD34^+CD10^+$ progenitors. CD62L was expressed on immature thymocytes, and its ligands were expressed at the cortico-medullary junction of the thymus, which suggested a possible role for this molecule in thymic homing. Our studies identify the earliest stage of lymphoid priming in human bone marrow.

Although much is known about the identity of progenitor stages in mouse lymphopoiesis, considerably less is understood about the critical stages of lymphoid commitment of human hematopoietic cells. Early models developed from mouse studies assumed strictly dichotomous pathways of lineage commitment[1]. Those ideas have evolved into models of gradual loss of lineage potential that can occur via multiple alternative pathways, although the physiological relevance of lineage potential demonstrated in certain *in vitro* assays continues to be debated[2–5]. A stage at which mouse bone marrow progenitors are 'lymphoid primed' before complete loss of myeloid potential has been defined on the basis of expression of the cell surface receptor Flt3, and cells at this stage have been called 'lymphoid-primed multipotent progenitors' (LMPPs)[2].

Critical species-specific differences create challenges for the 'translation' of knowledge about cellular hierarchies derived from mouse studies to the specifics of human hematopoiesis[6]. In addition, the source and stage in ontogeny of human hematopoiesis can influence the functional abilities, surface immunophenotypes and transcriptional profiles of the cells under study[6–8]. Most studies of the earliest progenitor stages in human hematopoiesis have used neonatal umbilical cord blood as the source of hematopoietic cells. However, understanding of how lymphopoiesis is regulated during steady-state adult hematopoiesis requires direct study of hematopoietic stem cells and progenitors from postnatal human bone marrow[8,9].

The stepwise process of the lymphoid differentiation of multipotent hematopoietic stem cells (HSCs) in human bone marrow has been assumed to begin with expression of the cell

surface antigen CD10 (CALLA or MME) on $CD34^+$ progenitors , based on the finding that CD10+ progenitors lacked myeloid and erythroid potential but were able to generate all lymphoid lineages[10]. However, more recent studies have shown that $CD34^+CD10^+$ cells, even those without expression of lineage markers (Lin^-: $CD3^-CD14^-CD15^-CD19^-CD56^-CD235a^-$),exhibit a strong bias toward B cell potential with relatively little T cell and natural killer (NK) cell potential[11,12]. $CD34^+Lin^-CD10^+$ cells that lack expression of CD24 are precursors of the $CD34^+Lin^-CD10^+CD24^+$ population but nonetheless show molecular evidence of commitment to the B cell lineage, with expression of several B cell specific genes[12]. Therefore, to understand the progenitor hierarchy of human lymphoid commitment, we sought to identify a stage of lymphoid priming that precedes commitment to the B lymphoid lineage, either before or independently of CD10 expression.

L-selectin (CD62L) is expressed on lymphocytes and mediates homing to peripheral lymphoid organs[13]. Studies have reported that upregulation of CD62L expression on c-Kit^+Lin^- Sca-1^+ mouse bone marrow cells correlates with loss of erythroid and megakaryocyte potential and efficient thymic engraftment[14–16]. In this study we have identified a $CD34^+Lin^-CD10^-$ progenitor subpopulation in human bone marrow with high expression of L-selectin and that was devoid of clonogenic myeloid or erythroid potential. In stromal cultures, these cells were able to generate B cells, NK cells and T cells, as well as monocytic and dendritic cells, similar to the LMPPs in mouse bone marrow that have been reported before[2]. $CD34^+Lin^-CD10^-CD62L^{hi}$ cells (called '$CD10^-CD62L^{hi}$ cells' here) rapidly engrafted immunodeficient mice, producing B cells and myeloid cells. Despite evidence of lymphoid skewing, comprehensive molecular analysis showed that $CD10^-CD62L^{hi}$ cells not only lacked B cell–specific transcripts but also had not initiated DNA recombination, on the basis of no expression of the recombinase component–

encoding genes *RAG1* and *RAG2* and minimal expression of *DNTT*, which encodes terminal deoxynucleotidyltransferase. Genome-wide expression and functional analysis identified the $CD10^{-}CD62L^{hi}$ progenitor population as a developmental intermediate between the multipotent $CD34^{+}Lin^{-}CD38^{-}$ population and the $CD34^{+}Lin^{-}CD10^{+}$ lymphoid progenitor population.

We also found that primitive lymphoid-restricted $CD34^{+}CD1a^{-}$ progenitors in human thymus expressed CD62L and that the vasculature at the cortico-medullary junction of human thymus expressed ligands for CD62L, which suggested the possibility that CD62L may have a role human thymic homing. We propose that the $CD10^{-}CD62L^{hi}$ progenitor in bone marrow represents the earliest stage at which adult human progenitors become lymphoid primed. The identification of this progenitor population will facilitate a more complete understanding of the regulation of lymphoid commitment from HSCs during normal and aberrant human hematopoiesis.

RESULTS

The lymphoid marker CD7 does not define lymphoid commitment

Given published reports linking expression of the lymphoid marker CD7 to early stages of lymphoid commitment in umbilical cord blood[17–20], we first investigated whether expression of CD7 was sufficient to identify human lymphoid commitment in bone marrow independently of CD10 expression. Examination of CD34+ cell populations depleted of lineage marker–expressing showed that the $CD34^{+}Lin^{-}CD38^{-}CD7^{+}$ population identified before in umbilical cord blood[17] was not detectable in human bone marrow (**Supplementary Fig. 1a**). However, as noted before[7], we detected low expression of CD7 on a small population of $CD34^{+}Lin^{-}CD38^{+}$ human bone marrow cells (2.8% ± 0.6%; $n = 5$ donors), most of which did not coexpress CD10

(**Fig. 1a**). Clonogenic assays demonstrated that CD7 expression alone was insufficient to define lymphoid restriction of the $CD34^+Lin^-CD10^-$ population of bone marrow; nonlymphoid clonogenic cells, particularly erythroid progenitors, were readily detectable in the $CD34^+$ Lin^- $CD10^-CD7^+$ population by assay of colony-forming unit–cells (CFU-C; **Fig. 1b**). Consistent with published studies of bone marrow and umbilical cord blood[7,10–12,21], $CD34^+Lin^-CD10^+$ progenitors were devoid of clonogenic myeloid or erythroid progenitors (**Fig. 1b**).

L-selectin^{hi} progenitors do not have CFU-C potential

CD45RA has been shown to be expressed on various lymphoid progenitor cells[10,17–19] and granulocyte-macrophage progenitors[22] Analysis of the $CD34^+Lin^-CD10^-$ subpopulation demonstrated the presence of both $CD45RA^-$ and $CD45RA^+$ fractions; in contrast, all $CD34^+Lin^-$ $CD10^+$ cells were $CD45RA^+$ (**Fig. 1c**). Erythroid potential was absent but clonogenic myeloid progenitors were still readily detectable, by assay of CFU–granulocyte-macrophage, in the $CD34^+Lin^-CD10^-CD45RA^+$ population (**Fig. 1d**). As expected, clonogenic erythroid potential was in megakarocytic-erythroid progenitors and common myeloid progenitors (**Fig. 1d**), neither of which express CD45RA.

Further refinement of the $CD10^-CD45RA^+$ population was necessary to identify those cells that lacked clonogenic myeloid potential. As noted above, CD62L is a cell surface receptor that mediates lymphocyte homing to peripheral nodes[13] and is expressed on certain mouse bone marrow progenitors that lack erythroid or megakaryocytic potential[14]. Analysis of the $CD34^+Lin^-$ $CD10^-$ $CD45RA^+$ population demonstrated that although most cells had low expression of CD62L, a distinct subpopulation ($9 \pm 1.5\%$, $n = 14$) of $CD34^+Lin^-CD10^-CD45RA^+$ cells in normal human bone marrow had high expression of CD62L (**Fig. 1c**). Functional screening of $CD34^+Lin^-$ fractions by CFU-C assay demonstrated that only the $CD34^+Lin^-CD10^-$

$CD45RA^+CD62L^{hi}$ population (called '$CD10^-CD62L^{hi}$ cells' here) and the $CD34^+Lin^-CD10^+$ population (called '$CD10^+$ cells' here) were devoid of clonogenic myelo-erythroid potential (**Fig. 1d** and **Supplementary Table 1**). Of note, the $CD34^+Lin^-CD10^-CD45RA^+$ population with intermediate expression of CD62L had low but detectable CFU-C potential (population B, **Supplementary Fig. 1b**,**c**), which suggested that progressive loss of multipotency correlated with increasing CD62L expression.

$CD10^+$ cells had low or undetectable expression of CD62L, and the $CD34^+Lin^-CD38^-$ population, which is enriched for HSCs and multipotent progenitor cells (MPPs)[21]had intermediate expression of CD62L (**Fig. 1e** and **Supplementary Fig. 1b**). Notably, $CD10^-CD62L^{hi}$ cells did not express CD7 (**Fig. 1f**). Thus, the progenitor subset with highest CD62L expression expressed neither CD10 nor CD7, markers that have been relied on for the isolation of human lymphoid progenitors. Analysis of bone marrow from 20 different donors whose ages ranged from infancy to adulthood consistently showed the presence of $CD10^-CD62L^{hi}$ cells (**Supplementary Fig. 2a–c**).

Lymphoid and monocyte potential of $CD10^-CD62L^{hi}$ cells

Culture in lymphoid conditions demonstrated that the $CD10^-CD62L^{hi}$ population robustly generated both B cells and NK cells (**Fig. 2a**). Consistent with published studies[11], $CD10^+$ cells (all of which were $CD19^-$ through depletion of lineage marker–expressing cells) generated mostly B cells with relatively weak potential to develop into NK cells. Cell output under B cell–NK cell lymphoid conditions tended to be higher in cultures initiated with $CD10^-CD62L^{hi}$ cells than in those initiated with $CD10^+$ cells (**Fig. 2b**). After *in vitro* culture under T cell conditions, $CD10^-CD62L^{hi}$ cells generated cells with the immunophenotype typical of thymocytes (expression of CD1A, CD7, CD4, CD8, CD3 and TCRab)[23] (**Fig. 2c**,**d** and **Supplementary Fig.**

3) and that expressed the T cell–associated genes *TCF7*, *GATA3*, *DNTT* and *RAG1* (**Supplementary Fig. 3**), as well as $CD56^+$ NK cells (some of which coexpressed CD8). Cell output was significantly higher in T cell cultures initiated with $CD10^-CD62L^{hi}$ cells than in those initiated with $CD10^+$ cells (**Fig. 2e**).

Although we did not detect clonogenic myeloid cells by CFU-C assay, both the $CD10^+$ and $CD10^-CD62L^{hi}$ subsets were able to generate low numbers of myeloid cells when cultured on stromal layers; however, cell output from both progenitor types was significantly lower than that of HSCs-MPPs (**Fig. 2f**). Most nonlymphoid cells generated from the $CD10^+$ and $CD10^-CD62L^{hi}$ populations in stromal coculture were $CD14^+CD33^+$ monocytes-macrophages or $CD209^+CD1a^+$ dendritic cells (**Supplementary Fig. 4**); $CD66b^+$ granulocytes were uncommon. We rarely noted erythroid differentiation in $CD10^+$ or $CD10^-CD62L^{hi}$ cultures, but erythroid cell production was robust in cultures from $CD38^-$ HSCs-MPPs.

The cloning efficiency of $CD10^-CD62L^{hi}$ cells in lymphoid cultures initiated with a single cell (~11%) and by limiting-dilution analysis (cloning efficiency, 1 cell in 5.3 cells for B cells–NK cells (95% confidence interval, 1 in 4.4–6.4), and 1 cell in 5.6 cells for T cell cultures (95% confidence interval, 1 in 4.6–6.9); **Fig. 3a**,**b**) was similar to that of $CD10^+$ cells (~12% from single cells). However, lineage analysis of clones demonstrated that the $CD10^-CD62L^{hi}$ population contained bi-potent B cell–NK cell progenitors, whereas the $CD10^+$ population contained predominantly unipotent B cell progenitors (**Fig. 3c**). We detected myeloid cells in 86% of clones that could be assigned a lineage in B cell–NK cell conditions (**Fig. 3d**) and in 97% of all clones assayed from T cell cultures (**Fig. 3e**). Consistent with the *in vitro* assays of lineage potential, intratibial transplantation of $CD10^-CD62L^{hi}$ progenitors into immunodeficient mice of the NSG strain (nonobese diabetic–severe combined immunodeficiency strain, deficient

in the IL-2Rg receptor for interleukin 2 (IL-2)) produced rapid marrow engraftment of both myeloid and B lymphoid cells (**Fig. 3f**,**g** and **Supplementary Fig. 5**). Differentiation of non–self-renewing progenitor cells into T lymphoid cells would not be expected in this xenogeneic adult mouse model.

In summary, our functional assays showed that the $CD10^{-}CD62L^{hi}$ population had full lymphoid potential, was less skewed toward the B lineage than was the $CD10^{+}$ population, and had greater potential to develop into T cells than did $CD10^{+}$ population. Although the population lacked clonogenic myelo-erythroid potential, some differentiation of the $CD10^{-}CD62L^{hi}$ population into myeloid cells (mostly monocytes-macrophages and dendritic cells) could be induced in stromal cocultures and in short-term engraftment assays. However, myeloid potential was significantly lower that of HSCs-MPPs and erythroid potential was absent.

Differentiation stages of HSCs and lymphoid progenitors

Given the lineage potential shown in the functional studies reported above, we next explored the stages of differentiation of the $CD10^{-}CD62L^{hi}$ and $CD10^{+}$ populations compared with that of the most primitive $CD34^{+}Lin^{-}CD38^{-}$ ('CD38-') HSC-MPP population. Expression of the differentiation marker CD38 increased progressively from the $CD34^{+}CD38^{-}$ population to the $CD10^{-}CD62L^{hi}$ population and was maximal in the $CD10^{+}$ population (n = 14 donors; **Fig. 4a**). Expression of the stem cell–associated receptors KIT, FLT3, integrin a_6**.** (CD49F) and PROM (CD133) was similar in $CD38^{-}$ and $CD10^{-}CD62L^{hi}$ populations but was downregulated in $CD10^{+}$ cells; THY1(CD90) had its highest expression on $CD38^{-}$ cells. HLA-DR was upregulated in both $CD10^{-}CD62L^{hi}$ and $CD10^{+}$ progenitor cells (**Fig. 4a**). After 1 week in lymphoid culture, $CD10^{+}$ cells differentiated and lost expression of the adhesion molecule CD34 faster than $CD10^{-}$

$CD62L^{hi}$ cells did (**Fig. 4b**). In addition, $CD10^{-}CD62L^{hi}$ cells were able to generate $CD34^{+}CD10^{+}$ cells *in vitro* (**Fig. 4b**), which suggested that $CD10^{-}CD62L^{hi}$ cells were precursors of the $CD10^{+}$ population.

Principal-component analysis of global gene-expression data from microarray analysis of three different bone marrow samples also placed the $CD10^{-}CD62L^{hi}$ progenitors in an intermediate position between the $CD38^{-}$ HSCs-MPPs and the $CD10^{+}$ progenitor cells (**Fig. 4c**). Gene expression of $CD10^{-}CD62L^{hi}$ progenitor cells clustered hierarchically with $CD38^{-}$ HSCs-MPPs rather than with $CD10^{+}$ progenitors (**Supplementary Fig. 6a**). By pairwise comparison with HSCs-MPPs, similar numbers of genes were upregulated in $CD10^{-}CD62L^{hi}$ and $CD10^{+}$ populations; approximately half of those upregulated genes were common to both progenitor types (**Supplementary Fig. 6b**). More than twice as many genes were downregulated in the $CD10^{+}$ population than were downregulated in the $CD10^{-}CD62L^{hi}$ population, and most downregulated genes in $CD10^{-}CD62L^{hi}$ cells were also downregulated in $CD10^{+}$ cells (**Supplementary Fig. 6b**). Thus, the differentiation of HSCs-MPPs involved many shared molecular pathways but additional transcriptional modulation seemed to occur after the $CD10^{-}CD62L^{hi}$ stage during the generation of $CD10^{+}$ cells.

Downregulation of HSC-associated genes in $CD10^{-}CD62L^{hi}$ cells

We then analyzed by microarray and quantitative PCR the expression patterns of genes known to regulate critical hematopoietic stages of differentiation to delineate the molecular relationships among the $CD38^{-}$, $CD10^{-}CD62L^{hi}$ and $CD10^{+}$ populations. All genes included in the heat maps had a difference in expression of at least twofold ($P < 0.05$ (moderated t-statistics)) and belonged to one of six different expression patterns (clusters 1–6; **Fig. 5a**,**b**). Genes encoding known HSC-related transcription factors (*TAL1*, *GATA2* and *PRDM16*) were significantly downregulated in

both $CD10^{-}CD62L^{hi}$ cells and $CD10^{+}$ cells relative to their expression in the $CD38^{-}$ population (cluster 1, **Fig. 5a**). Genes of the *HOXB* family were also downregulated during the transition from the $CD38^{-}$ HSC-MPP stage to the $CD10^{-}CD62L^{hi}$ LMPP stage with no further significant change at the $CD10^{+}$ stage (cluster 1, **Fig. 5a**). In contrast, expression of genes of the *HOXA* family decreased later in differentiation at the $CD10^{+}$ progenitor stage (clusters 2 and 3, **Fig. 5a**). We noted reciprocal patterns of expression for members of the polycomb repressive complexes PRC1 (encoded by *PCGF2*, *PHC2,* and *SCML4*; cluster 1, **Fig. 5a**) and PRC2 (encoded by *SUZ12*, *EZH2* and *EED*; cluster 5, **Fig. 5a**)[24]. These analyses showed a highly coordinated program of transcriptional regulation as HSC lost multipotency, became lymphoid primed and then committed to B lymphopoiesis.

Lymphoid differentiation stages of CD10-$CD62L^{hi}$ and $CD10^{+}$ cells

Analysis of genes upregulated only in the $CD10^{-}CD62L^{hi}$ population (cluster 4, **Fig. 5b**) showed a profile consistent with the dual lymphoid and monocyte potential of this population. Specifically, genes associated with T cell and NK cell lineages (*CD2* and *CD3E*)[14,25–27] and genes encoding lymphoid cytokine receptors (*IL2RG*, *IL10RA*, *IL10RB*, *IL17RA* and *IFNGR1*) were upregulated, as were myeloid-associated genes (*MPO*, *CSF1R* and *CSF2R*; **Fig. 5b**). Consistent with the cell surface expression , *FLT3* was expressed in both HSCs-MPPs and $CD10^{-}CD62L^{hi}$ cells but not in $CD10^{+}$ cells (cluster 3; **Fig. 5b**). Consistent with the B cell–skewed differentiation potential of the $CD10^{+}$ population, genes known to be expressed specifically during commitment to the B cell lineage (*EBF1*, *PAX5*, *IL7R*, *CD79A*, *CD79B*, *VPREB1*, *VPREB3*, *CD19*, *CD22*, *CD24* and *CD27*) had high expression in $CD10^{+}$ cells (cluster 6; **Fig. 5a**–**c**). Notably, none of those B cell–specific genes were expressed in either $CD34^{+}CD38^{-}$ cells or $CD10^{-}CD62L^{hi}$ cells.

Detailed analysis by quantitative PCR showed that although expression of genes encoding molecules essential for lymphoid commitment was highest in $CD10^+$ cells, upregulation of certain genes of early lymphoid differentiation began at the $CD10^-CD62L^{hi}$ stage. Expression of *TCF3* (which encodes the transcription factor E2A) increased 2.1-fold during the transition from $CD38^-$ cell to $CD10^-CD62L^{hi}$ cell and increased 4.4-fold in the transition from $CD10^-CD62L^{hi}$ cell to $CD10^+$ cell (**Fig. 5c**). Similarly, *DNTT* expression increased 8.0-fold during the transition from $CD38^-$ cell to $CD10^-CD62L^{hi}$ cell and increased 12.0-fold in the transition from $CD10^-CD62L^{hi}$ cell to $CD10^+$ cell (**Fig. 5c**). In contrast, *RAG1* expression was limited to $CD10^+$ cells (**Fig. 5c**), which demonstrated that the mechanisms of DNA rearrangement for genes encoding T cell antigen receptors and immunoglobulins were not fully initiated in the $CD10^-CD62L^{hi}$ population.

To investigate further the degree of heterogeneity of the three populations, we assayed the expression of key genes in single cells (**Fig. 5d**). These analyses showed that the HSC genes *TAL1* (which encodes the transcription factor SCL (TAL1)) and *MPL* (which encodes the thrombopoietin receptor) were expressed exclusively in $CD38^-$ cells, and expression of *RAG1* and *PAX5* (which encodes the transcription factor PAX5) was limited to $CD10^+$ cells. We detected expression of *TCF3* in a similar percentage of $CD10^-CD62L^{hi}$ and $CD10^+$ cells. Detectable *FLT3* expression in single cells was limited almost exclusively to the $CD10^-CD62L^{hi}$ population (**Fig. 5d**). Thus, the $CD38^-$ HSC-MPP, $CD10^-CD62L^{hi}$ and $CD10^+$ populations had distinct molecular profiles, consistent with their functional 'readout' *in vitro*. Whereas the $CD10^+$ population was committed to B lymphopoiesis, the $CD10^-CD62L^{hi}$ population included cells with evidence of early lymphoid priming but no expression of genes associated with commitment to the B cell lineage (**Supplementary Fig. 7**).

CD62L and ligand expression in human thymus

We analyzed by flow cytometry and gene expression the coexpression of receptor-ligand pairs that have been reported before in mouse studies as being important in the homing of cells to and settling of cells in the thymus[28–30]. The chemokine receptor CXCR4 was expressed at similar abundance in $CD10^{-}CD62L^{hi}$ and $CD10^{+}$ populations (**Fig. 6a**). However PSGL-1, the ligand for P-selectin, and the activation and memory marker CD44, both had higher expression in $CD10^{-}$ $CD62L^{hi}$ cells than in $CD10^{+}$ cells (**Fig. 6a**). In addition, the gene encoding the chemokine receptor CCR7, which is expressed on mouse early thymic progenitors and mediates the migration of early thymocytes[28–30], was significantly upregulated in the $CD10^{-}CD62L^{hi}$ population relative to its expression in either $CD10^{+}$ cells or the $CD38^{-}$ population (**Fig. 6b**). We noted no consistent differences between the populations in their expression of the chemokine CCR9 (data not shown).

We next examined the expression of CD62L in progenitor populations from human thymus. CD62L expression was higher in $CD34^{+}$ thymic progenitors than in the more mature $CD34^{-}$ thymocytes (which represent >95% of all thymocytes; **Fig. 6c**). After further delineation of the $CD34^{+}$ thymocyte population, we found that most CD62L-expressing cells were in the $CD34^{+}CD1a^{-}$ subset rather than in the more mature $CD34^{+}CD1a^{+}$ subset (**Fig. 6c**). MECA-79 detects a carbohydrate epitope found on the family of CD62L ligands known as 'peripheral node addressins'[31]. We detected staining of MECA-79 in the thymic vasculature specifically in a subset of P-selectin-positive endothelial cells at the cortico-medullary junction of the thymus, the site of entry of marrow-derived precursors into the thymus (**Fig. 6d–j**), which suggested a possible role for L-selectin in homing to the human thymus.

DISCUSSION

Our studies presented here have demonstrated that 'lymphoid priming' in human bone marrow begins before the onset of CD10 expression in a subset of $CD34^+$ progenitors with high expression of the homing molecule CD62L. Several pieces of evidence indicated that the $CD10^-$ $CD62L^{hi}$ population was a precursor of the more B cell–restricted, $CD10^+$ stage of lymphopoiesis. First, it is widely assumed that all human B cell differentiation passes through a $CD10^+$ progenitor stage, and cultures initiated with $CD10^-CD62L^{hi}$ cells were able to generate $CD10^+$ progenitors before differentiating into $CD19^+$ B cells. In addition, although the $CD10^-$ $CD62L^{hi}$ population had greater NK potential, the number of B cells generated in culture was at least equivalent to that generated in cultures of $CD10^+$ cells. Patterns of the expression of genes and cell-surface antigens were also consistent with a model that positions the $CD10^-CD62L^{hi}$ population before CD10 expression.

A published study has described a $CD10^+$ subset in the $CD34^+CD38^{neg–lo}$ population with lymphoid, monocytic and dendritic cell potential but no erythroid potential[21]. However, this $CD10^+$ 'multilymphoid progenitor' (MLP) also expressed the B cell–specific gene *PAX5*. Notably, the strategy for the isolation of these MLP included cells with intermediate expression of CD38, similar to expression in the $CD10^-CD62L^{hi}$ population and higher than that in the most primitive HSC fraction. We propose that lymphoid priming begins with upregulation of CD38 (relative to its expression in HSCs) and that B cell commitment is initiated with the onset of CD10 expression and further upregulation of CD38 expression.

Most human hematopoietic studies have used umbilical cord blood (UCB), largely because this source of human cells is more readily accessible than is bone marrow. Bone marrow progenitors have a much lower proliferative output than their immunophenotypic homologs in

UCB [7,17,32–34] or than HSCs from either source [35], which makes *in vivo* assessment of rare, non–self-renewing bone marrow progenitor populations difficult and sometimes unfeasible. However, UCB does not represent steady-state postnatal hematopoiesis, and substantial differences between progenitors from UCB and bone marrow are known to exist in terms of immunophenotype and function[6]. Notably, the functional and molecular profiles of $CD10^-$ $CD62L^{hi}$ bone marrow progenitors (which do not express CD7) are similar to those of $CD34^+CD38^-CD7^+$ UCB progenitors[20]. Moreover, the $CD10^-CD62L^{hi}$ immunophenotype described here is less reliable for the identification of a pure lymphoid-primed population in UCB than in bone marrow; a distinct $CD62L^{hi}$ population is difficult to detect in UCB, and $CD34^+Lin^-CD10^-CD45RA^+CD62L^+$ cell populations in UCB include small but readily detectable numbers of CFU-C (Q-L.H. and G.M.C., unpublished data). The differences in lineage potentials of cells with similar immunophenotypes in UCB and bone marrow, as well as the intrinsic functional differences that would be expected between cells that are detected transiently in the postnatal circulation and those that are generated throughout life in the bone marrow microenvironment, highlight the critical need for studies that focus on human bone marrow.

Much elegant data has been generated in mouse studies to both support and challenge the classic idea that the lymphoid and the myelo-erythroid pathways emerge separately from a multipotent progenitor stage[1–4,36]. The 'lymphoid-primed' LMPPs in mouse bone marrow retain full lymphoid and some myeloid potential but have lost erythro-megakaryocytic potential, whereas common lymphoid progenitors (CLPs) represent a more mature, lymphoid-restricted progenitor population. Cell surface expression of Flt3 has been used to isolate LMPPs from a subpopulation of $c\text{-}Kit^+Lin^-Sca\text{-}1^+$ cells in mouse bone marrow[2], and the IL-7 receptor IL-7Ra is

used to define mouse CLPs in the c-Kit^{-}Lin^{-}Sca-1^{lo} population[1]. Given our functional and molecular data, the CD10^{-}CD62L^{hi} human bone marrow progenitor seems most similar to the mouse LMPPs, and the CD10^{+} progenitor is more analogous to the mouse CLPs. However, despite upregulation of *FLT3* at the transcriptional level, the cell-surface expression of FLT3 has not been found to be useful as a marker for discriminating between human HSCs and LMPPs[21] (and reported here). Notably, studies have reported that upregulation of CD62L expression in c-Kit^{+}Lin^{-}Sca-1^{+} mouse bone marrow cells correlates with high expression of Flt3 and loss of erythroid and megakaryocyte potential, which suggests that CD62L expression might be used as an alternative marker for discriminating between mouse multipotent progenitors and LMPPs[14].

The myeloid potential of the CD10^{-}CD62L^{hi} population consisted mostly of monocyte-macrophage and dendritic cells. The absence of clonogenic myeloid-erythroid potential in CFU-C assays suggested that the CD10^{-}CD62L^{hi} population does not represent a precursor to the main myelo-erythroid pathways initiated by common myeloid progenitors and granulocyte-macrophage progenitors. Instead, we favor the proposal that the CD10^{-}CD62L^{hi} cells are 'lymphoid-primed' progenitors that precede CD10 expression and are able to generate limited numbers of monocytes-macrophages and dendritic cells. This type of residual myeloid and dendritic potential has been reported for even more lymphoid-committed progenitors[10,17,21]. A published paper has noted that mouse IL-7Ra^{+} CLPs, despite their complete lack of either CFU activity or *in vivo* myeloid potential, can generate myeloid cells in stromal cocultures, which suggests that myeloid differentiation may be an alternative pathway found in certain *in vitro* conditions[5]. Nonetheless, it is clear that the capacity for myeloid differentiation *in vitro* progressively wanes as lymphoid commitment proceeds and that this residual, mostly monocytic, potential is retained after erythroid potential is lost.

We note both differences and similarities between the $CD10^{-}CD62L^{hi}$ cells and the mouse LMPPs in their gene expression[2,36]. In both mouse LMPPs and human $CD10^{-}CD62L^{hi}$ cells, genes encoding the transcription factor TAL-1 and the cytokine receptor MPL are substantially downregulated relative to their expression in HSCs, whereas *KIT* expression is retained[36,37]. Expression of the gene encoding E2A, which is essential for the development of mouse LMPPs[38], is also upregulated during generation of the $CD10^{-}CD62L^{hi}$ population from HSCs-MPPs, but B cell–specific genes such as *EBF1* and *PAX5* are not. In contrast, components of the molecular machinery required for DNA recombination seem to have high expression in mouse LMPPs[36], but in our human studies, *RAG1* and *RAG2* were expressed at the $CD10^{+}$ stage and *DNTT* expression was significantly higher in $CD10^{+}$ cells than in $CD10^{-}CD62L^{hi}$ cells.

The identification of a lymphoid-primed precursor prior to the previously reported $CD10^{+}$ 'CLP'[10] raises the question of whether $CD10^{-}CD62L^{hi}$ cells are recruited to the thymus to initiate T cell differentiation. Controversy about the identity of precursors that seed the mouse thymus has continued for over a decade, and it seems likely that more than one type of bone marrow progenitor may be able to initiate thymopoiesis. Experimental restrictions make it impossible to definitively prove the identity of the bone marrow precursors that normally seed the human thymus. The $CD10^{+}CD24^{-}$ population in bone marrow probably represents a lymphoid progenitor that seeds the human thymus, given the finding of a similar immunophenotypic subset among human thymocytes[12]. The thymocyte data presented here have provided evidence that the $CD10^{-}CD62L^{hi}$ cells may be an additional or alternative thymic precursor population. It should be noted that although CD62L expression was highest on $CD34^{+}CD1a^{-}$ progenitors, $CD10^{-}CD62L^{hi}$ bone marrow cells are not precursors of the most primitive ($CD7^{-}$) subset of $CD34^{+}CD1a^{-}$ thymocytes. $CD34^{+}CD1a^{-}CD7^{-}$ thymocytes have high myeloid and erythroid

potential in clonogenic assays[39] and do not express CD62L. It is not clear at this time whether CD62L becomes upregulated as $CD34^+CD1a^-CD7^-$ MPPs differentiate into $CD34^+CD1a^-CD7^+$ thymocytes or whether CD7 is rapidly upregulated when $CD7^-CD62L^{hi}$ LMPPs engage with the thymic microenvironment. PSGL-1–P-selectin interactions are critical mediators of homing to mouse thymus[40]. As PSGL-1 had abundant expression on both HSC-MPP and $CD10^-CD62L^{hi}$ bone marrow cells, it is possible that homing to human thymus involves the same mechanism. However, the high expression of L-selectin in the primitive $CD34^+CD1a^-$ thymocyte population and the endothelial expression of L-selectin ligands in the human thymus, specifically in the cortico-medullary region, raises the possibility that in addition to being involved in the homing of lymphocytes to peripheral lymphoid organs, L-selectin may have a role in progenitor homing to human thymus. We have noted expression of CD62L in a subset of $CD34^+Lin^-CD10^-$ cells (but not $CD34^+CD10^+$ cells) in mobilized peripheral blood (data not shown), but the physiological relevance and lineage potential of this mobilized population is as yet unclear. Of note, although interactions with L-selectin have not been described in homing to mouse thymus, CD62L expression has been used to identify a population of mouse bone marrow progenitors that efficiently and rapidly reconstitute the mouse thymus after transplantation[15,16], and a population of $c\text{-}Kit^+Lin^-Sca\text{-}1^+CD62L^+$ $RAG\text{-}1^-$ progenitors is found in both mouse bone marrow and mouse thymus[16].

The reliance on CD10 expression as a marker of lymphoid commitment in previous studies of hematopoietic progenitors in human bone marrow has until now meant that states of differentiation could be compared only between multipotent progenitors and progenitors committed to the B cell lineage. The identification of a progenitor in human bone marrow primed for full lymphoid differentiation, and before B cell commitment, will now permit delineation of

the molecular regulation of the first stages of lymphoid commitment in human hematopoiesis. It will also allow understanding of how these processes are affected during aberrant hematopoiesis in disease states.

METHODS

Methods and any associated references are available in the online version of the paper.

Accession codes. GEO: microarray data, GSE35685.

Note: Supplementary information is available in the online version of the paper.

ACKNOWLEDGMENTS

We thank J. Scholes, F. Codrea, X. Li, and S. Dandekar ; and D. Kohn, G. Dravid, S. Sandoval and M. Corselli for advice on the manuscript. Supported by the US National Institutes of Health (P01 HL073104 and RO1 HL077912),and the California Institute of Regenerative Medicine (RC1-00108 and RM1-01717 to G.M.C.; and RN1-00557-1 to H.K.A.M.), the UCLA Broad Stem Cell Research Center Flow Cytometry Core Resource, the UCLA Genotyping and Sequencing Core, and the UCLA Jonsson Comprehensive Cancer Center Genomics Shared Resource.

AUTHOR CONTRIBUTIONS

L.A.K. designed, did and analyzed experiments and wrote the paper; Q.-L.H. designed, did and analyzed experiments, R.S. did bioinformatics analysis of microarray data; S.G. and Y.Z. assisted in experiments; C.P. did experiments; H.K.A.M. supervised bioinformatics analysis; and G.M.C. designed and analyzed experiments and wrote the paper.

COMPETING FINANCIAL INTERESTS

The authors declare no competing financial interests.

Published online at http://www.nature.com/doifinder/10.1038/ni.2378.

<jrn>1. Kondo, M., Weissman, I.L. & Akashi, K. Identification of clonogenic common lymphoid progenitors in mouse bone marrow. *Cell* **91**, 661–672 (1997).</jrn>

<jrn>2. Adolfsson, J. *et al.* Identification of Flt3+ lympho-myeloid stem cells lacking erythro-megakaryocytic potential a revised road map for adult blood lineage commitment. *Cell* **121**, 295–306 (2005).</jrn>

<jrn>3. Forsberg, E.C., Serwold, T., Kogan, S., Weissman, I.L. & Passegue, E. New evidence supporting megakaryocyte-erythrocyte potential of flk2/flt3^{+} multipotent hematopoietic progenitors. *Cell* **126**, 415–426 (2006).</jrn>

<jrn>4. Schlenner, S.M. & Rodewald, H.R. Early T cell development and the pitfalls of potential. *Trends Immunol.* **31**, 303–310 (2010).</jrn>

<jrn>5. Richie Ehrlich, L.I., Serwold, T. & Weissman, I.L. In vitro assays misrepresent in vivo lineage potentials of murine lymphoid progenitors. *Blood* **117**, 2618–2624 (2011).</jrn>

<jrn>6. Payne, K.J. & Crooks, G.M. Immune-cell lineage commitment: translation from mice to humans. *Immunity* **26**, 674–677 (2007).</jrn>

<jrn>7. Rossi, M.I. *et al.* B lymphopoiesis is active throughout human life, but there are developmental age-related changes. *Blood* **101**, 576–584 (2003).</jrn>

<jrn>8. Mold, J.E. *et al.* Fetal and adult hematopoietic stem cells give rise to distinct T cell lineages in humans. *Science* **330**, 1695–1699 (2010).</jrn>

<jrn>9. Leavy, O. Haematopoiesis: Baby tolerance. *Nat. Rev. Immunol.* **11**, 78 (2011).</jrn>

<jrn>10. Galy, A., Travis, M., Cen, D., Chen, B. & Human, T. B, natural killer, and dendritic cells arise from a common bone marrow progenitor cell subset. *Immunity* **3**, 459–473 (1995).</jrn>

<jrn>11. Ichii, M. *et al.* The density of CD10 corresponds to commitment and progression in the human B lymphoid lineage. *PLoS ONE* **5**, e12954 (2010).</jrn>

<jrn>12. Six, E.M. *et al.* A human postnatal lymphoid progenitor capable of circulating and seeding the thymus. *J. Exp. Med.* **204**, 3085–3093 (2007).</jrn>

<jrn>13. Rosen, S.D. Ligands for L-selectin: homing, inflammation, and beyond. *Annu. Rev. Immunol.* **22**, 129–156 (2004).</jrn>

<jrn>14. Cho, S. & Spangrude, G.J. Enrichment of functionally distinct mouse hematopoietic progenitor cell populations using CD62L. *J. Immunol.* **187**, 5203–5210 (2011).</jrn>

<jrn>15. Perry, S.S. *et al.* L-selectin defines a bone marrow analog to the thymic early T-lineage progenitor. *Blood* **103**, 2990–2996 (2004).</jrn>

<jrn>16. Perry, S.S., Welner, R.S., Kouro, T., Kincade, P.W. & Sun, X.H. Primitive lymphoid progenitors in bone marrow with T lineage reconstituting potential. *J. Immunol.* **177**, 2880–2887 (2006).</jrn>

<jrn>17. Hao, Q.L. *et al.* Identification of a novel, human multilymphoid progenitor in cord blood. *Blood* **97**, 3683–3690 (2001).</jrn>

<jrn>18. Storms, R.W., Goodell, M.A., Fisher, A., Mulligan, R.C. & Smith, C. Hoechst dye efflux reveals a novel $CD7^{+}CD34^{-}$ lymphoid progenitor in human umbilical cord blood. *Blood* **96**, 2125–2133 (2000).</jrn>

<jrn>19. Haddad, R. *et al.* Molecular characterization of early human T/NK and B-lymphoid progenitor cells in umbilical cord blood. *Blood* **104**, 3918–3926 (2004).</jrn>

<jrn>20. Hoebeke, I. *et al.* T-, B- and NK-lymphoid, but not myeloid cells arise from human $CD34^{+}CD38^{-}CD7^{+}$ common lymphoid progenitors expressing lymphoid-specific genes. *Leukemia* **21**, 311–319 (2007).</jrn>

<jrn>21. Doulatov, S. *et al.* Revised map of the human progenitor hierarchy shows the origin of macrophages and dendritic cells in early lymphoid development. *Nat. Immunol.* **11**, 585–593 (2010).</jrn>

<jrn>22. Manz, M.G., Miyamoto, T., Akashi, K. & Weissman, I.L. Prospective isolation of human clonogenic common myeloid progenitors. *Proc. Natl. Acad. Sci. USA* **99**, 11872–11877 (2002).</jrn>

<jrn>23. La Motte-Mohs, R.N., Herer, E. & Zuniga-Pflucker, J.C. Induction of T-cell development from human cord blood hematopoietic stem cells by Delta-like 1 in vitro. *Blood* **105**, 1431–1439 (2005).</jrn>

<jrn>24. Majewski, I.J. *et al.* Opposing roles of polycomb repressive complexes in hematopoietic stem and progenitor cells. *Blood* **116**, 731–739 (2010).</jrn>

<jrn>25. Blom, B. & Spits, H. Development of human lymphoid cells. *Annu. Rev. Immunol.* **24**, 287–320 (2006).</jrn>

<jrn>26. Biassoni, R., Ferrini, S., Prigione, I., Moretta, A. & Long, E.O. CD3-negative lymphokine-activated cytotoxic cells express the CD3 epsilon gene. *J. Immunol.* **140**, 1685–1689 (1988).</jrn>

<jrn>27. Lanier, L.L., Chang, C., Spits, H. & Phillips, J.H. Expression of cytoplasmic CD3 epsilon proteins in activated human adult natural killer (NK) cells and CD3 g, d, e complexes in fetal NK cells. Implications for the relationship of NK and T lymphocytes. *J. Immunol.* **149**, 1876–1880 (1992).</jrn>

<jrn>28. Misslitz, A. *et al.* Thymic T cell development and progenitor localization depend on CCR7. *J. Exp. Med.* **200**, 481–491 (2004).</jrn>

<jrn>29. Krueger, A., Willenzon, S., Lyszkiewicz, M., Kremmer, E. & Forster, R. CC chemokine receptor 7 and 9 double-deficient hematopoietic progenitors are severely impaired in seeding the adult thymus. *Blood* **115**, 1906–1912 (2010).</jrn>

<jrn>30. Zlotoff, D.A. *et al.* CCR7 and CCR9 together recruit hematopoietic progenitors to the adult thymus. *Blood* **115**, 1897–1905 (2010).</jrn>

<jrn>31. Streeter, P.R., Rouse, B.T. & Butcher, E.C. Immunohistologic and functional characterization of a vascular addressin involved in lymphocyte homing into peripheral lymph nodes. *J. Cell Biol.* **107**, 1853–1862 (1988).</jrn>

<jrn>32. Arakawa-Hoyt, J. *et al.* The number and generative capacity of human B lymphocyte progenitors, measured in vitro and in vivo, is higher in umbilical cord blood than in adult or pediatric bone marrow. *Bone Marrow Transplant.* **24**, 1167–1176 (1999).</jrn>

<jrn>33. Kim, D.K. *et al.* Comparison of hematopoietic activities of human bone marrow and umbilical cord blood CD34 positive and negative cells. *Stem Cells* **17**, 286–294 (1999).</jrn>

<jrn>34. De Smedt, M. *et al.* T-lymphoid differentiation potential measured in vitro is higher in CD34+CD38-/lo hematopoietic stem cells from umbilical cord blood than from bone marrow and is an intrinsic property of the cells. *Haematologica* **96**, 646–654 (2011).</jrn>

<jrn>35. Bhatia, M., Wang, J.C., Kapp, U., Bonnet, D. & Dick, J.E. Purification of primitive human hematopoietic cells capable of repopulating immune-deficient mice. *Proc. Natl. Acad. Sci. USA* **94**, 5320–5325 (1997).</jrn>

<jrn>36. Månsson, R. *et al.* Molecular evidence for hierarchical transcriptional lineage priming in fetal and adult stem cells and multipotent progenitors. *Immunity* **26**, 407–419 (2007).</jrn>

<jrn>37. Luc, S. *et al.* Down-regulation of Mpl marks the transition to lymphoid-primed multipotent progenitors with gradual loss of granulocyte-monocyte potential. *Blood* **111**, 3424–3434 (2008).</jrn>

<jrn>38. Dias, S., Mansson, R., Gurbuxani, S., Sigvardsson, M. & Kee, B.L. E2A proteins promote development of lymphoid-primed multipotent progenitors. *Immunity* **29**, 217–227 (2008).</jrn>

<jrn>39. Hao, Q.L. *et al.* Human intrathymic lineage commitment is marked by differential CD7 expression: identification of CD7- lympho-myeloid thymic progenitors. *Blood* **111**, 1318–1326 (2008).</jrn>

<jrn>40. Rossi, F.M. *et al.* Recruitment of adult thymic progenitors is regulated by P-selectin and its ligand PSGL-1. *Nat. Immunol.* **6**, 626–634 (2005).</jrn>

Figure 1 Identification of bone marrow progenitors that lack myeloid and erythroid clonogenic potential. (**a**) Expression of CD10 and CD7 on $CD34^{+}Lin^{-}$ bone marrow cells. Numbers in (or adjacent to) outlined areas indicate percent cells in each throughout. (**b**) Methylcellulose CFU-C assay of the myeloid and erythroid clonogenic output of various $CD34^{+}$ Lin^{-} subsets. BFU-E, burst-forming unit, erythroid; GM, granulocyte-macrophage; GEMM, granulocyte-erythrocyte-monocyte-macrophage. Total, $n = 4$; $CD10^{-}CD7^{-}$ and $CD10^{-}CD7^{+}$, $n = 2$; $CD10^{+}$, $n = 5$, all n's refer to independent bone marrow samples. (**c**) Strategy for the isolation of $CD34^{+}Lin^{-}$ $CD45RA^{+}10^{+}$ ($CD10^{+}$) cells and $CD34^{+}Lin^{-}CD45RA^{+}CD10^{-}CD62L^{hi}$ ($CD10^{-}CD62L^{hi}$) cells by flow cytometry (representative of $n > 30$ independent bone marrow samples; for full gating strategy see **Supplementary Fig 2** (**d**) Myeloid and erythroid clonogenic capacity of various $CD34^{+}Lin^{-}$ subsets (For number of independent bone marrow samples assayed, and t-test of CFU-C in $CD10^{-}CD62L^{hi}$ relative to all other populations shown, see **Supplementary Table 1a**,**b**). IL-$3R^{lo}CD45RA^{-}$, common myeloid progenitor; IL-$3R^{-}CD45RA^{-}$, megakarocytic-erythroid progenitor; $IL3R^{lo}$ $CD45RA^{+}$, granulocyte-macrophage progenitor. (**e**) CD62L expression on subsets of the $CD34^{+}Lin^{-}$ populations. (**f**) Expression of CD62L and CD7 on gated $CD34^{+}Lin^{-}CD10^{-}$ cells, assessed by flow cytometry. Numbers in quadrants indicate percent cells in each throughout. $*P < 0.05$, $**P < 0.01$ and $***P < 0.001$. (t-tests). Data are representative of seven independent experiments (**a**), five independent experiments (**b**), thirty experiments with over thirty independent bone marrow samples (**c**), nine independent experiments (**d**), thirty experiments with over thirty independent bone marrow samples (**e**), three independent experiments with three independent bone marrow samples (**f**); error bars (**b**,**d**), s.e.m.

Figure 2 Lympho-myeloid potential of bone marrow progenitors. (**a**) Expression of CD19 (B cells) and CD56 (NK cells) from $CD34^+Lin^-$ cells cultured for 4 weeks in B cell-NK cell lymphoid conditions (on OP9 stromal cells with KIT ligand (KL), FLT3 ligand (FL) and thrombopoietin), initiated with $CD10^-CD62L^{hi}$ cells (left) or $CD10^+$ cells (right), assessed by flow cytometry. (**b**) Cell output of $CD34^+Lin^-$ populations in B cell–NK cell lymphoid cultures initiated with $CD10^-CD62L^{hi}$ or $CD10^+$ cells (key), presented relative to cell number at day 0. (**c**,**d**) Flow cytometry of $CD34^+Lin^-$ cells cultured for 4–8 weeks in T cell conditions (on OP9 stromal cells expressing the Notch ligand DLL1, in the presence of KL, FL and IL-7), initiated with $CD10^-CD62L^{hi}$ cells (top row, **c**; **d**) or $CD10^+$ cells (bottom row, **c**). (**e**) Cell output of bulk cultures of $CD34^+Lin^-$ populations initiated with $CD10^-$ $CD62L^{hi}$ cells or $CD10^+$ cells and cultured in T cell conditions (presented as in **b**). $*P < 0.038$ (1-way ANOVA). (**f**) Cell growth of bone marrow $CD34^+Lin^-$ populations in myelo-erythroid cocultures (OP9 stroma with IL-3, thrombopoietin, KL, erythropoietin and FL) initiated with HSCs ($CD34^+Lin^-$ $CD38^-$), $CD10^-$ $CD62L^{hi}$ cells or $CD10^+$ cells (presented as in **b**). $*P < 0.0001$, for $CD38^-$ versus $CD10^-CD62L^{hi}$ or $CD10^+$, or $*P = 0.49$ for $CD10^-CD62L^{hi}$ versus $CD10^+$ (1-way ANOVA). Data are from one representative of ten independent experiments (**a**), one representative of ten independent experiments (**b**), one representative of six experiments (**c**) one representative of three experiments (**d**) or are from six experiments (**e**), or three independent experiments (**f**; error bars (**e**,**f**), s.e.m.).

Figure 3 Lineage potential of $CD10^-$ $CD62L^{hi}$ cells by *in vitro* clonal analysis and *in vivo* transplantation studies. (**a**,**b**) Limiting dilution analysis of $CD10^-CD62L^{hi}$ cells grown in B cell–NK cell conditions (**a**) or T cell conditions (**b**), presented as frequency of wells lacking B cells–NK cells ($B\text{-}NK^-$ wells) or T cells (T^- wells). (**c**) Lineage analysis of clones from single $CD10^-$

$CD62L^{hi}$ or $CD10^{+}$ cells in B cell–NK cell lymphoid coculture, presented as frequency of wells with clonal growth containing NK cells (NK), B cells (B) or both (B & NK). (**d**) Flow cytometry of clones generated in B cell–NK cell conditions from one to three $CD10^{-}CD62L^{hi}$ cells showing NK cell potential ($CD56^{+}$), myeloid potential ($CD14^{+}CD15^{+}$) and dendritic cell potential ($CD1a^{+}$) of one clone (far left and middle left); B cell potential ($CD19^{+}$) and dendritic cell potential ($CD1a^{+}$; middle right); or coexpression of myeloid and dendritic cell markers from a single-cell clone (far right). (**e**) Flow cytometry of a single clone generated in T cell conditions showing T cell potential ($CD4^{+}CD8^{+}$) and myeloid potential ($CD4^{dim}CD14^{+}CD15^{+}$). (**f**) Flow cytometry of bone marrow from a mouse of the NSG strain, analyzed 2 weeks after transplantation of 1×10^{5} irradiated $CD34^{-}$ carrier cells only (negative control; left) or 3×10^{4} $CD34^{+}Lin^{-}CD10^{-}CD62L^{hi}$ cells (center) or 1.5×10^{5} $CD34^{+}Lin^{-}$ cells (right), showing human engraftment (top row; cells positive for HLA class 1 and human CD45), B cells ($CD19^{+}$) and myeloid cells (CD14, CD15, & $CD33^{+}$) from gated human cells (middle row), and back-gating of B cells and myeloid cells from plots above (bottom row). SSC, side scatter; FSC, forward scatter. (**g**) Frequency of human myeloid cells and human B cells among the total human cells in **f**. Each symbol represents an individual mouse; small horizontal lines indicate the mean. Data are from three experiments (**a**,**b**; error bars, s.e.m.) three experiments (**c**), three experiments (**d**),three experiments (**e**), one experiment (**f**) or one experiment with three mice per group (**g**).

Figure 4 $CD10^{-}CD62L^{hi}$ cells represent an intermediate stage of differentiation between HSCs and $CD10^{+}$ progenitors. (**a**) Expression of key cell-surface markers on various $CD34^{+}Lin^{-}$ populations (key), assessed by flow cytometry (top row, left; bottom row), and summary of those results (top right), presented as mean florescence intensity (MFI). $*P < 0.010$ and $**P < 0.001$ (t-tests). (**b**) Flow cytometry of B cell–NK cell lymphoid cultures initiated with $CD38^{-}$, $CD10^{-}$

$CD62L^{hi}$ or $CD10^{+}$ cells and assessed at 1 week. (**c**) Unsupervised whole-genome principal-component analysis of $CD38^{-}$, $CD10^{-}CD62L^{hi}$ or $CD10^{+}$ populations from human bone marrow. Data are from eighteen experiments with two or three independent samples per marker (or 14 samples for CD38; **a**), two independent experiments (**b**) orthree experiments with three independent bone marrow samples (**c**).

Figure 5 $CD10^{-}CD62L^{hi}$ cells represent a distinct progenitor population with a unique expression profile that combines HSC and early lymphoid cell genes. (**a**) Expression of genes encoding transcription factors (**a**) or cytoplasmic and cell-surface molecules (**b**) with a difference in expression of more than twofold by pair-wise comparison ($P < 0.05$) and defined as follows based on statistical analysis (not heat-map appearance): cluster 1, upregulated only in $CD38^{-}$ cells relative to two other equivalent populations ($CD38^{-} > (CD10^{-}CD62L^{hi} = CD10^{+})$; cluster 2, $CD38^{-} > CD62L^{hi} > CD10^{+}$; cluster 3, $(CD38^{-} = CD10^{-}CD62L^{hi}) > CD10^{+}$; cluster 4, $CD10^{-}CD62L^{hi} > (CD38^{-} = CD10^{+})$; cluster 5, $(CD10^{-}CD62L^{hi} = CD10^{+}) > CD38^{-}$; cluster 6, $CD10^{+} > (CD10^{-}CD62L^{hi} = CD38^{-})$. (**c**) Quantitative PCR analysis of selected genes, presented relative to expression in $CD10^{-}CD62L^{hi}$ cells. *P £ 0.050, **$P < 0.010$ and ***$P < 0.001$ (1-way ANOVA). (**d**) Quantitative PCR analysis of selected genes in single cells, presented as the frequency of single cells expressing the gene. Data are representative of three independent experiments (**a**,**b**),three experiments with three biological replicates (**c**; mean and s.e.m.) or one experiment with 13 cells assayed per gene (**d**).

Figure 6 High CD62L expression and progenitor recruitment **[Author: Of what? Revised]** to human thymus. (**a**) Expression of homing molecules on $CD10^{-}CD62L^{hi}$ cells and $CD10^{+}$ cells, assessed by flow cytometry (gated as $CD34^{+}Lin^{-}$). (**b**) Quantitative PCR analysis of *CCR7* gene expression in $CD38^{-}$, $CD10^{-}CD62L^{hi}$ and $CD10^{+}$ cells. *P £ 0.05 ().(**c**) CD62L expression in

human $CD34^+$ or $CD34^-$ thymocytes (top) and $CD34^+CD1A^+$ and $CD34^+CD1A^-$ thymocytes (bottom), assessed by flow cytometry. (**d**) Chromagen immunohistochemistry showing MECA-79 staining at the cortico-medullary junction of the thymus. Scale bars, 200 mm. (**e**–**g**) Fluorescence immunohistochemistry of region as in **d** showing costaining of MECA-79 (**e**) with blood vessels positive for vascular endothelial cadherin (VE-cadherin (CD144); **f**) and a merged image (**g**). Scale bars, 100 mm. (**h**–**j**) Fluorescence immunohistochemistry showing costaining of MECA-79 (**h**) in a subset of P-selectin–positive blood vessels (**i**) at the cortico-medullary junction of the thymus, and a merged image (**j**). Scale bars, 100 mm. Data are representative of three experiments with three biological replicates (**a**), three experiments with three biological replicates (**b**; mean and s.e.m.), three experiments with three biological replicates (**c**), one experiment (**d**–**j**).

ONLINE METHODS

Isolation of bone marrow cells.

Normal human bone marrow and thymic cells were obtained from healthy donors via the Pathology Tissue Core of the University of California, Los Angeles, Cincinnati Children's Hospital, or AllCells according to guidelines approved by Institutional Review Board of the University of California, Los Angeles. Samples were enriched for $CD34^+$ cells by the magnetic-activated cell-sorting (MACS) system (Miltenyi Biotec).

Samples enriched for $CD34^+$ cells were incubated with combinations of monoclonal antibodies specific for human molecules (allophycocyanin-indotricarbocyanine–conjugated antibody to (anti-CD34; 581; (Biolegend), phycoerythrin-indodicarbocyanine–anti-CD45RA (HI100), allophycocyanin–anti-CD38 (HIT2), phycoerythrin-indotricarbocyanine–anti-CD10

(HI10a), phycoerythrin–anti-CD62L (DREG-56), phycoerythrin– or phycoerythrin-indodicarbocyanine–anti-CD7 (M-T701) and fluorescein isothiocyanate–labeled lineage-depletion antibodies anti-CD3 (SK7), anti-CD14 (M2E2), anti-CD19 (4G7), anti-CD56 (MY31) and anti-CD235a (GA-R2; all from Becton Dickinson). The DNA-intercalating dye DAPI (4',6-diamidino-2-phenylindole) was added for analysis of viability. A 'no-antibody' control defined negative gates. Additional analyses used the following antibodies: Alexa Fluor 647–anti-CD127 (HIL-7R-M21), allophycocyanin–anti-CD117 (YB5.B8), allophycocyanin–anti-CD184 (anti-CXCR4; 12G5), allophycocyanin–anti-PSGL-1 (anti-CD162 or anti-SELPLG; KPL-1), phycoerythrin–anti-Flt3 (anti-CD135; 4G8), allophycocyanin–anti-CD44 (G44-26), allophycocyanin–anti-CD62L (DREG-56), phycoerythrin-indodicarbocyanine–anti-CD90 (5E10) and phycoerythrin–anti-HLA-DR (L234; all from BD). Cells were isolated on a FACSAria (355-, 405-, 488-, 561- and 633-nm lasers; BD Immunocytometry Systems).

B cell–NK cell lymphoid cultures.

Cells isolated by flow cytometry were plated in bulk on OP9 stroma in 48-well plates or as single cells or by limiting dilution on OP9 or MS5 stroma in 96-well plates with an automated cell-deposition unit. Cells were cultured in lymphoid medium (RPMI-1640 medium (Irvine Scientific) with 5% FCS (Biowhittaker), 50 mM 2-mercaptoethanol (Sigma), penicillin-streptomycin, L-glutamine (Gemini Bio Products)) with IL-7 (5 ng/ml), Flt3 ligand (5 ng/ml) and thrombopoietin (5 ng/ml), with or without IL-3 (5 ng/ml) for first 3–5 of culture (cytokines from R&D Systems). Clones were recorded as being positive if they included more than 100 cells. Cloning efficiency of single cells was defined as follows: (positive wells / total wells) × 100 (limiting-dilution plating information, **Supplementary Table 2**

T cell lymphoid cultures.

Cells were plated in bulk on 6-well or 96-well plates or as single cells or by limiting dilution (with an automated cell-deposition unit) on established OP9 stroma expressing the Notch ligand DL1 in lymphoid medium with IL-7 (5 ng/ml), Flt3 ligand (5 ng/ml) and stem-cell factor (1 ng/ml; R&D Systems)[41].

Myelo-erythroid cultures and CFU assay.

Populations were plated on OP9 stroma in DMEM with 10% FBS, with IL-3 (5 ng/ml), Flt3 ligand (5 ng/ml), stem-cell factor (5 ng/ml), thrombopoietin (50 ng/ml) and erythropoietin (4 U/ml; R&D Systems). CFU assays were done as described[39].

Lineage-specific analysis.

Cells were collected from transplanted mice and cultured, then were stained with the following human-specific monoclonal antibodies (alls from BD): anti-CD45 (HI30; for all human hematopoietic cells); anti-HLA-A, HLA-B and HLA-C (G46-2.6; for all human cells); anti-CD19 (4G7 and SJ25C1; for B lymphoid cells); anti-CD56 (MY31; for NK cells); anti-CD209 (DCN46; for dendritic cells); anti-CD1A (HI149), anti-CD3 (SK7), anti-CD4 (RPA-T4), anti-CD7(M-T701), anti-CD8 (RPA-T8) and anti-TCRab (WT31), for T lymphoid cells); anti-CD235a (GA-R2; for erythroid cells); anti-CD14 (M5E2) and anti-CD11B (ICRF44), for monocytic cells); anti-CD14 (M5E2), anti-CD15 (W6D3) and anti-CD33 (WM53); for myeloid cells); or anti-CD66B (G10F5; for granulocytic cells). A Fortessa or LSRII (BD) was used for flow cytometry, and data were analyzed with FlowJo software. T cell differentiation was assessed by RT-PCR of human $CD45^+$ cells and mouse $CD29^-$ cells isolated at 4–5 weeks from T cell lymphoid cultures.

***In vivo* studies.**

Adult mice of the NSG strain (Jackson Laboratories) were used for *in vivo* experiments according to protocols approved by the Institutional Animal Care and Use Committee of University of California Los Angeles. Adult NSG mice were irradiated (375 cGy) before intratibial injection of 3×10^4 $CD10^-CD62L^{hi}$ cells ($n = 3$ mice) or 2×10^4 to 15×10^4 $CD34^+Lin^-$ bone marrow cells ($n = 3$ mice), each with 1×10^5 'carrier' cells (irradiated (3,000 cGy) $CD34^-$ UCB cells) and were killed 2 weeks later for analysis by flow cytometry. Total human engraftment was defined as cells positive for HLA-A, HLA-B, HLA-C and human CD45. Negative control mice received only irradiated carrier cells.

Quantitative PCR analysis.

After cell isolation with a FACSAria, RNA was extracted with a Qiagen RNAEsay Microkit (Qiagen) and reverse-transcribed with Omniscript RT, OLIGO DT, and RNAguard (Pharmacia Biotech). An ABI Viia7 was used for real-time PCR with Taqman Mastermix and TaqMan probe–based gene-expression analysis probes, (List of probes, see **Supplementary Table 3**) (Applied Biosystems). Reactions were done in technical and biological triplicates. Nine candidate reference genes were analyzed with geNorm^{plus} software for optimal reference genes[42]. Quantitative PCR results were normalized to the geometric means of results obtained for the reference genes *ACTB* and *B2M* through the use of the change-in-cycling-threshold methods ($\Delta\Delta C_T$).

Single-cell quantitative PCR was done on a Fluidigm Biomark 48.48 gene expression chip with Taqman probes and results were analyzed with Real-Time Software v3.0.2 (Fluidigm)

at the University of California, Los Angeles GeneSeq Core. The gene encoding b_2-microglobulin was used as a positive control for presence of cDNA.

Microarray analysis.

RNA from bone marrow from three different donors was extracted with Microkit (Qiagenand hybridized onto Affymetrix U133 Plus 2.0 Array (Affymetrix). The robust multichip average method[43] was used to obtain normalized expression from the three populations. The Microarray Suite 5 (MAS5) algorithm[44] was used for present, marginal or absent 'calls' for all replicates. Replicate arrays from the three populations were hierarchically clustered with Spearman rank correlation (distance metric) and average linkage (agglomeration) method. Only probe sets considered 'present' by the MAS5 method in all replicates in any of the three populations (24,067 probes) were used for hierarchical clustering. The number of genes with a difference in expression in Venn diagrams was calculated with the R/Bioconductor software[45] package Limma[46] at a *P* value of less than 0.01 and change in threshold of ± twofold. For genes with multiple probe sets, the probe set with the lowest *P* value was chosen. Probe sets not mapped to a gene with an official symbol were excluded. Genes were considered for inclusion in the heat map only if they had a difference in expression of ± twofold and the difference was significant at a *P* value of less than 0.05 relative to expression by the other population of cells in at least one condition (Limma). Gene set enrichment analysis was done as described[47]. For presentation, Cluster 3.0 software (clustering)[48] and Java TreeView software (dendrograms and heat maps)[49] were used.

Immunohistochemistry.

Human thymuses were frozen at –80 °C and embedded in optimum cutting temperature compound (Tissue-Tek) and sections 5 mm in thickness were stained with hematoxylin and eosin. For immunohistochemistry, sections were fixed in 10% neutral buffered formalin, then were incubated with primary antibody (anti-MECA-79 (1:83 dilution; sc-19602; Santa Cruz Biotechnology) and/or anti-VE-cadherin (1:83 dilution; BV6; Chemicon International)), followed by incubation with secondary antibody (anti-rat () and/or anti-mouse horseradish conjugated-peroxidase (Vector). For fluorescence immunohistochemistry, Tyramide Signal Amplification Alexa Fluor 594 and/or Tyramide Signal Amplification Alexa Fluor 488 was applied (Invitrogen Molecular Probes, Cat# T20925, T20912). For chromagen staining, DAB (3,3-diaminobenzidine tetrahydrochloride) was applied, followed by hematoxylin (Jackson Immunoresearch). Sections were viewed with Axioimager with Apotome Imagining System (10×), and images were captured with an Axiocam MRm camera (florescence) or HRc camera (chromagen; Zeiss).

Statistical analysis.

Prism version 5 (GraphPad Software Inc) was used for statistical analysis. The two-way analysis of variance was used for comparison of growth potential. The mean and s.e.m. were calculated for total CFU output of populations, mean fluorescence intensity and quantitative PCR, and the one-way analysis of variance with a Tukey post-test was used for statistical analysis. ELDA software[50] was used for limiting dilution analysis.

<jrn>41. Holmes, R. & Zuniga-Pflucker, J.C. The OP9–DL1 system: generation of T-lymphocytes from embryonic or hematopoietic stem cells in vitro. *Cold Spring Harb. Protoc.* (2009). </jrn>

<jrn>42. Vandesompele, J., *et al.* Accurate normalization of real-time quantitative RT-PCR data by geometric averaging of multiple internal control genes. *Genome Biol* **3**, XX–XX (2002). </jrn>

<jrn>43. Bolstad, B.M., Irizarry, R.A., Astrand, M. & Speed, T.P. A comparison of normalization methods for high density oligonucleotide array data based on variance and bias. *Bioinformatics* **19**, 185–193 (2003).</jrn>

<jrn>44. Liu, W.M. *et al.* Analysis of high density expression microarrays with signed-rank call algorithms. *Bioinformatics* **18**, 1593–1599 (2002).</jrn>

<jrn>45. Gentleman, R.C. *et al.* Bioconductor: open software development for computational biology and bioinformatics. *Genome Biol.* **5**, R80 (2004).</jrn>

<bok>46. Smyth, G.K. *Bioinformatics and Computational Biology Solutions using R and Bioconductor, R.* (Springer, New York, 2005).</bok>

<jrn>47. Subramanian, A. *et al*. Gene set enrichment analysis: a knowledge-based approach for interpreting genome-wide expression profiles. *Proc. Natl. Acad. Sci. USA* **102**, (2005).</jrn>

<jrn>48. de Hoon, M.J., Imoto, S., Nolan, J. & Miyano, S. Open source clustering software. *Bioinformatics* **20**, 1453–1454 (2004).</jrn>

<jrn>49. Saldanha, A.J. Java Treeview–extensible visualization of microarray data. *Bioinformatics* **20**, 3246–3248 (2004).</jrn>

<jrn>50. Hu, Y. & Smyth, G.K. ELDA: extreme limiting dilution analysis for comparing depleted and enriched populations in stem cell and other assays. *J. Immunol. Methods* **347**, 70–78 (2009).</jrn>

Figure 1

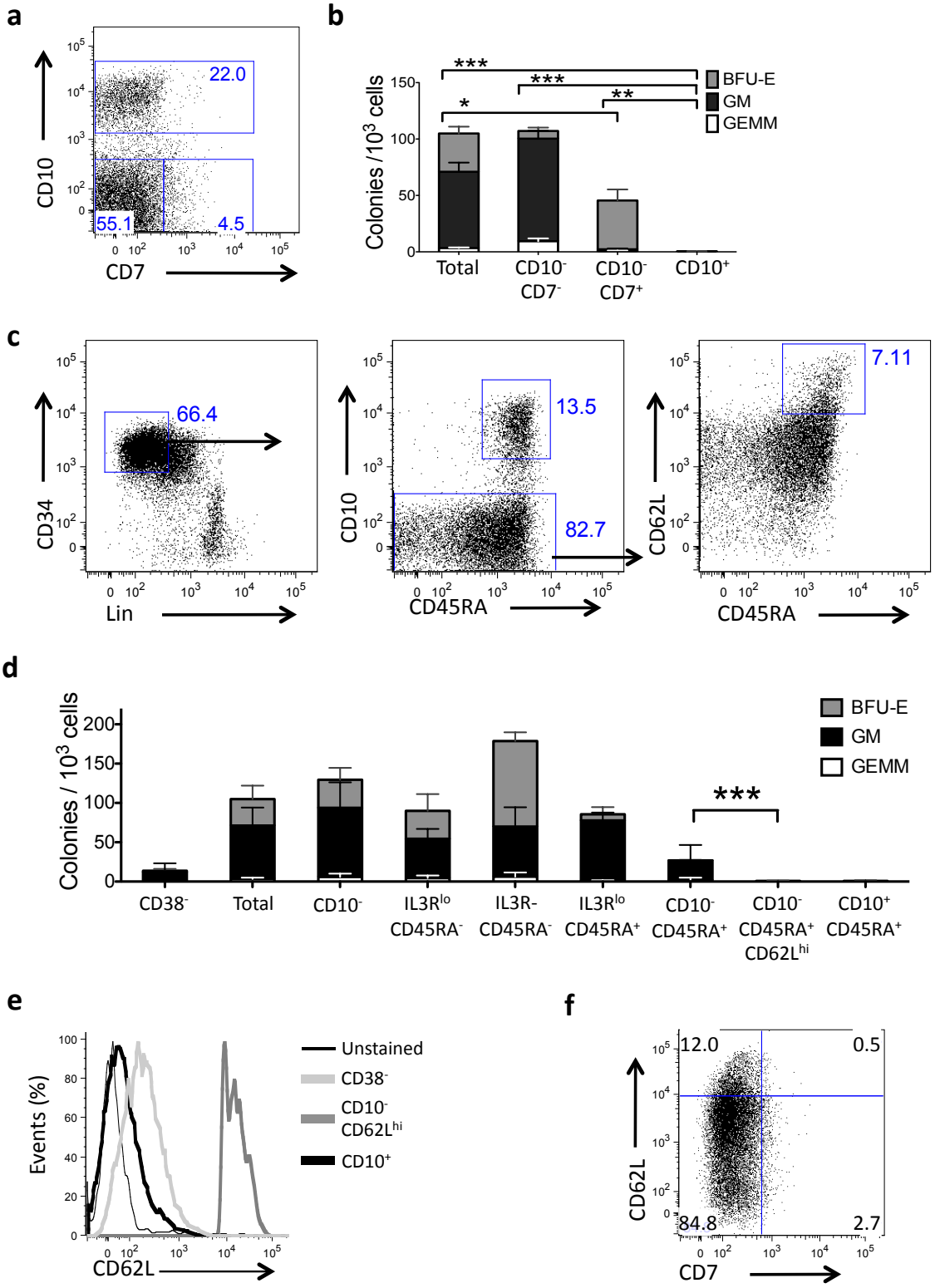
a
CD10
CD7
22.0
55.1
4.5
b
Colonies /10^3 cells
BFU-E
GM
GEMM
***
***
**
*
Total
CD10- CD7-
CD10- CD7+
CD10+
c
CD34
Lin
66.4
CD10
CD45RA
13.5
82.7
CD62L
CD45RA
7.11
d
Colonies / 10^3 cells
BFU-E
GM
GEMM
***
CD38-
Total
CD10-
IL3Rlo CD45RA-
IL3R- CD45RA-
IL3Rlo CD45RA+
CD10- CD45RA+
CD10- CD45RA+ CD62Lhi
CD10+ CD45RA+
e
Events (%)
CD62L
Unstained
CD38-
CD10- CD62Lhi
CD10+
f
CD62L
CD7
12.0
0.5
84.8
2.7

Figure 2

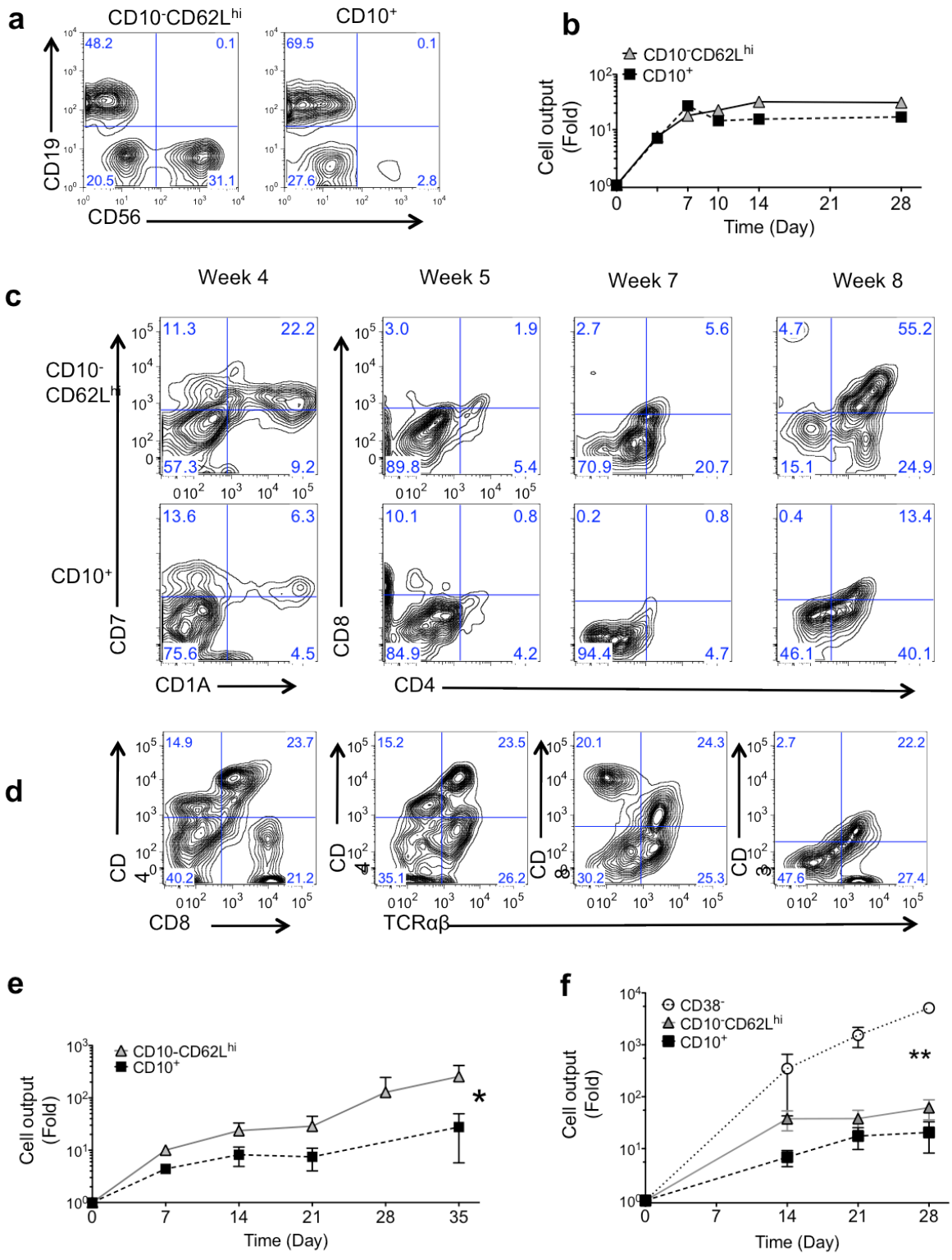
a
CD10-CD62Lhi
CD10+
48.2
0.1
20.5
31.1
69.5
0.1
27.6
2.8
CD19
CD56
b
CD10-CD62Lhi
CD10+
Cell output (Fold)
Time (Day)
c
Week 4
Week 5
Week 7
Week 8
CD10-CD62Lhi
CD10+
11.3
22.2
57.3
9.2
3.0
1.9
89.8
5.4
2.7
5.6
70.9
20.7
4.7
55.2
15.1
24.9
13.6
6.3
75.6
4.5
10.1
0.8
84.9
4.2
0.2
0.8
94.4
4.7
0.4
13.4
46.1
40.1
CD7
CD8
CD1A
CD4
d
14.9
23.7
40.2
21.2
15.2
23.5
35.1
26.2
20.1
24.3
30.2
25.3
2.7
22.2
47.6
27.4
CD4
CD8
CD8
TCRαβ
e
CD10-CD62Lhi
CD10+
Cell output (Fold)
Time (Day)
*
f
CD38-
CD10-CD62Lhi
CD10+
Cell output (Fold)
Time (Day)
**

Figure 3

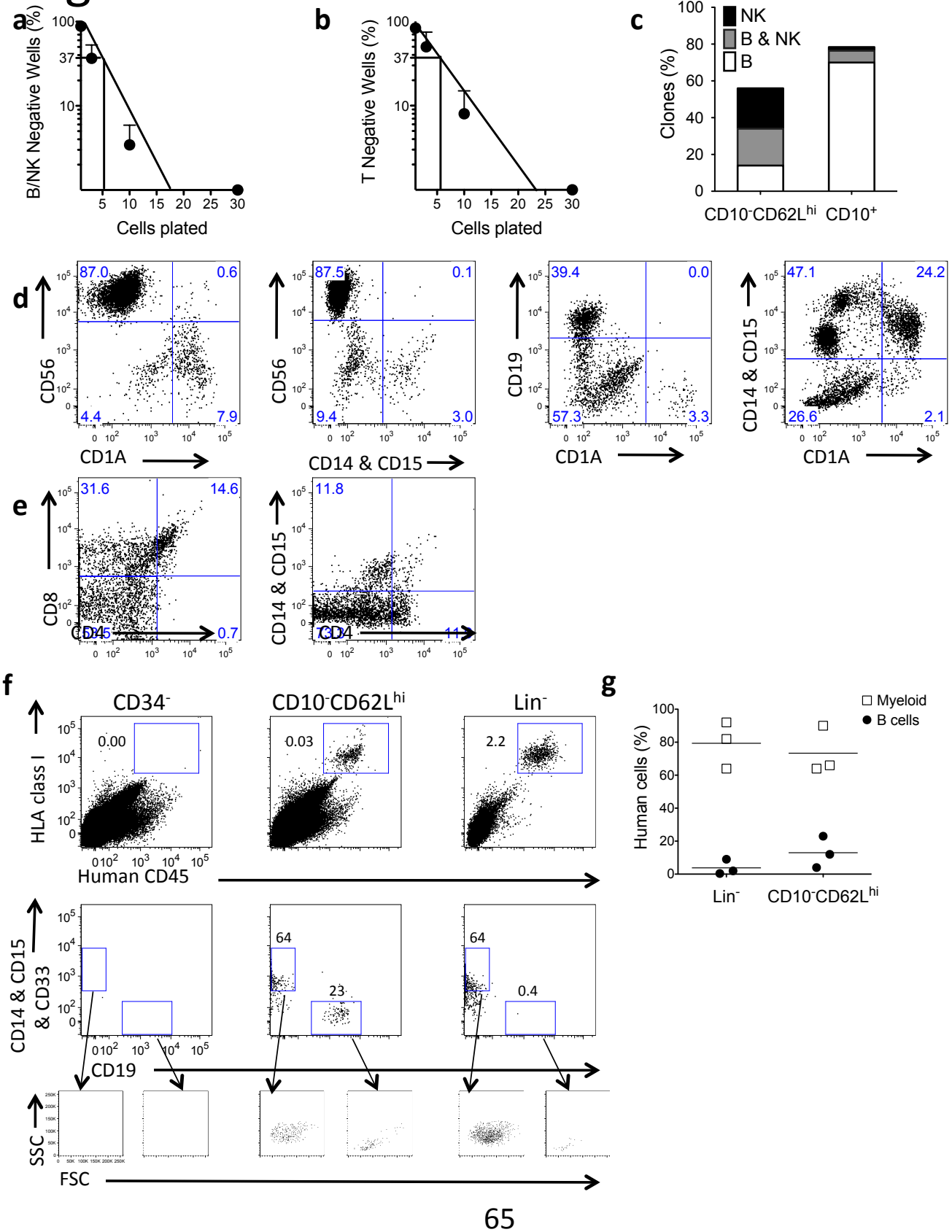
a
B/NK Negative Wells (%)
100
37
10
5 10 15 20 25 30
Cells plated
b
T Negative Wells (%)
100
37
10
5 10 15 20 25 30
Cells plated
c
Clones (%)
100
80
60
40
20
0
NK
B & NK
B
CD10-CD62Lhi
CD10+
d
CD56
CD1A
87.0
0.6
4.4
7.9
CD56
CD14 & CD15
87.5
0.1
9.4
3.0
CD19
CD1A
39.4
0.0
57.3
3.3
CD14 & CD15
CD1A
47.1
24.2
26.6
2.1
e
CD8
CD45
31.6
14.6
0.7
CD14 & CD15
CD4
11.8
11
f
CD34-
CD10-CD62Lhi
Lin-
HLA class I
Human CD45
0.00
0.03
2.2
CD14 & CD15 & CD33
CD19
64
23
64
0.4
SSC
FSC
g
Human cells (%)
100
80
60
40
20
0
Myeloid
B cells
Lin-
CD10-CD62Lhi

Figure 4

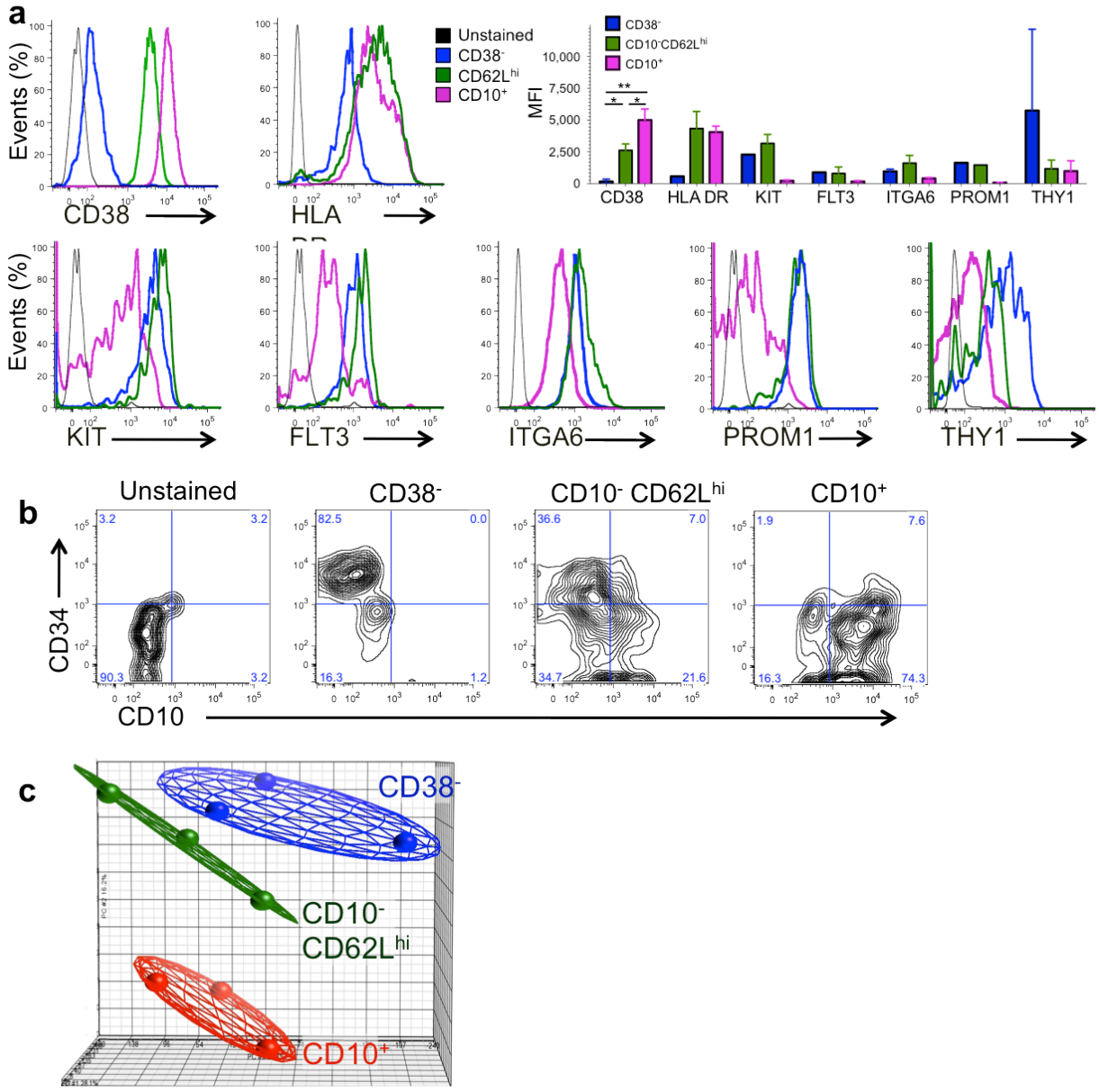
a
Events (%)
CD38
HLA
Unstained
CD38-
CD62Lhi
CD10+
MFI
CD38-
CD10-CD62Lhi
CD10+
CD38
HLA DR
KIT
FLT3
ITGA6
PROM1
THY1
KIT
FLT3
ITGA6
PROM1
THY1
b
Unstained
CD38-
CD10- CD62Lhi
CD10+
CD34
CD10
3.2
3.2
90.3
3.2
82.5
0.0
16.3
1.2
36.6
7.0
34.7
21.6
1.9
7.6
16.3
74.3
c
CD38-
CD10-
CD62Lhi
CD10+

Figure 5

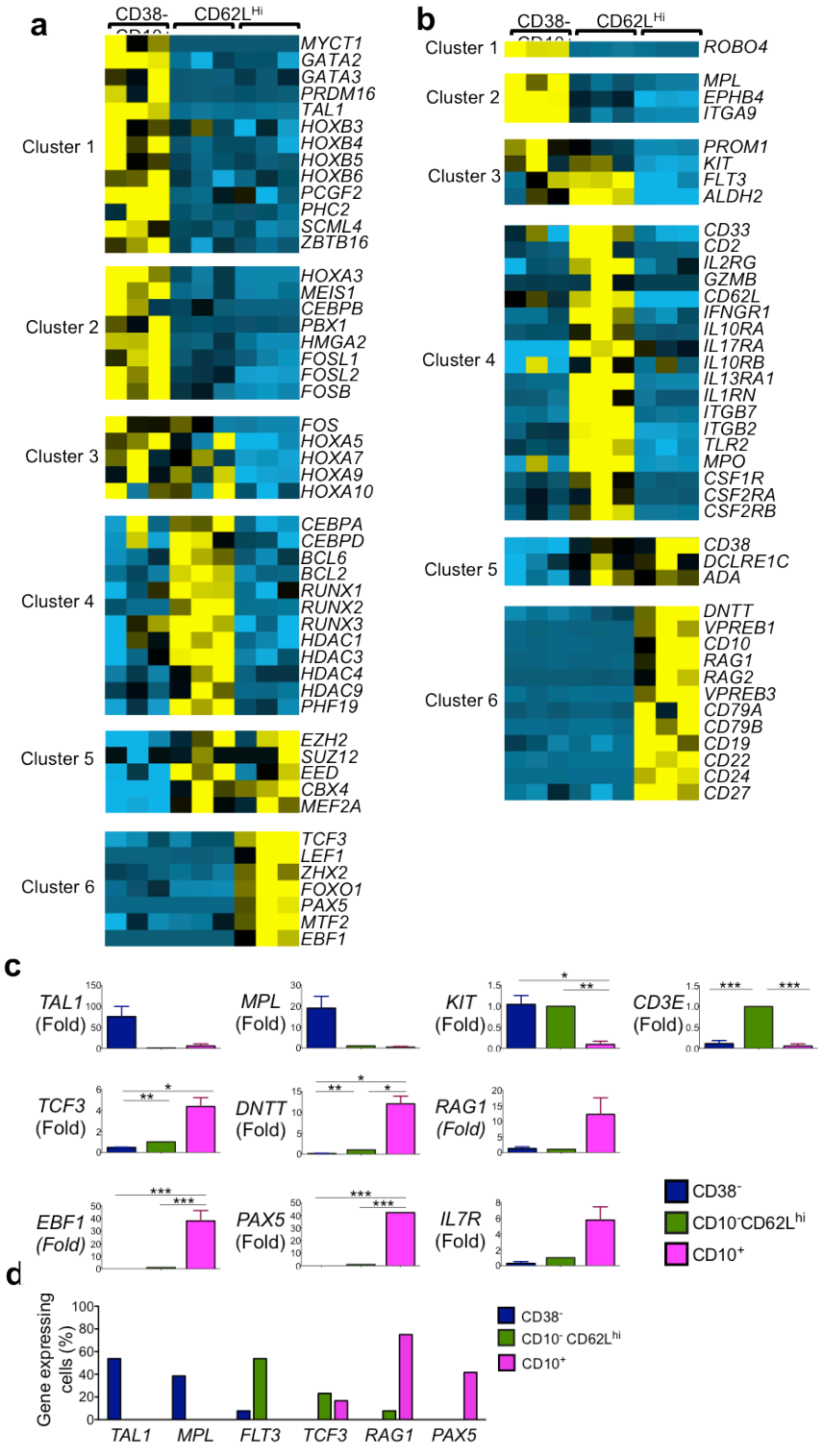
a
CD38-
CD62L Hi
Cluster 1
MYCT1
GATA2
GATA3
PRDM16
TAL1
HOXB3
HOXB4
HOXB5
HOXB6
PCGF2
PHC2
SCML4
ZBTB16
Cluster 2
HOXA3
MEIS1
CEBPB
PBX1
HMGA2
FOSL1
FOSL2
FOSB
Cluster 3
FOS
HOXA5
HOXA7
HOXA9
HOXA10
Cluster 4
CEBPA
CEBPD
BCL6
BCL2
RUNX1
RUNX2
RUNX3
HDAC1
HDAC3
HDAC4
HDAC9
PHF19
Cluster 5
EZH2
SUZ12
EED
CBX4
MEF2A
Cluster 6
TCF3
LEF1
ZHX2
FOXO1
PAX5
MTF2
EBF1
b
CD38-
CD62L Hi
Cluster 1
ROBO4
Cluster 2
MPL
EPHB4
ITGA9
Cluster 3
PROM1
KIT
FLT3
ALDH2
Cluster 4
CD33
CD2
IL2RG
GZMB
CD62L
IFNGR1
IL10RA
IL17RA
IL10RB
IL13RA1
IL1RN
ITGB7
ITGB2
TLR2
MPO
CSF1R
CSF2RA
CSF2RB
Cluster 5
CD38
DCLRE1C
ADA
Cluster 6
DNTT
VPREB1
CD10
RAG1
RAG2
VPREB3
CD79A
CD79B
CD19
CD22
CD24
CD27
c
TAL1 (Fold)
MPL (Fold)
KIT (Fold)
CD3E (Fold)
TCF3 (Fold)
DNTT (Fold)
RAG1 (Fold)
EBF1 (Fold)
PAX5 (Fold)
IL7R (Fold)
CD38-
CD10-CD62L hi
CD10+
d
Gene expressing cells (%)
CD38-
CD10- CD62L hi
CD10+
TAL1
MPL
FLT3
TCF3
RAG1
PAX5

Figure 6

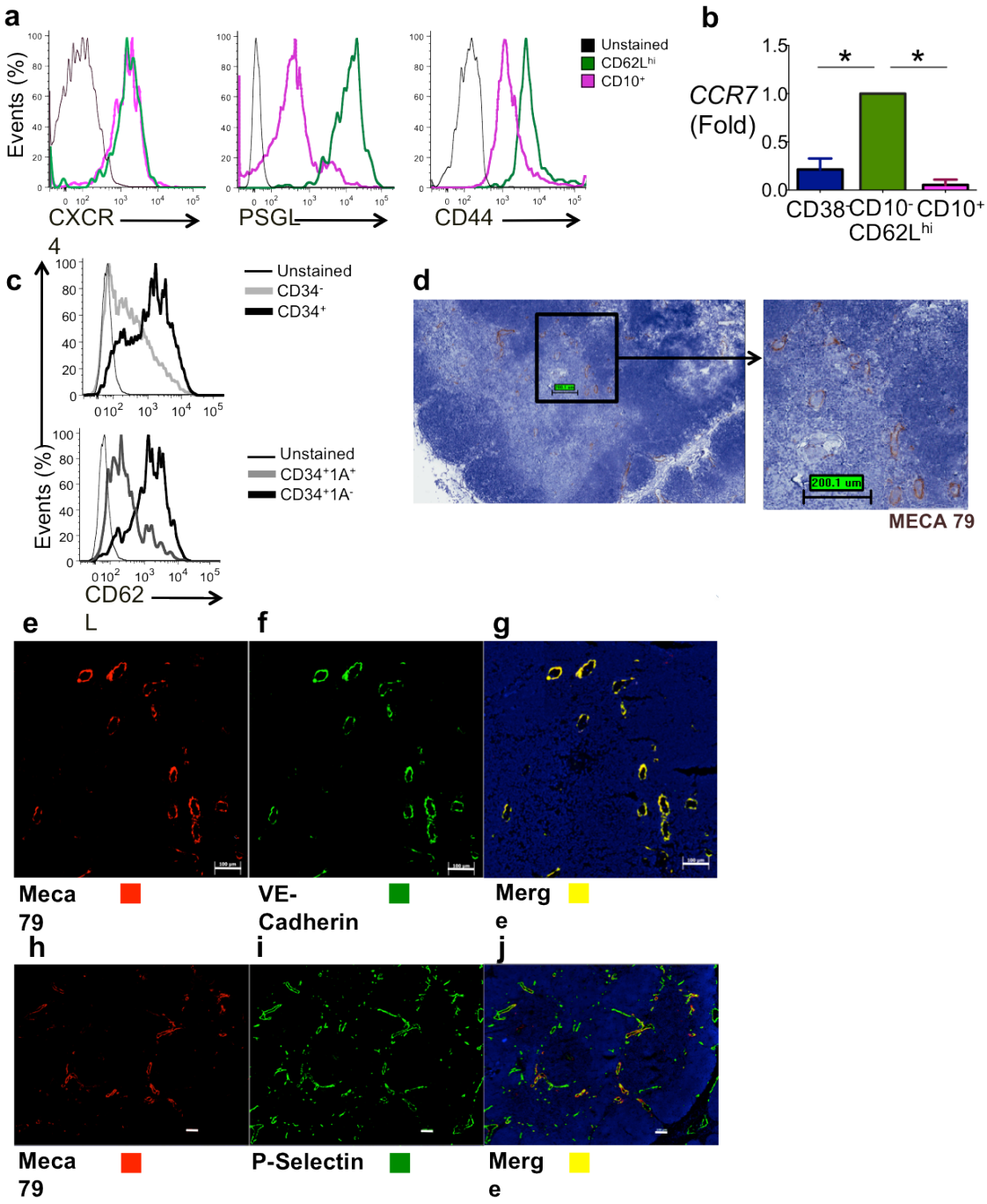
a
Events (%)
CXCR4
PSGL
CD44
Unstained
CD62L^hi
CD10+
b
CCR7 (Fold)
1.5
1.0
0.5
0.0
*
*
CD38-CD10-CD62L^hi
CD10+
c
Unstained
CD34-
CD34+
Unstained
CD34+1A+
CD34+1A-
Events (%)
CD62L
d
200.1 um
MECA 79
e
Meca 79
f
VE-Cadherin
g
Merge
h
Meca 79
i
P-Selectin
j
Merge

Supplemental Figure 1

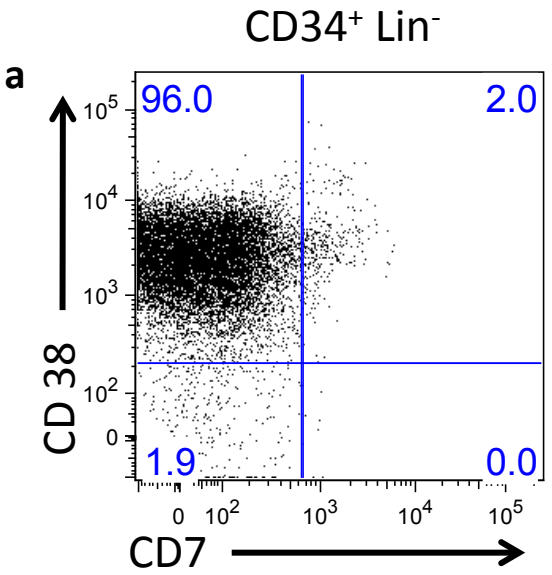

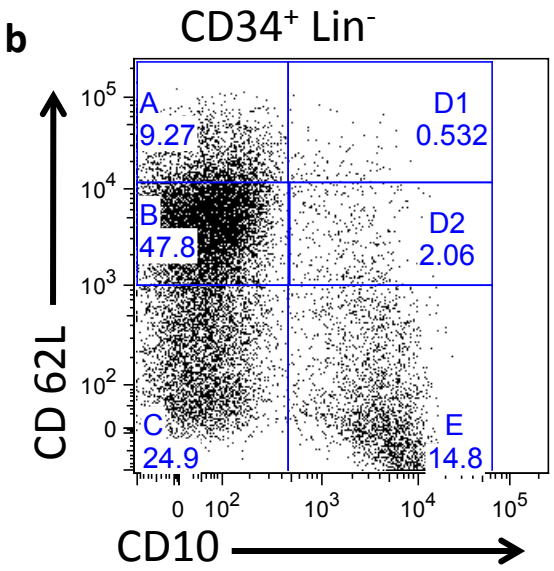

c

Population	C.F.U./ 10^3 cells plated
A	0.6
B	3.1
C	59.0
D1 &D2	0.5
E	0.0

Supplementary Figure 1. Relationship of CD7, CD38, CD10 and CD62L expression on CD34$^+$lin$^-$ cells and CFU potential of progenitor subsets.
Representative experiment of (**a**) CD38 and CD7 expression on CD34+lin- cells from BM (*n*=6), (**b**) CD62L and CD10 expression on CD34$^+$lin$^-$ BM cells (% of each subset within CD34+lin- population is shown) (*n*=30). (**c**) Table of CFUs for populations gated as in (**a**) (n=2-9). CFUs are given in # of colonies/10^3 BM cells plated.

Supplemental Figure 2

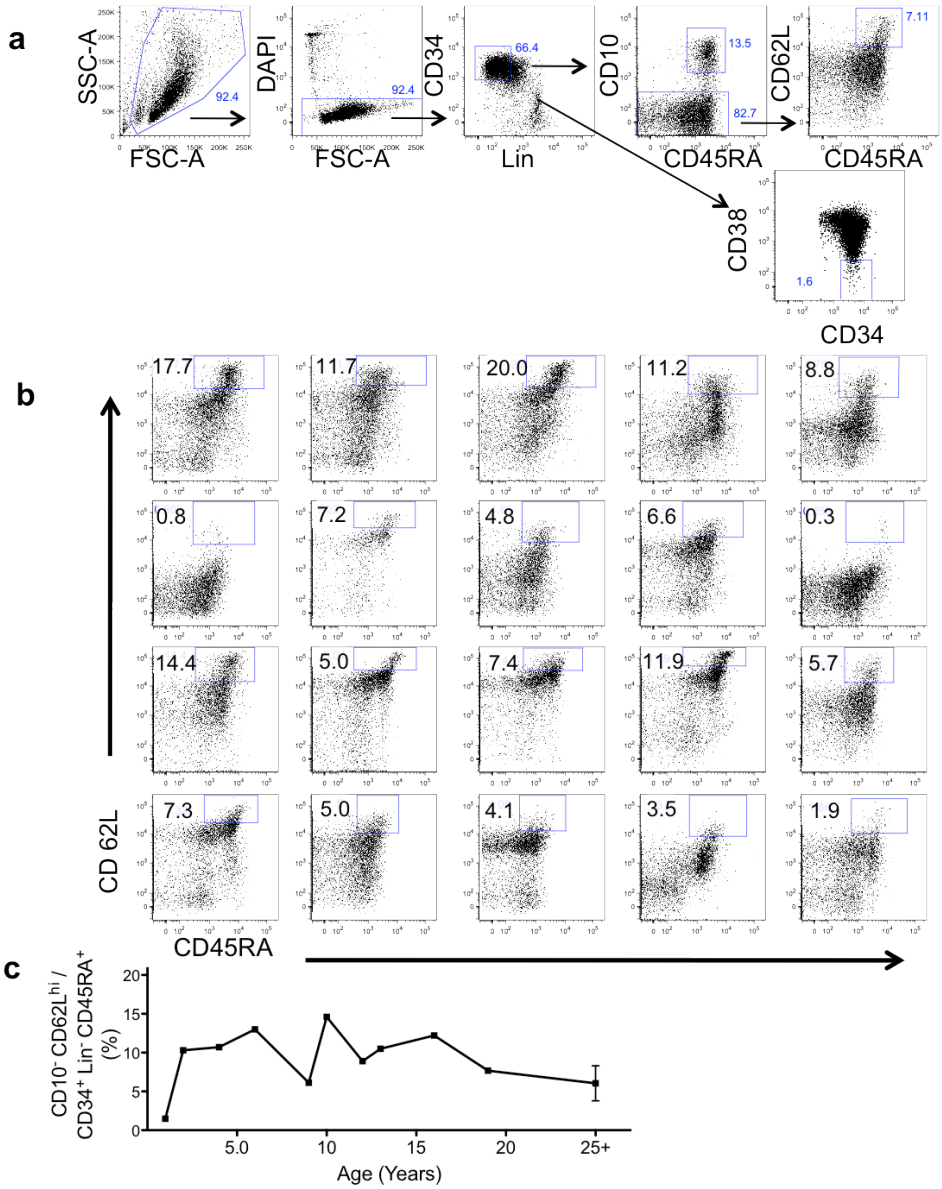

Supplementary Figure 2. CD10^{-}CD62L^{hi} profiles amongst different bone marrow donors

(**a**) Gating strategy for isolation of CD10^{-}CD62L^{hi}, CD10^{+} and CD38^{-} cell populations (**b**) Flow cytometric analysis of CD62L vs CD45RA of 20 independent human BMs. Cells were previously gated as DAPI^{-} CD34^{+} Lin^{-} CD10^{-} as shown in (**a**). (**c**) Relationship of frequency of CD10^{-}CD62L^{hi} cells within the CD34^{+}lin^{-}CD45RA^{+} population to age. 17 BM donors in which age was known are shown (1 year to adult; *n* = 7 adults > 25y). Note: at 1 year of age, CD34^{+}lin^{-} cells are predominantly CD10^{+}.

Supplemental Figure 3

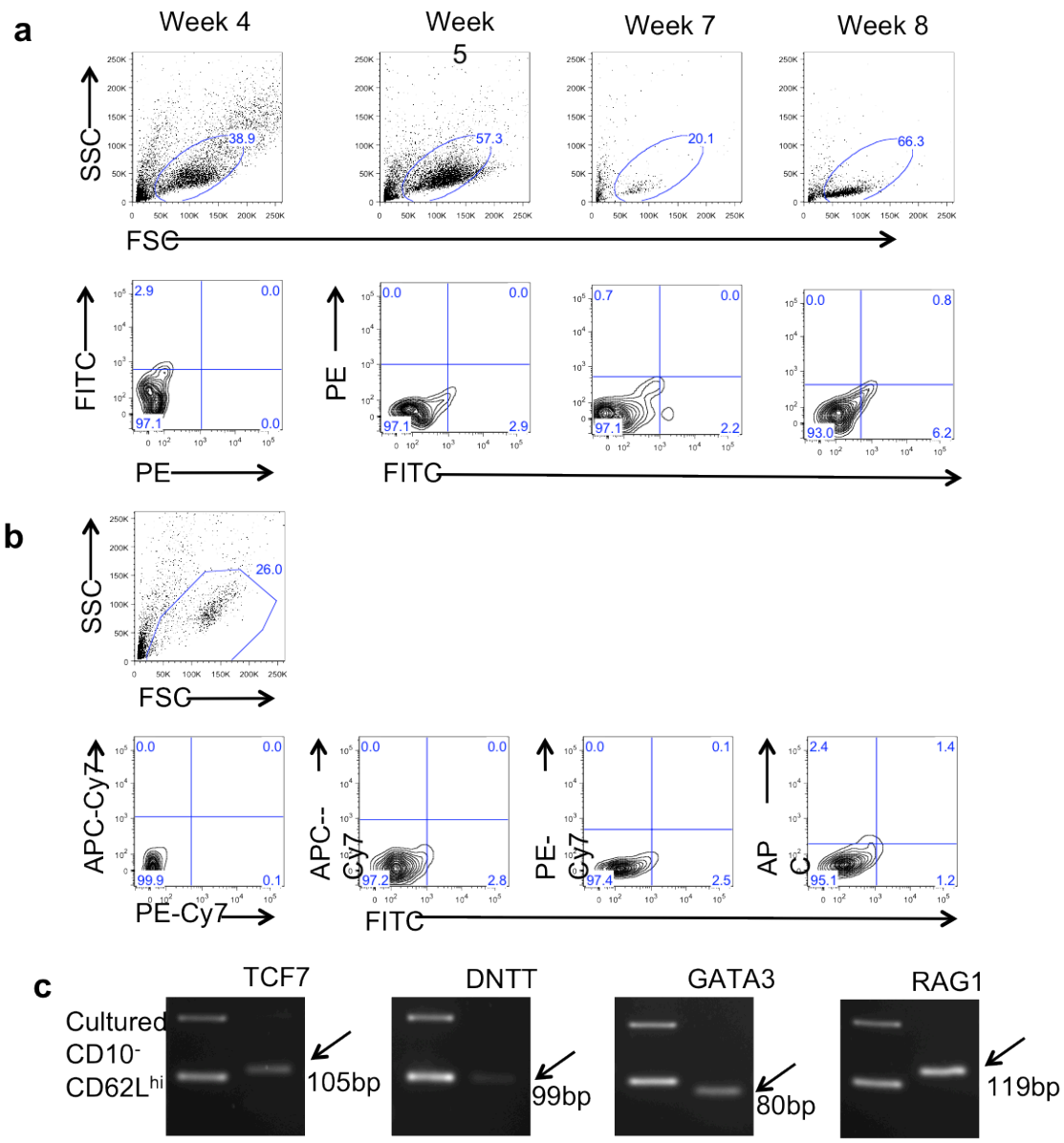

Supplementary Figure 3. T cell cultures generated from CD10⁻CD62L^{hi} cells. Analysis of T cell cultures initiated with CD10-CD62L^{hi} cells (**a,b**) Unstained Flow Cytometry analysis of T Lymphoid cultures in companion to (**a**) Figure 2c (Week 4 CD7-FITC, CD1A-PE, Weeks 5, 7, 8 CD8-PE, CD4-FITC) (n=6) or (**b**) Figure 2d (TCRαβ-FITC, CD4-APC-Cy7, CD8-PE-Cy7, CD3-APC) (n=2). (**c**) Semi-quantitative RT-PCR analyses of T cell associated genes from total cells harvested at 4-6 weeks from 2 independent experiments. 1kb ladder shown at left of each transcript.

Supplemental Figure 4

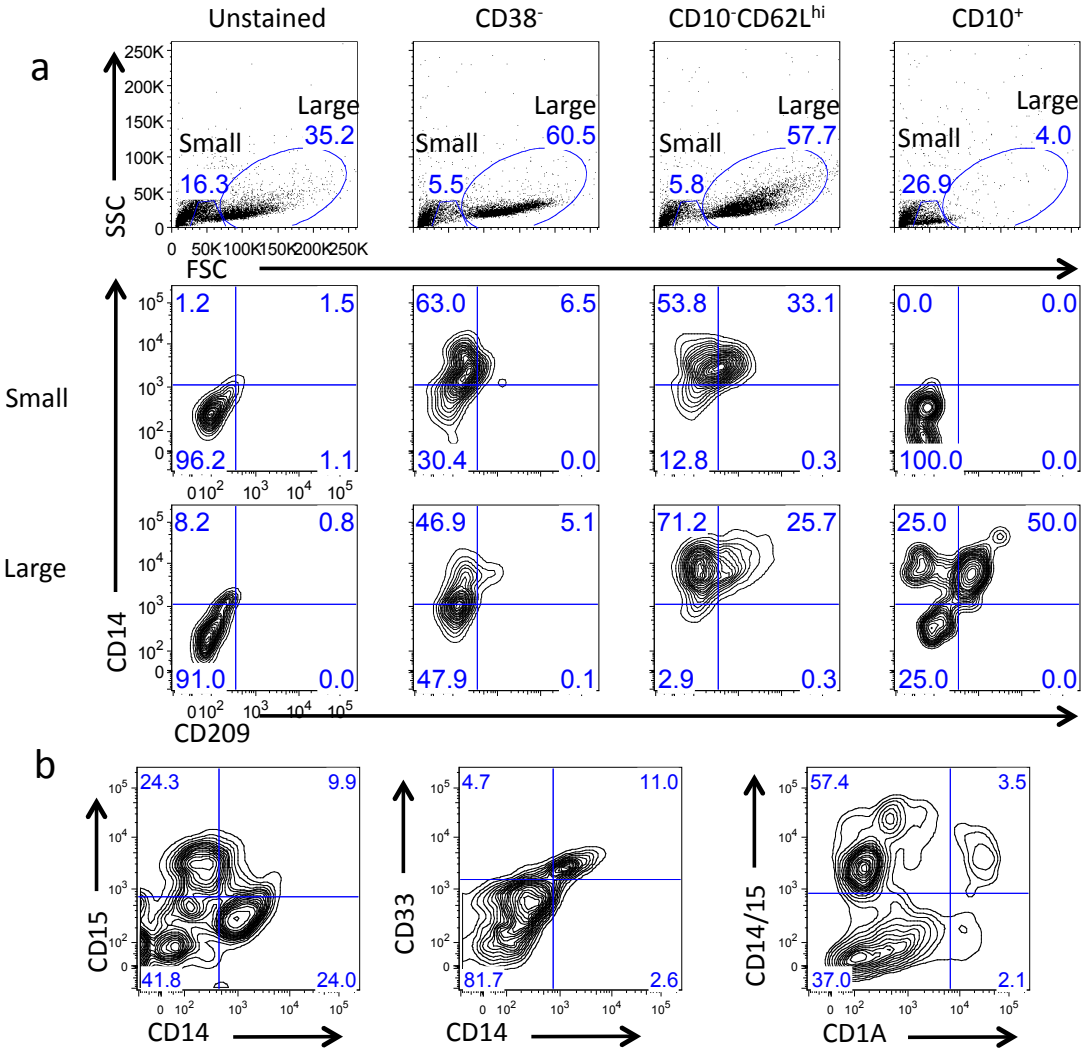

Supplementary Figure 4. The CD10-CD62L^{hi} population has monocytic potential in myeloid stromal co-cultures

(**a**) Flow Cytometry analysis of 2 week myelo-erythroid co-cultures (OP9 with SCF, FLT-3, TPO, IL3 and EPO) initiated with CD38-, CD10-CD62L^{hi} or CD10+ cells. Far left panels show unstained controls. Monocytes/macrophages (CD14) and dendritic cells (CD209) were detected after initial gating on CD45+ cells (not shown). FSC and SSC gating (top row) are shown to analyze small (middle row) and large (bottom row) cells separately. Glycophorin and CD66b expression were rarely detected. Data representative of 3 independent experiments. (**b**) Co-expression of myeloid (CD14, CD15 and CD33) and dendritic (CD1A+) markers in myelo-erythroid cultures initiated with CD10-CD62L^{hi} cells. Data representative of 3 independent experiments.

Supplemental Figure 5

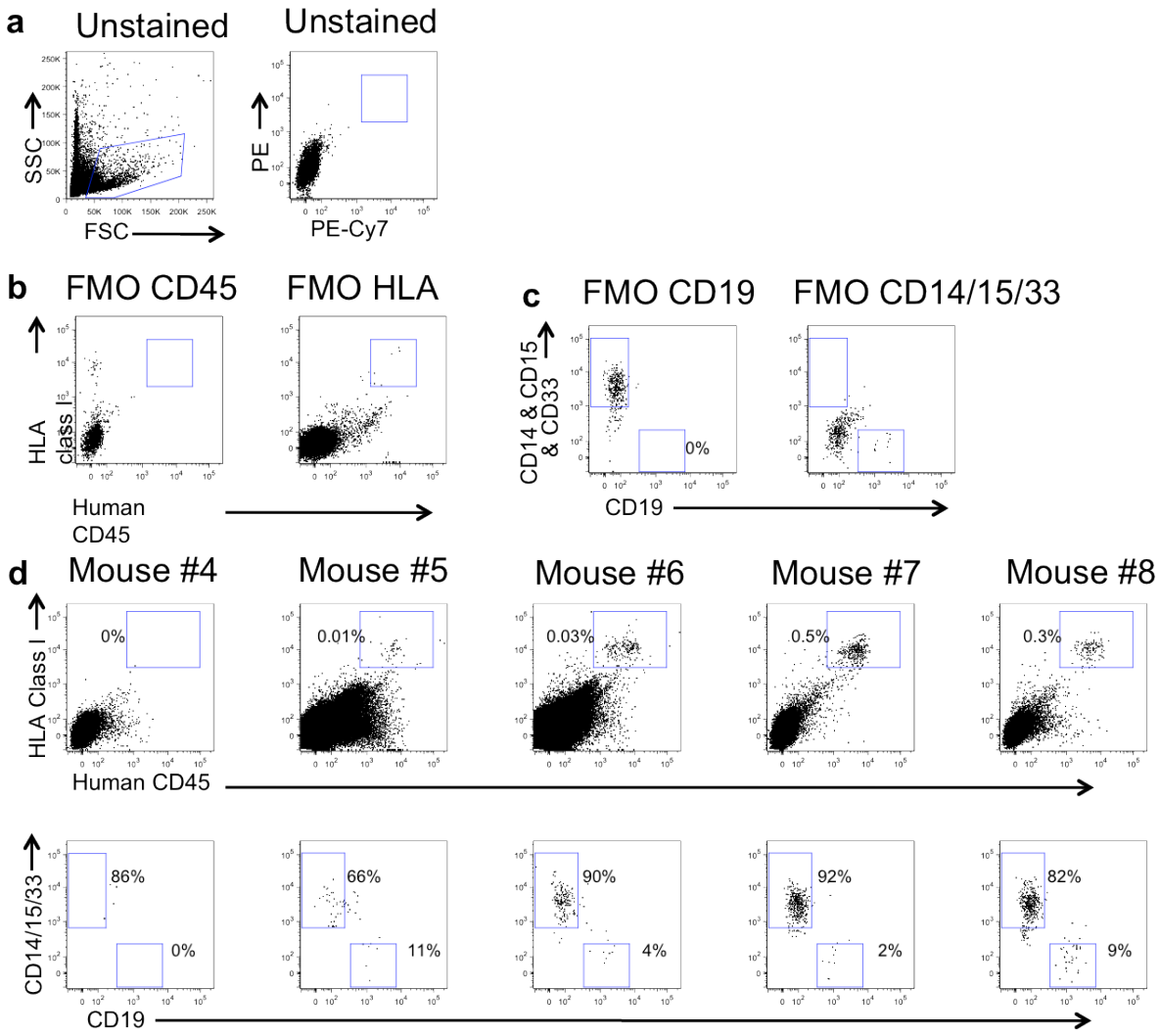

Supplementary Figure 5. Additional in vivo reconstitution data.
Flow cytometry analysis of NSG mice transplanted with human BM populations and analyzed 2wk post transplant. (**a-d**) Data from 5 additional animals not included in Fig 3f. Mouse #4 received 100,000 irradiated $CD34^-$ carrier cells only (negative control), Mice #5 and #6 received 30,000 $CD34^+lin^-CD10^-$ $CD62L^{hi}$ cells, Mouse #7 received 150,000 $CD34^+lin^-$ cells, and Mouse #8 received 30,000 $CD34^+lin^-$ cells. **(a)** Unstained controls for PE (hCD45) and PE-Cy7 (HLA-class 1), **(b, c)** Fluorescence minus one (FMO) controls from composite of cells from animals #7 and #8, **(b)** is gated from FSC vs SSC as shown in (**a**), (**c**) is gated on $CD45^+HLA^+$ cells as shown in (**d**). (**d**) Human engraftment shown top row as $hCD45^+$ & HLA-class 1^+ cells, bottom row shows B (CD19+) cells and myeloid (CD14, CD15, & CD33+) cells from gated human cells.

Supplemental Figure 6

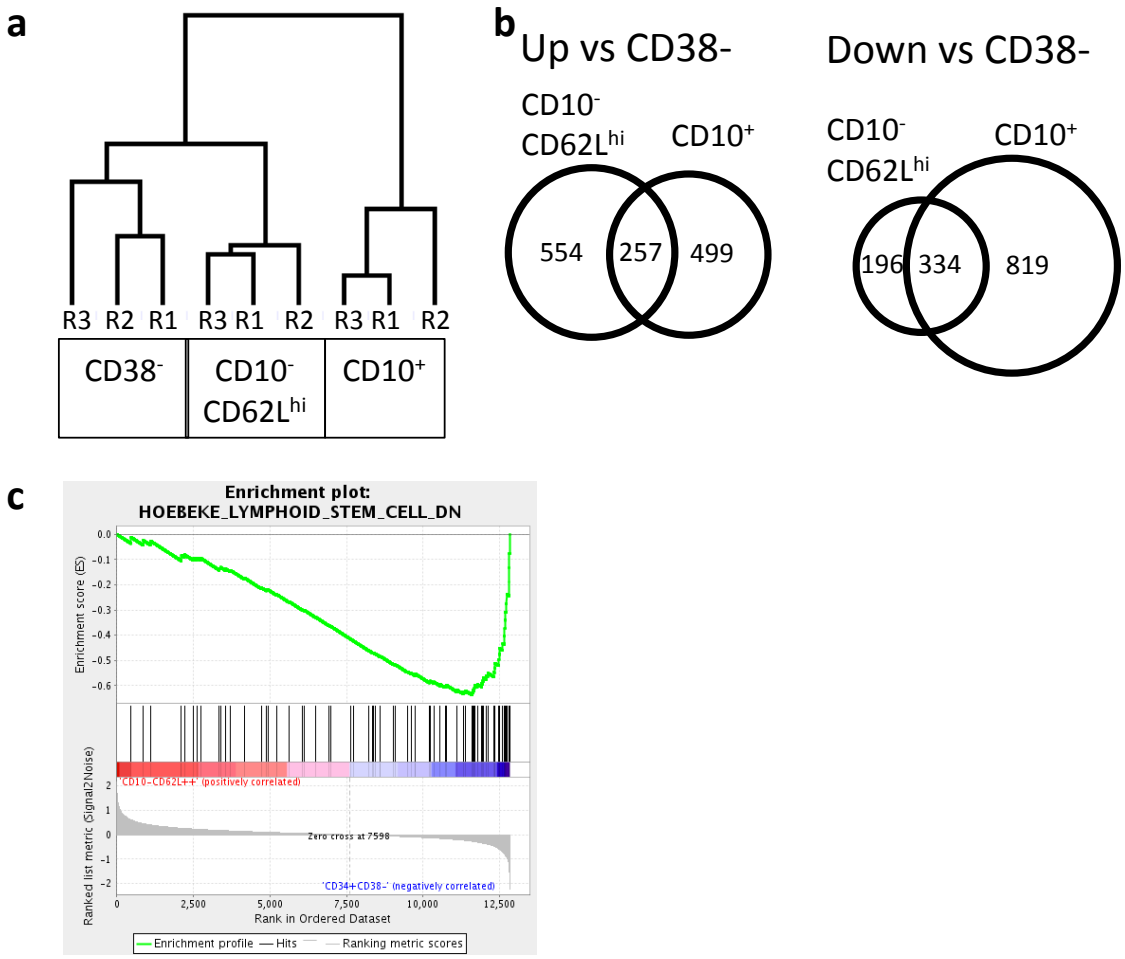

Supplementary Figure 6. Global gene expression analysis places CD10$^-$CD62L^{hi} population in intermediate position between CD38$^-$ and CD10$^+$,with similar profile to umbilical cord blood CD34$^+$CD38$^-$CD7$^+$ lymphoid progenitors

Microarray datasets from three independent BM samples. (**a**) Hierarchical clustering of global gene expression using Spearman rank correlation and average linkage method. (**b**) Venn Diagram showing pair-wise comparisons of global gene expression. Shown are number of genes that are > 2 fold differentially up-regulated or down-regulated relative to CD38$^-$, p<0.01. (**c**) Gene Set Enrichment Analysis (GSEA) comparing gene expression between BM CD10$^-$CD62L^{hi} and BM CD38$^-$ and published CD34$^+$CD38$^-$CD7$^+$ UCB[20]. Overall the set of genes down-regulated in BM CD10$^-$CD62L^{hi} (LMPP) compared to BM CD38$^-$ (HSC-MPP) was similar to the set of genes down-regulated in UCB CD34$^+$CD38$^-$CD7$^+$ (MLP) compared to UCB CD34$^+$CD38$^-$CD7$^-$ (HSC-MPP) from Hoebeke et al. (FDR q-value 1.6180314E-4, Normalized Enrichment Score -2.398794).

Supplemental Figure 7

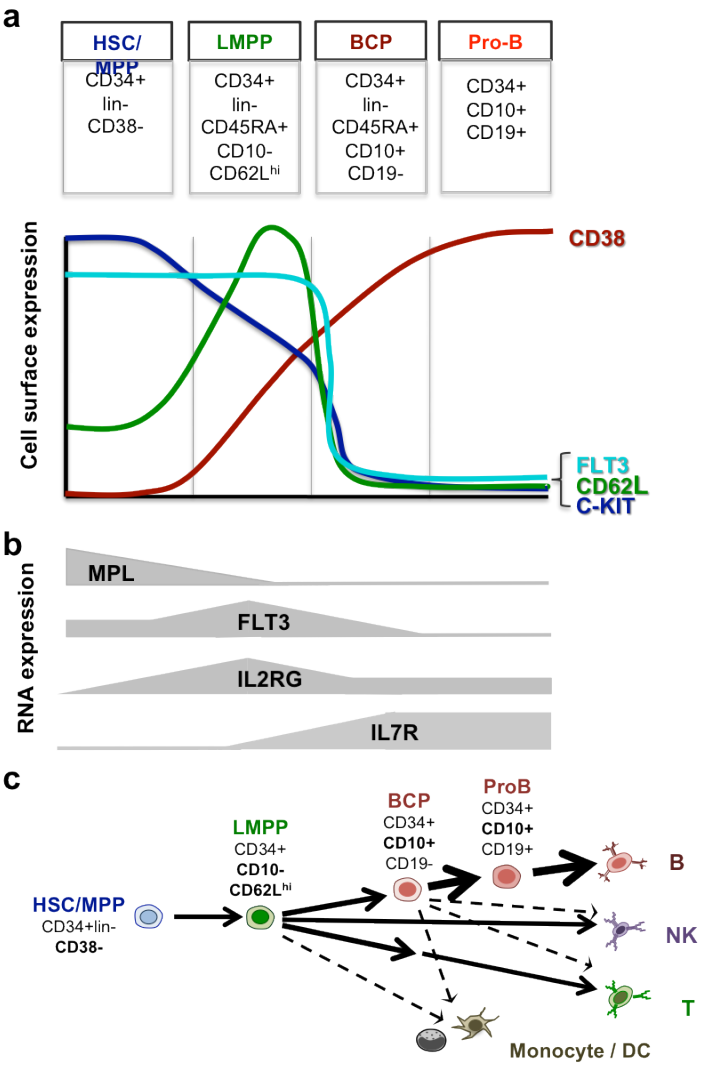

Supplementary Figure 7. Stages of lymphoid priming and B cell commitment in human bone marrow.

(a, b) Changes in relative expression of key cytokine receptors in BM progenitor populations listed above, (**a**) protein expression by flow cytometry and (**b**) gene expression by array and/ or qPCR. Note, although *FLT3* transcripts are increased in the CD10^{-}CD62L^{hi} LMPP population, expression by flow cytometry is similar in HSC-MPP and LMPP. (**c**) Proposed model of progenitor relationships during early stages of lymphoid commitment in human bone marrow. CD34^{+}lin^{-}CD10^{+} cells are predominantly B cell progenitors (BCP) whereas CD10-CD62L^{hi} cells readily generate all three lymphoid lineages; dashed lines represent less prominent lineage differentiation pathways.

Supplemental Table 1

a

$CD34^+Lin^-$

	Experiment 1		Experiment 2		Experiment 3		Experiment 4	
Colonies	85	84	66	93	318	332	209	168
CFU-GEMM	6	4	50	4	2	6	9	4
CFU-E	42	52	2	66	196	205	157	104
CFU-GM	37	28	14	23	120	121	43	60

$CD10^-$

	Experiment 1		Experiment 2		Experiment 3		Experiment 4	
Colonies	81	70	153	164	255		208	426
CFU-GEMM	0	5	6	9	6		12	26
CFU-E	61	50	93	111	177		132	287
CFU-GM	20	15	54	44	72	No Data	62	113

MEP

	Experiment 1		Experiment 2	
Colonies	204	193	130	188
CFU-GEMM	13	2	2	8
CFU-E	69	89	30	66
CFU-GM	122	102	98	114

CMP

	Experiment 1		Experiment 2	
Colonies	39	102	118	102
CFU-GEMM	2	2	9	5
CFU-E	4	44	47	48
CFU-GM	33	56	62	48

$CD38^-$

	Experiment 1		Experiment 2	
Colonies	23	20	7	5
CFU-GEMM	0	0	0	0
CFU-E	0	0	5	2
CFU-GM	23	20	2	3

GMP

	Experiment 1		Experiment 2	
Colonies	88	64	92	99
CFU-GEMM	0	0	1	2
CFU-E	0	0	16	16
CFU-GM	88	64	75	80

$CD10^-CD45RA^+$

	Experiment 1		Experiment 2		Experiment 3	
Colonies	11	35	9	60	24	50
CFU-GEMM	0	0	0	2	0	0
CFU-E	0	0	0	0	0	0
CFU-GM	11	35	9	58	24	50

$CD10^+CD45RA^+$

	Experiment 1		Experiment 2		Experiment 3		Experiment 4		Experiment 5	
Colonies	1	0	1	0	0	1	3	0	4	3
CFU-GEMM	0	0	0	0	0	1	0	0	0	0
CFU-E	1	0	0	0	0	0	2	0	3	2
CFU-GM	0	0	1	0	0	0	1	0	1	1

$CD10^-CD45RA^+CD62L^{Hi}$

	Experiment 1		Experiment 2		Experiment 3		Experiment 4		Experiment 5	
Colonies	0	0	0	2	2	1	0	0	1	0
CFU-GEMM	0	0	0	1	1	1	0	0	0	0
CFU-E	0	0	0	1	1	0	0	0	1	0
CFU-GM	0	0	0	0	0	0	0	0	0	0
	Experiment 6		Experiment 7		Experiment 8		Experiment 9			
Colonies	2	1	0	1	0	0	0	0		
CFU-GEMM	0	0	0	0	0	0	0	0		
CFU-E	0	0	0	0	0	0	0	0		
CFU-GM	2	1	0	1	0	0	0	0		

b

	$CD38^-$	Total	$CD10^-$	CMP	MEP	GMP	$CD10^-CD45RA^+$	$CD62L^{hi}$ $CD10^-CD45RA^+$	$CD10^-CD45RA^+$
N (Number of indpendent BM tested, each in duplicate)	2	4	4	2	2	2	3	9	5
P-value (t-test compared to $CD10^-CD45RA^+CD62L^{Hi}$)	<0.001	<0.001	<0.001	<0.00	<0.00	<0.00	<0.001	N/A	0.0932

Supplementary Table 1. Colony Forming Unit assay raw data

(**a**) Raw data for Colony Forming Unit Assays. All data is from subsets shown of human BM CD34+ Lin- cells. Each experiment represents duplicate plates from one flow cytometry sorted BM. (**b**) *P*-values of unpaired t-tests comparing CFU output from $CD10^-$ $CD62L^{hi}$ to each population shown (*N*=number of times that cell population was tested using a different donor, all in duplicate).

Supplemental Table 2

a

#Cells Seeded/ Well MS5	# Wells Seeded		
	Experiment 1	Experiment 2	Experiment 3
1	168	100	60
3	12	35	20
10	12	9	6
30	9	4	4
100	9	1	2
300	0	1	0

b

#Cells Seeded/ Well OP9-DL1	# Wells Seeded		
	Experiment 1	Experiment 2	Experiment 3
1	120	100	60
3	9	35	20
10	9	9	6
30	6	23	5
100	6	1	1
300	0	1	0

Supplementary Table 2. Set up for limiting dilution experiments

Number of wells seeded at each cell number for limiting dilution analysis on (**a**) MS5 stroma (n=3 independent samples) (see Fig 3a) or (**b**) OP9DL1 stroma (n=3 independent samples) (see Fig3b)

Supplemental Table 3

All primer probes are manufactured by ABI

Gene Name	Probe Name	Amplicon Size
TAL1	Hs01097987_m1	84
MPL	Hs00180489_m1	83
KIT	Hs00174029_m1	64
FLT3	Hs00174690_m1	58
RAG1	Hs01920694_s1	119
DNTT	Hs00172743_m1	99
CD3E	Hs01062241_m1	88
TCF7	Hs00175273_m1	105
GATA3	Hs00231122_m1	80
E2A	Hs00413032_m1	74
EBF1	Hs00395513_m1	96
PAX5	Hs00172003_m1	72
IL7R	Hs00902334_m1	161
CCR9	Hs01890924_s1	146
CCR7	Hs01013469_m1	58
SELPLG	Hs00380945_m1	68
B2M	Hs00984230_m1	81
ACTB	Hs99999903_m1	171

Supplementary Table 3. List of qPCR probes
List of ABI Taqman Probes and amplicon size used for qPCR analysis.

Chapter 3

Lymphoid Development in Humans with Deficiencies in the IL2Rgamma chain Pathway

Chapter 3 presents my in-progress research in on early B-lymphoid and mature B cells in human bone marrow from patients with Severe Combined Immune Deficiency caused by defects in IL2RG signaling. We demonstrate that the earliest stages of B lymphoid development are unaffected by defects in IL2RG signaling in these patients.

Lisa Ann Kohn designed, performed, collected, and analyzed experiments, and is finishing experiments and writing the paper.

Lymphoid Development in Humans with Deficiencies

in the IL2Rgamma chain Pathway

Authors:

Lisa A. Kohn,[1] Christopher Seet,[1] Jessica Scholes,[2] Felicia Codrea,[2] Rebecca Chan,[1] Sania Zaidi,[1] Yuhua "Judy" Zhu,[1] Satiro De Oliveira,[3] Neena Kapoor,[4] Ami Shah,[4] Hisham Abdel-Azim,[4] Donald B. Kohn,[3] Gay M. Crooks[1,2,3]

[1] Department of Pathology and Laboratory Medicine, David Geffen School of Medicine at University of California Los Angeles

[2] Broad Stem Cell Research Center Flow Cytometry Core, University of California Los Angeles

[3]Department of Pediatrics, David Geffen School of Medicine at University of California Los Angeles

[3] Division of Research Immunology and Bone Marrow Transplant, Childrens Hospital Los Angeles

Abstract

Despite the best efforts of scientists to elucidate the workings of the immune system through the study of model systems, critical differences exist between species that require the direct study of human cells. Illustrating this point is the difference in phenotype between SCID patients with mutations in the gamma chain signaling pathways and mice with similar mutations in which humans produce B cells but mice lack B cells. To address these differences, our studies examine bone marrow from SCID patients to determine the stage of lymphoid differentiation blockage. These studies are made possible by recent findings of human post-natal BM LMPP.

Key Words

Severe Combined Immunodeficiency

Common Gamma Chain

Human Bone Marrow

Common Lymphoid Progenitor

Lymphoid-primed Multipotent Progenitor

Introduction

The stepwise process of differentiation from multipotent hematopoietic stem cells (HSC) into functional lymphocytes consists of passing through many intermediate progenitor stages prior to becoming a mature lymphoid cell. Severe Combined Immune Deficiency (SCID) is a genetic syndrome characterized by a profound or absolute deficiency in functional T lymphoid cells. Depending on the specific mutation, B and Natural Killer (NK) cell production are also affected. Multiple genetic mutations can cause this syndrome, several are caused by defects in cytokine signaling.

The most common form of SCID, X-linked SCID (X-SCID), is caused by a null mutation in the *IL2RG* gene, whose protein product is known as the common gamma chain (γc). (1) *IL2RG* encodes a type I cytokine receptor chain that acts as the common signaling chain shared between the interleukin receptors IL-2, IL-4, IL-7, IL-9, IL-15 and IL-21. (2-7) Mutation of *IL2RG* results in complex phenotype due to an inability to differentiate or function in response to multiple lymphoid cytokines.(2) This deficiency in γc is characterized by an absence of peripheral T and NK cells, and present but functionally impaired B cells.(2, 8)

After the γc dimerizes with one of the above ligands, its signaling is mediated by the hematopoietic restricted tyrosine kinase Janus-activated kinase 3 (JAK3)-signal transducer and activator of transcription (STAT) pathway. JAK3 is directly associated with γc dependent cytokines.(9, 10) Disruption of the gene encoding JAK3 causes Jak3-

SCID, an autosomal form of SCID with an otherwise identical clinical phenotype to X-SCID.(11, 12)

Although humans with mutations in IL2RG or JAK3 have normal numbers of circulating B cells, mice with similar mutations are unable to develop B cells.(13-15) The lack of B cell development in IL2RG and Jak3(16-18) null mice has been specifically attributed to deficient IL7 signaling, as IL7Rα knock-out mice are unable to develop B cells.(19) In mice, IL7 critically regulates expression of early B cell factor (EBF) in the early stages of B lineage commitment in bone marrow (BM), especially at the CLP and pre-proB stages and B cell development is arrested at the pre-proB stage. (20-22) Patients with IL7Rα defects have a normal number of B cells, similar to patients with defects in IL2RG or JAK3 and unlike IL7R knock-out mice. (23) All stages of hematopoiesis, from early progenitors to many categories of mature lymphoid cells, have been examined in mice that are null for *IL2RG, IL7Rα, or IL7R*.(20) However, examination of hematopoietic progenitors in humans with SCID is more difficult, as it requires an invasive BM draw. Despite the experimental hurdles, it is important to directly investigate mechanisms of human lymphoid commitment, especially because cytokine deficiencies result in different phenotypes in humans and mice.

We applied thus applied the identification of the human LMPP progenitor population in normal BM (24) to the clinically relevant question how the lack of IL2RG signaling affects the regulation of the lymphoid commitment. Because SCID patients have normal numbers of circulating B cells, we hypothesized that the earliest stages of B lymphoid

development will be unaffected in these patients, and that we would be able to detect both B1 and non-B1 mature populations. These studies demonstrate that the earliest stages of B lymphoid development are unaffected by defects in IL2RG signaling in these human patients. These results demonstrate the critical differences between lymphopoiesis in mice and humans, and the importance of overcoming experimental hurdles in order to directly investigate human lymphoid commitment.

Methods

Collection of bone marrow, cord blood and peripheral blood cells

Human bone was collected from patients with Severe Combined Immunodeficiency at University of California, Los Angeles (UCLA) and Childrens Hospital of Los Angeles (CHLA). Normal human adult BM and peripheral blood were obtained from healthy donors via the Pathology Tissue Core at UCLA. Umbilical cord blood (CB) was collected from normal deliveries at UCLA. All materials were collected according to protocols approved by the UCLA and CHLA Investigational Review Boards.

Cell Isolation and Analysis

Mononuclear cells were isolated by density gradient centrifugation using Ficoll-Paque (GE Healthcare). Samples were enriched for CD34+ cells by the magnetic-activated cell-sorting (MACS) system (Miltenyi Biotec). Samples enriched for CD34+ progenitor cells were incubated with combinations of monoclonal antibodies specific for human molecules (allophycocyanin- indotricarbocyanine–conjugated (APC-Cy7) anti-CD34 (581; Biolegend); and phycoerythrin-indodicarbocyanine (PERCP-Cy5.5)–anti-CD45RA (HI100), allo-phycocyanin (APC)–anti-CD38 (HIT2), phycoerythrin-indotricarbocyanine (PE-Cy7)– anti-CD10 (HI10a), phycoerythrin (PE)–anti-CD62L (DREG-56), PE–anti-CD7 (M-T701), PE –anti-CD127 (aka IL7Ralpha) (HIL-7R-M21), fluorescein isothiocyanate (FITC) anti-CD7(M-T701), APC anti-CD19 (4G7 and SJ25C1), PE or APC-Cy7 anti-CD3 (SK7), FITC anti-CD56 (MY31), APC anti-CD4 (RPA-T4), PE-Cy7 anti-CD8 (RPA-T8), PE anti-CD24 (ML5), FITC anti-CD20 (L27), PE anti-CD20 (2H7), PERCP-Cy5.5 anti-IgM (MHM-88, Biolegend), FITC anti-CD27 (M-T271), APC anti-

CD43 (IG10), FITC anti-CD45RO(UCHL1), and FITC–labeled lineage-depletion antibodies anti-CD3 (SK7), anti- CD14 (M2E2), anti-CD19 (4G7), anti-CD56 (MY31) and anti-CD235a (GA-R2; all from Becton Dickinson unless noted).

Cells were isolated on a FACSAria (355-, 405-, 488-, 561- and 633-nm lasers; BD Immunocytometry Systems). The DNA-intercalating dye DAPI (4′,6-diamid- ino-2-phenylindole) was added for analysis of viability. A 'no-antibody' control defined negative gates. B1 cell gating was defined using the florescent minus one technique.

Quantitative PCR analysis

After isolation of cells with a FACSAria, RNA was extracted with a Qiagen RNAEsay Microkit (Qiagen) and reverse-transcribed with Omniscript RT, OLIGO DT, and RNAguard (Pharmacia Biotech). An ABI Viia7 was used for real-time PCR with Taqman Mastermix and TaqMan probe– based gene-expression analysis (probes (Applied Biosystems). Reactions were done in technical triplicates, optimal reference genes were previously determined(24, 25). Quantitative PCR results were normalized to *B2M* through the use of the change-in-cycling-threshold methods (ΔΔCT).

Statistical analysis

Prism version 5 (GraphPad Software Inc) was used for statistical analysis and graphic generation. Flow cytometry data were analyzed with FlowJo software.

Results

Clinical and Demographic Characteristics of Subjects

Clinical data of the SCID patients and normals are presented in Table I. BM from 6 patients with SCID was examined, along with 4 normal adult BMs and 3 normal umbilical cord bloods. Three of the SCID patients have X-SCID, and one had JAK3-SCID. As an age matched control, we also examined BM from two patients with Adenosine Deaminase (ADA)-SCID who were on PEG-ADA therapy at the time of BM collection.

SCID patients' T cells are of maternal origin

As expected based on findings in peripheral blood, patients with SCID demonstrated a markedly reduced frequency of T lymphoid cells (CD3+) in their BM compared to typical BM and cord blood (**Fig. 1a**). Of the patients who were analyzed, 3 of 4 had detectable maternal engraftment of lymphocytes based on Fluorescent In Situ Hybridization (FISH). Consistent with maternal engraftment, T cells in all SCID patients were predominantly CD45RO+ cells, in contrast to normal adult BM and cord blood. The ratio of mature CD45R0+ cells to immature CD45RA+ cells was higher within the SCID patients than in either the normal BM or cord blood samples (**Fig. 1b**). Concordant with their phenotype all SCID patients had less than 1% NK cells (CD56+)(**Fig. 1c**).

LMPP and CLP generation is not dependent on IL2Rg expression

Within both the normal and patient BM samples examined, the primitive markers CD34 and CD38 were detected amongst Lin- hematopoietic cells (**Fig. 2a**). We have

previously shown that during differentiation of HSC into CD34+lin-CD45RA+ CD62L LMPP, *IL2RG* is significantly up-regulated and continues to increase between the LMPP and CLP stages.(24) We thus investigated whether absence of IL2RG would affect the earliest stages of human lymphoid commitment. Analysis of BM showed that the CLP (CD10+CD45RA+) and LMPP (CD10-CD45RA+CD62L^{hi}) populations were readily detectable BM from two infants with X-SCID and one with Jak3-SCID (**Figs. 2b and 2c**). Thus signaling through the common gamma chain is not required for the earliest stage of lymphoid commitment.

IL7Rα is detected in the absence of the common gamma chain

Consistent with BM from normal infants, most CD34+ cells from X-SCID and Jak3-SCID were B cell progenitors, expressing an immunophenotype CD10+ CLPs or Pro-B cells. In all examined samples, robust CLP and Pro-B populations could be phenotypically detected. (**Fig. 3a**). Surface expression of IL7Rα (which typically partners with γc) was detected in the early CLP (CD34+CD10+CD19-), an expression pattern also seen in normal BM (**Fig. 3b**). (26) IL7Rα's alternative dimerization partner, Thymic Stromal Lymphopoietin (TSLP, gene name *CRLF2*), was not detected by flow cytometry on any population of cells (data not shown). Thus signaling through the common gamma chain is not required for normal generation of B lymphoid progenitors, or surface IL7Ralpha expression.

Early B Cell Production is maintained in the absence of IL7 signaling

Despite the lack of functional γc, X-SCID and JAK3 patients were able to produce several stages of mature B cells, including cells that expressed surface immunoglobulin (IgM) (**Figs. 4a, 4b, and 4c**). These cells were not of exclusively fetal origin B1 cells, as the majority of detected cells did not show the B1 phenotype ($CD20^{+}CD3^{-}CD43^{+}CD27^{+}$) (**Figs. 4d and 4e**). Consistent with their normal counter parts, early CLP and Pro-B cells had detectable levels of the early lymphoid genes Rag1 and TDT, and also expressed EBF1. (**Figs. 5a, 5b, and 5c**).

Discussion

A potential explanation for circulating B cells found in patients with SCID is that the cells are of the B-1 cell population, a population of spontaneously IgM secreting B cells of fetal origin that arise from a distinct hematopoietic progenitor.(27, 28) Recent developments have identified a potential B1 population in human UCB and peripheral blood. (29) In our studies, the majority of B cells interrogated did not express the B1 phenotype.

References

1. Noguchi M, Yi H, Rosenblatt HM, Filipovich AH, Adelstein S, Modi WS, et al. Interleukin-2 receptor gamma chain mutation results in X-linked severe combined immunodeficiency in humans. Cell. 1993 Apr 9;73(1):147-57.
2. Leonard WJ. Cytokines and immunodeficiency diseases. Nat Rev Immunol. 2001 Dec;1(3):200-8.
3. Russell SM, Keegan AD, Harada N, Nakamura Y, Noguchi M, Leland P, et al. Interleukin-2 receptor gamma chain: a functional component of the interleukin-4 receptor. Science. 1993 Dec 17;262(5141):1880-3.
4. Noguchi M, Nakamura Y, Russell SM, Ziegler SF, Tsang M, Cao X, et al. Interleukin-2 receptor gamma chain: a functional component of the interleukin-7 receptor. Science. 1993 Dec 17;262(5141):1877-80.
5. Asao H, Okuyama C, Kumaki S, Ishii N, Tsuchiya S, Foster D, et al. Cutting edge: the common gamma-chain is an indispensable subunit of the IL-21 receptor complex. J Immunol. 2001 Jul 1;167(1):1-5.
6. Kondo M, Takeshita T, Ishii N, Nakamura M, Watanabe S, Arai K, et al. Sharing of the interleukin-2 (IL-2) receptor gamma chain between receptors for IL-2 and IL-4. Science. 1993 Dec 17;262(5141):1874-7.
7. Kimura Y, Takeshita T, Kondo M, Ishii N, Nakamura M, Van Snick J, et al. Sharing of the IL-2 receptor gamma chain with the functional IL-9 receptor complex. Int Immunol. 1995 Jan;7(1):115-20.
8. Buckley RH. Primary immunodeficiency diseases due to defects in lymphocytes. N Engl J Med. 2000 Nov 2;343(18):1313-24.
9. Witthuhn BA, Silvennoinen O, Miura O, Lai KS, Cwik C, Liu ET, et al. Involvement of the Jak-3 Janus kinase in signalling by interleukins 2 and 4 in lymphoid and myeloid cells. Nature. 1994 Jul 14;370(6485):153-7.
10. Johnston JA, Kawamura M, Kirken RA, Chen YQ, Blake TB, Shibuya K, et al. Phosphorylation and activation of the Jak-3 Janus kinase in response to interleukin-2. Nature. 1994 Jul 14;370(6485):151-3.
11. Macchi P, Villa A, Giliani S, Sacco MG, Frattini A, Porta F, et al. Mutations of Jak-3 gene in patients with autosomal severe combined immune deficiency (SCID). Nature. 1995 Sep 7;377(6544):65-8.
12. Russell SM, Tayebi N, Nakajima H, Riedy MC, Roberts JL, Aman MJ, et al. Mutation of Jak3 in a patient with SCID: essential role of Jak3 in lymphoid development. Science. 1995 Nov 3;270(5237):797-800.
13. DiSanto JP, Muller W, Guy-Grand D, Fischer A, Rajewsky K. Lymphoid development in mice with a targeted deletion of the interleukin 2 receptor gamma chain. Proc Natl Acad Sci U S A. 1995 Jan 17;92(2):377-81.
14. Sugamura K, Asao H, Kondo M, Tanaka N, Ishii N, Ohbo K, et al. The interleukin-2 receptor gamma chain: its role in the multiple cytokine receptor complexes and T cell development in XSCID. Annu Rev Immunol. 1996;14:179-205.
15. Cao X, Shores EW, Hu-Li J, Anver MR, Kelsall BL, Russell SM, et al. Defective lymphoid development in mice lacking expression of the common cytokine receptor gamma chain. Immunity. 1995 Mar;2(3):223-38.

16. Thomis DC, Gurniak CB, Tivol E, Sharpe AH, Berg LJ. Defects in B lymphocyte maturation and T lymphocyte activation in mice lacking Jak3. Science. 1995 Nov 3;270(5237):794-7.
17. Park SY, Saijo K, Takahashi T, Osawa M, Arase H, Hirayama N, et al. Developmental defects of lymphoid cells in Jak3 kinase-deficient mice. Immunity. 1995 Dec;3(6):771-82.
18. Nosaka T, van Deursen JM, Tripp RA, Thierfelder WE, Witthuhn BA, McMickle AP, et al. Defective lymphoid development in mice lacking Jak3. Science. 1995 Nov 3;270(5237):800-2.
19. Peschon JJ, Morrissey PJ, Grabstein KH, Ramsdell FJ, Maraskovsky E, Gliniak BC, et al. Early lymphocyte expansion is severely impaired in interleukin 7 receptor-deficient mice. J Exp Med. 1994 Nov 1;180(5):1955-60.
20. Kikuchi K, Kasai H, Watanabe A, Lai AY, Kondo M. IL-7 specifies B cell fate at the common lymphoid progenitor to pre-proB transition stage by maintaining early B cell factor expression. J Immunol. 2008 Jul 1;181(1):383-92.
21. Kikuchi K, Lai AY, Hsu CL, Kondo M. IL-7 receptor signaling is necessary for stage transition in adult B cell development through up-regulation of EBF. J Exp Med. 2005 Apr 18;201(8):1197-203.
22. Dias S, Silva H, Jr., Cumano A, Vieira P. Interleukin-7 is necessary to maintain the B cell potential in common lymphoid progenitors. J Exp Med. 2005 Mar 21;201(6):971-9.
23. Puel A, Ziegler SF, Buckley RH, Leonard WJ. Defective IL7R expression in T(-)B(+)NK(+) severe combined immunodeficiency. Nat Genet. 1998 Dec;20(4):394-7.
24. Kohn LA, Hao QL, Sasidharan R, Parekh C, Ge S, Zhu Y, et al. Lymphoid priming in human bone marrow begins before expression of CD10 with upregulation of L-selectin. Nat Immunol. 2012 Oct;13(10):963-71.
25. Vandesompele J, De Preter K, Pattyn F, Poppe B, Van Roy N, De Paepe A, et al. Accurate normalization of real-time quantitative RT-PCR data by geometric averaging of multiple internal control genes. Genome Biol. 2002 Jun 18;3(7):RESEARCH0034.
26. Ryan DH, Nuccie BL, Ritterman I, Liesveld JL, Abboud CN, Insel RA. Expression of interleukin-7 receptor by lineage-negative human bone marrow progenitors with enhanced lymphoid proliferative potential and B-lineage differentiation capacity. Blood. 1997 Feb 1;89(3):929-40.
27. Montecino-Rodriguez E, Leathers H, Dorshkind K. Identification of a B-1 B cell-specified progenitor. Nat Immunol. 2006 Mar;7(3):293-301.
28. Dorshkind K, Montecino-Rodriguez E. Fetal B-cell lymphopoiesis and the emergence of B-1-cell potential. Nat Rev Immunol. 2007 Mar;7(3):213-9.
29. Griffin DO, Holodick NE, Rothstein TL. Human B1 cells in umbilical cord and adult peripheral blood express the novel phenotype CD20+ CD27+ CD43+ CD70. J Exp Med. 2011 Jan 17;208(1):67-80.
30. Rossi MI, Yokota T, Medina KL, Garrett KP, Comp PC, Schipul AH, Jr., et al. B lymphopoiesis is active throughout human life, but there are developmental age-related changes. Blood. 2003 Jan 15;101(2):576-84.

Table I: Source of Hematopoietic Samples
Alternative Title: Patient Characteristics

Cell Source	Clinical Genotype	Phenotype	Age at Analysis	Sex
Bone Marrow	IL2Rγ SCID (1)	T- B+ NK-	3 months	M
Bone Marrow	IL2Rγ SCID (2)	T- B+ NK-	2 weeks	M
Bone Marrow	IL2Rγ SCID (3)	T- B+ NK-	8 weeks	M
Bone Marrow	JAK3 SCID	T- B+ NK-	3 months	F
Bone Marrow	ADA SCID (1)	T- B+ NK+[a]	3 months	F
Bone Marrow	ADA SCID (2)	T- B- NK+	21 months	F
Bone Marrow	Normal	T+ B+ NK+	6 yrs	Unknown
Bone Marrow	Normal	T+ B+ NK+	Adult (>20yrs)	Unknown
Bone Marrow	Normal	T+ B+ NK+	Adult (>20yrs)	Unknown
Bone Marrow	Normal	T+ B+ NK+	Adult (>20yrs)	Unknown
Cord Blood	Normal	T+ B+ NK+	Neonatal	Unknown
Cord Blood	Normal	T+ B+ NK+	Neonatal	Unknown
Cord Blood	Normal	T+ B+ NK+	Neonatal	Unknown

[a]Patient on exogenous ADA therapy at time of phenotyping

IL2Rγ SCID IL2Rgamma deficient Severe Combined Immune Deficiency aka X linked Severe Combined Immune Deficiency
JAK3 SCID Janus Associated Kinase 3 deficient Severe Combined Immune Deficiency
ADA SCID Adenosine Deaminase Severe Combined Immune Deficiency
T T cell
B B cell
NK Natural Killer cell
+ Cell type present
- Cell type absent

Figure Caption List

Fig. 1 T cell deficiency in SCID patients
(**a**) The percentage of mature $CD34^-$ human bone marrow or cord cells that are $CD3^+$ T cells as detected by flow cytometry (**b**) Ratio of mature CD45R0+ cells to immature CD45RA+ cells amongst human bone marrow CD3+ T cells as detected by flow cytometry

Fig. 2 Lack of gamma chain signaling does not block early lymphoid commitment
(**a**) CD34 and CD38 expression on CD34 enriched lineage negative (Lin^-) hematopoietic cells (Lineage includes CD3, CD14, CD19, CD56 and Glycophorin a) (**b**) Common Lymphoid Progenitors ($CD10^+CD45RA^+$) are detected within CD34+Lin^- hematopoietic cells from all sources (**c**) Lymphoid-primed multipotent progenitors ($CD10^-$ $CD62L^{hi}CD45RA^+$) are detected within CD34+$CD10^-Lin^-$ hematopoietic cells from all sources

Fig. 3 IL7Rα is detected in the absence of the common gamma chain signaling pathway
(**a**) CD10 and CD19 expression on $CD34^+$ hematopoietic progenitor cells (**b**) IL7Rα expression on Common Lymphoid Progenitors ($CD34^+CD10^+CD19^-$) (red) and unstained controls (black)

Fig. 4 B Cell Differentiation is maintained in the absence of IL7 signaling
(**a**) CD19 and CD20, (**b**) CD24 and CD20, or (**c**) membrane bound IgM and CD20 expression on $CD34^-$ hematopoietic cells. (**d**) CD3 and CD20 expression on $CD34^-$ cells (**e**) B1 cells ($CD43^+CD27^+$) within $CD3^-CD20^+$ B cells

Fig. 5 V(D)J recombination and early B cell differentiation is maintained in the absence of IL7 signaling
Quantitative PCR analysis of gene expression, presented relative to expression in CD34+CD10+ CLP cells for (**a**) DNA nucleotidylexotransferase (*DNTT*, aka *TDT*) (**b**) Recombination activating gene 1 (*RAG1*) (**c**) Early B Cell Factor 1 (*EBF1*)

Fig. 1 Patients with SCID show decreased frequency of NK and T cells, and predominately mature T cells

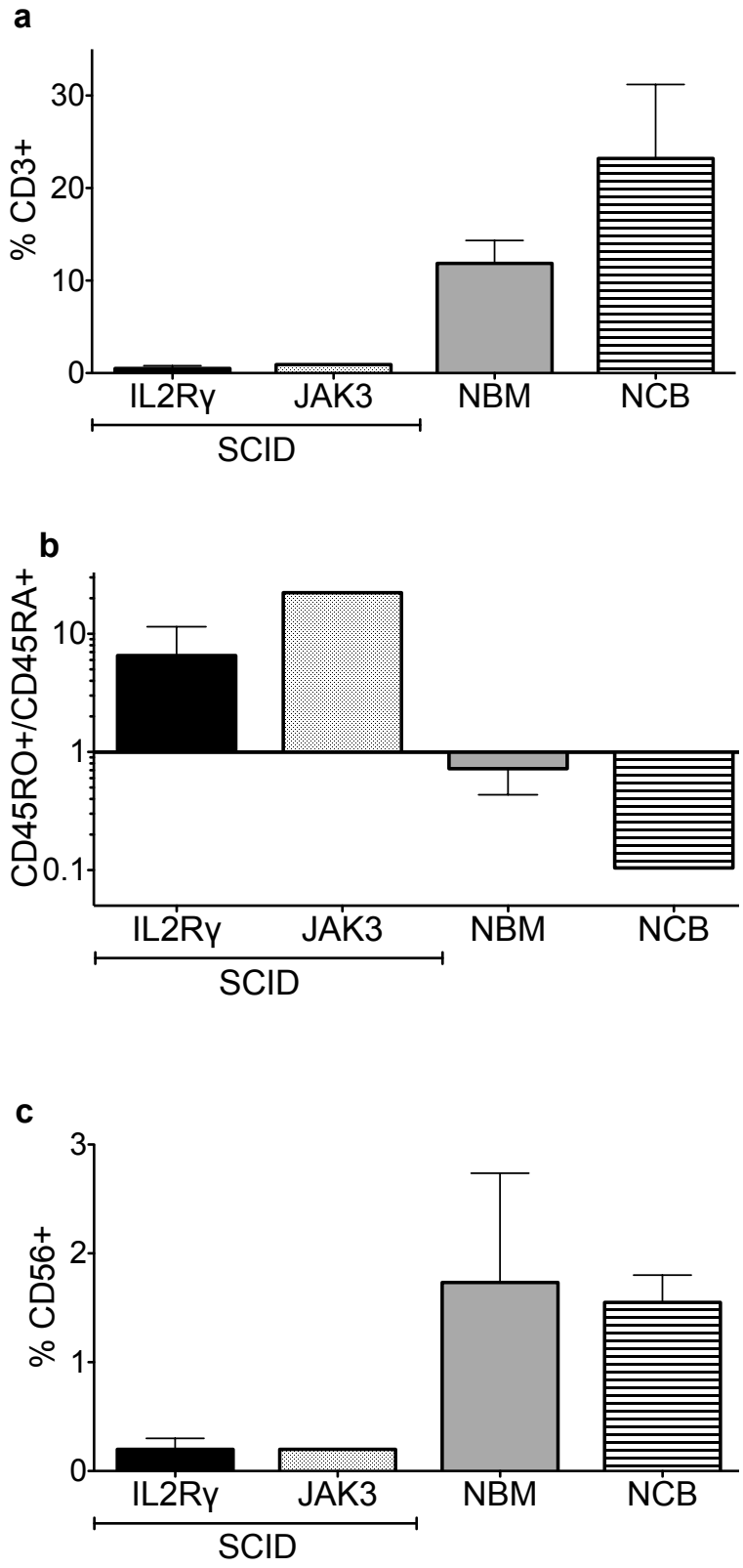

Fig. 2 Lack of IL7 signaling does not block early lymphoid commitment

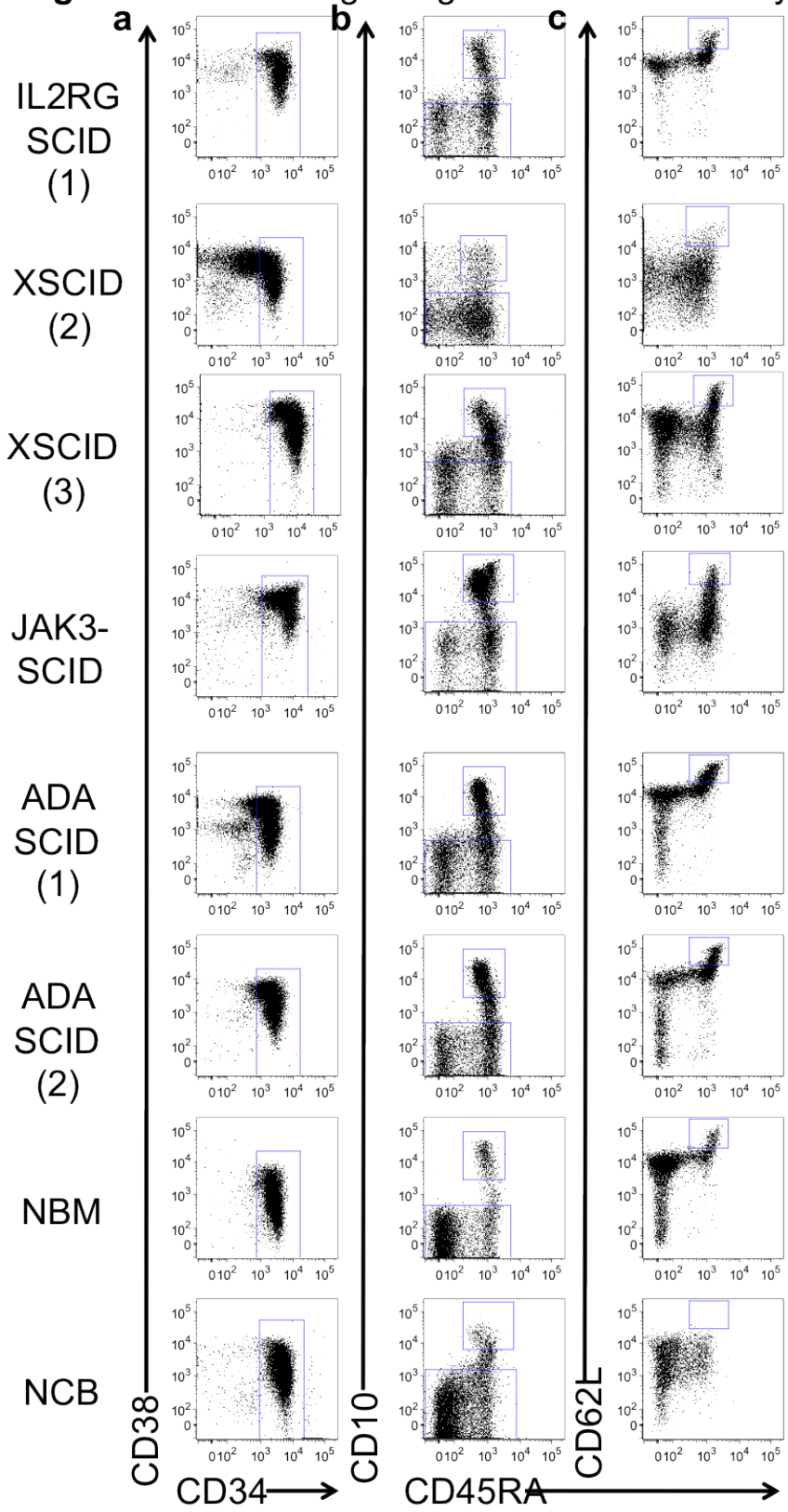

Fig. 3 IL7Rα is detected in the absence of the common gamma chain

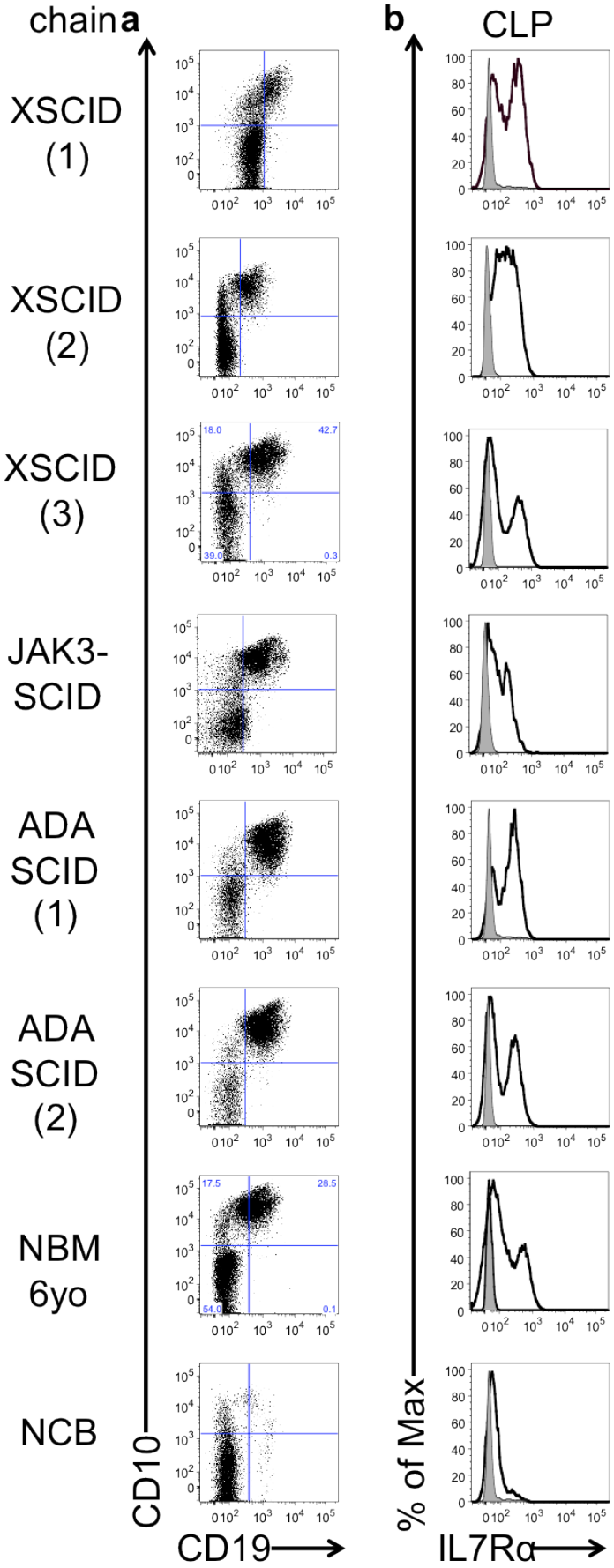

Fig. 4 Early B Cell Production is maintained in the absence of IL7 signaling

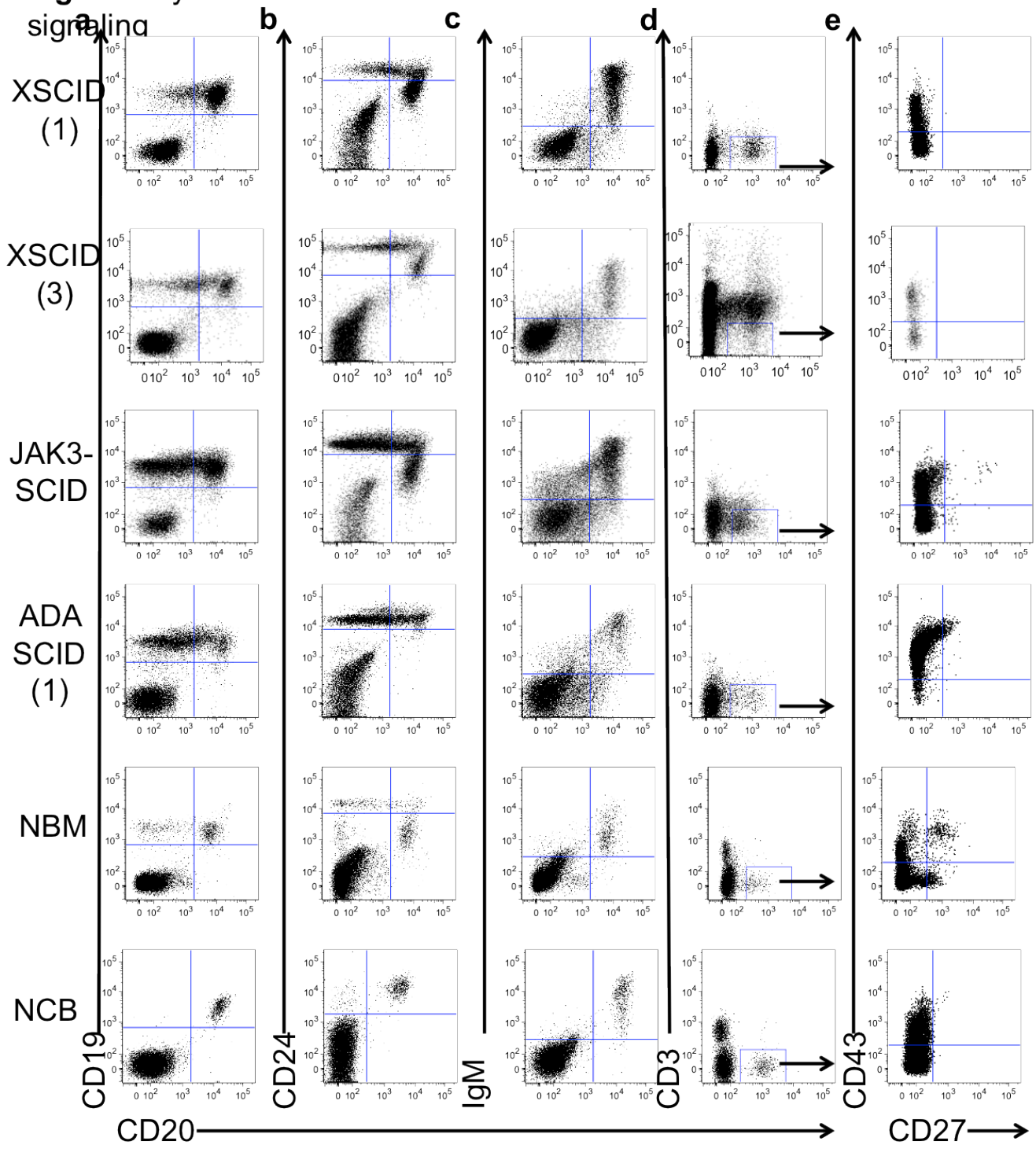

Fig. 5 V(D)J recombination and early B cell differentiation is maintained in the absence of IL7 signaling

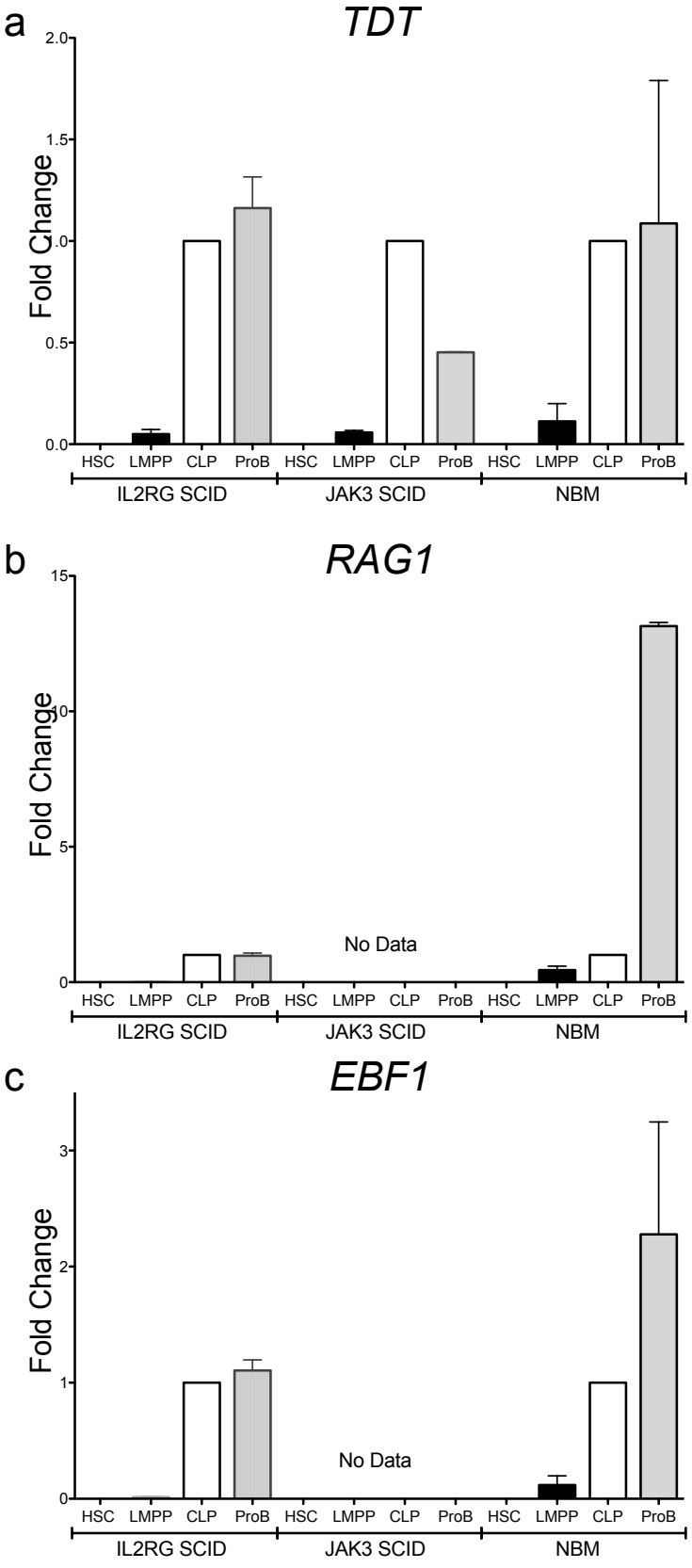

Chapter 4
Rapid Thymic Reconstitution Following Bone Marrow Transplantation in Neonatal Mice is VEGF-Dependent

Chapter 4 presents research in which I participated on comparing thymic reconstitution in neonatal and adult mice post transplantation. Neonates undergo more rapid and efficient thymic reconstitution than adults, even when BM engraftment is minimal and in the absence of pre-transplantation radiation. Inhibition of VEGF prior to transplantation prevents rapid thymic reconstitution in neonates, but has no effect on thymic reconstitution in adults.

Lisa Ann Kohn designed, performed, collected, and analyzed experiments.

Biol Blood Marrow Transplant.

2012 May; 18(5): 683–689. Published online 2012 January 25. doi:

10.1016/j.bbmt.2012.01.006

PMCID: PMC3334422

Rapid Thymic Reconstitution Following Bone Marrow Transplantation in Neonatal Mice is VEGF-Dependent

Andrew R. Cuddihy,1,2,* Batul T. Suterwala,1,* Shundi Ge,1 Lisa A. Kohn,1 Julie Jang,1 Jacob Andrade,1 Xiaoyan Wang,3 and Gay M. Crooks1

From the 1Department of Pathology and Laboratory Medicine, University of California Los Angeles, Los Angeles, California;

2Myeloma Research Group, Central Clinical School, Alfred Hospital/Monash University, Melbourne, Victoria, 3004, Australia;

3Department of Biostatistics, University of California Los Angeles, Los Angeles, California.

Financial disclosure: See Acknowledgments on page 689.

*A.R. Cuddihy and B.T. Suterwala contributed equally to this article. Correspondence and reprint requests: Gay M. Crooks, MD, Department of Pathology & Laboratory Medicine, David Geffen School of Medicine, University of California Los Angeles, A7- 149 CHS, 10833 Le Conte Avenue, Los Angeles, CA 90095- 1732 (e-mail: gcrooks@mednet.ucla.edu).

Abstract

Age-related differences in thymic function influence the rapidity of T cell reconstitution following hematopoietic stem cell transplantation (HSCT). In adults, thymic reconstitution is delayed until after marrow engraftment is established, and is significantly improved by approaches that increase marrow chimerism, such as pre-transplant irradiation. In contrast, we show that neonatal mice undergo more rapid and efficient thymic reconstitution than adults, even when bone marrow engraftment is minimal and in the absence of pre-transplant radiation. We have previously shown that the neonatal thymus produces high levels of vascular endothelial growth factor (VEGF) that drives angiogenesis locally. In this report we show that inhibition of VEGF prior to HSCT prevents rapid thymic reconstitution in neonates, but has no effect on thymic reconstitution in adults. These data suggest that the early, radiation independent, thymic reconstitution unique to the neonatal host is mediated through VEGF, and reveals a novel pathway that might be targeted to improve immune reconstitution post-HSCT.

INTRODUCTION

Immune reconstitution following allogeneic he- matopoietic stem cell transplantation (HSCT) is frequently slow and imperfect, with consequent morbidity from opportunistic infections [1-5]. Several factors contribute to immune dysfunction after allogeneic HSCT, including the presence of graft- versus-host disease, immune suppressive medications, and damage to the thymic microenvironment from con- ditioning regimens and age-related involution [1-3].

Mature tolerant T cells are generated after HSCT through a complex stepwise process that begins with homing and engraftment in the marrow. Pretransplan tation conditioning facilitates the initial stage of HSC engraftment and proliferation in the marrow, with subsequent differentiation into progeny that are re- cruited to the thymus to generate donor-derived thy- mocytes [3]. In murine studies, more than 2 weeks are required for donor-derived CD41CD81 cells to first appear in the thymus after transplantation [6]. In the clinical setting, severe T lymphopenia persists in patients for at least 100 days posttransplantation [1-5].

The paradigm that assumes robust thymic reconstitution requires pretransplantation condition- ing is challenged by observations made over several decades in the setting of HSCT for Severe Combined Immune Deficiency (SCID). When newborns and young infants with SCID undergo HSCT from HLA-matched siblings, T cell reconstitution can often be accomplished without pretransplantation condi- tioning [7-10]. In addition, T cell reconstitution occurs rapidly and is more robust when HSCT for SCID is performed in the newborn period [3,11,12], suggesting that neonatal thymus is particularly permissive to reconstitution with donor cells.

Postnatal thymic growth in immune-competent humans and mice is most rapid during the neonatal period [13-15]. Our group has shown that during the first few days of murine postnatal life, the thymus is a site of vigorous thymocyte proliferation and vascular endothelial growth factor (VEGF)- dependent angiogenesis [13]. Under the influence of lo- cally produced VEGF, neonatal thymic vasculature is a dense network of capillaries. Beyond the first week of life, as VEGF

dependence is lost, the capillaries meta- morphose to a mature hierarchic adult vasculature. Blocking VEGF during the neonatal period not only causes loss of vascular density and capillary pruning, but also reduces thymocyte numbers [13]. In the current studies, we show that the unique pattern of thymic re- constitution after bone marrow transplantation (BMT) in the neonate is likely influenced by the same VEGF- mediated mechanisms that contribute to robust thymo- poiesis during normal neonatal development.

MATERIALS AND METHODS

BMT and VEGF Inhibition

In all experiments, unfractionated bone marrow (BM; 1 107 cells/animal) from 6- to 8-week-old C57Bl6/J (CD45.2) mice was transplanted intrave- nously into neonatal (1 day old, via facial vein) or adult (6 weeks old, via retro-orbital injection) Non-Obese Diabetic (NOD)/SCID/IL-2Rg2/2 (NSG; CD45.1) mice (Jackson Research Laboratories, Bar Habor, ME). Where indicated, mice were sublethally irradi- ated 2 hours pre-BMT with 150 cGy (neonates) or 270 cGy (adults) using a Cs-137 source [13]. For the timed transplant experiments in 1-, 4-, 7-, and 10- day-old NSG mice, 1

107 unfractionated C57Bl6/J BM (CD45.2) cells were injected intra- hepatically without pretransplantation irradiation. In all indicated experiments, neonates and adults received either VEGF-Trap or hFc control (25 mg/kg) (Regeneron Pharmaceuticals, Tarrytown, NY) [16] 24 hours prior to BMT (and 22 hours prior to irradiation). Mice were kept in specific pathogen-free facilities at

Children's Hospital Los Angeles and University of California Los Angeles under approved protocols.

In Vivo Labeling of Thymic Vasculature

Mice were anesthetized and perfused with a mixture of biotinylated tomato lectin (10 mg/kg; Vector Labo- ratories, Burlingame, CA) and streptavidin-Cy3 (3.1 mg/kg; Jackson ImmunoResearch, West Grove, PA) via facial vein (neonates) or cardiac injection (adults). Two minutes later, mice were perfused with PBS fol- lowed by 4% paraformaldehyde. Isolated thymi were fixed in 4% paraformaldehyde [13]. Sections (200 mm each) of 3% agarose-embedded thymi were examined for lectin labeling using a Leica TCS SP1 confocal mi- croscope with a Plan Apo 10/0.4NA objective Tokyo, Japan and images acquired using Leica LCS software. Where indicated, mice received either 25 mg/kg hFc or VEGF trap intraperitoneally 24 hours before the lectin staining. Due to the difficulty in identifying and dissecting thymi from nontransplanted adult NSG mice, thymi from NOD SCID b2m2/2 were used to study the vasculature of adult immune deficient mice. Analysis

Mice were euthanized 3 or 6 weeks posttransplan- tation for analysis of engraftment. Single cell suspen- sions were created from thymi and BM of all animals. The cells were incubated with Mouse BD Fc Block (BD Biosciences, San Jose, CA) followed by incubation with rat anti-mouse CD45.2 (FITC) to identify donor cells and rat anti-mouse CD4 (APC) and CD8 (PE) antibodies (all BD Biosciences). Cells were acquired on a FACSCalibur or LSRII (BD Bio- sciences), and data were analyzed using FlowJo soft- ware (Tree Star, Ashland, OR). For morphological analyses, 5-mm sections of paraffin-embedded thymi were stained

with hematoxylin and eosin H&E and ex- amined using an Olympus BX51 microscope fitted with a 4 /0.13 phl objective Tokyo, Japan. Images were acquired with an Olympus DP 72 digital color camera (Tokyo, Japan) and DP2-BSW software.

Statistical Analysis

Data were analyzed using the Wilcoxon rank sum test or mixed model analysis of variance to account for inter-experiment variability. P values \.05 were considered significant. All statistical analyses were per- formed with statistical software SAS version 9.1 [17].

RESULTS

Neonatal Murine Thymus Is Uniquely Permissive to Rapid and Robust Reconstitution after BMT, Independent of Pretransplantation Conditioning

To examine if the impact of radiation on thymic and BM reconstitution is affected by recipient age, immune-deficient neonatal and adult mice underwent allogeneic BMT with or without prior conditioning with sublethal doses of total body irradiation. Six weeks after transplantation, donor chimerism in the BM was significantly higher in all irradiated compared with nonirradiated mice, regardless of age at transplantation (Figure 1A; P \ .001). Thus, pretransplantation irradi- ation, even at sublethal doses, is required for efficient BM engraftment irrespective of the host age. Despite similar patterns of BM chimerism in both age groups, a profound difference was seen in the pat- tern of thymic reconstitution between neonatal and adult recipients. In parallel with BM chimerism, reconstitution of the thymus in adults

was almost un- detectable in nonirradiated recipients, and was signifi- cantly increased with irradiation (Figure 1B; P \ .001).

Thymic reconstitution was significantly greater in mice that received transplantations as neonates when compared with adult recipients, irrespective of irradia- tion (Figure 1B; P \ .01 for irradiated and P \ .001 for nonirradiated cohorts). In addition, thymic reconstitu- tion in neonates was rapid; even in the absence of irra- diation, donor cells were detected in the thymus as early as 48 hours (data not shown) and efficiently reconstituted the thymus at 1 and 2 weeks posttrans- plantation when compared with BM reconstitution (Figure 1C). By 2 weeks, most donor thymocytes had progressed to the double positive (DP; CD41CD81) stage (Figure 1D).

Thymic Vasculature in Immune-Deficient and Immune-Competent Mice Is VEGF-Dependent during the Neonatal Period

We have previously reported that the thymic vas- culature in immune-competent neonatal mice consists of a dense capillary network that is VEGF- dependent [13]. By adulthood, the vasculature has matured to a hierarchic pattern losing most of the capillaries and becoming VEGF-independent [13]. Although largely devoid of thymocytes, thymi of immune-deficient neonatal mice have the same dense capillary network as immune-competent neonatal mice, and this vascular phenotype is similarly lost by adulthood (Figure 2A). As with immune- competent mice, inhibition of VEGF in the immune-deficient neonatal thymus causes loss of dense capillaries and the appearance of an adult vas- cular pattern (Figure 2B).

The Window of Efficient, Radiation-Independent Thymic Reconstitution Closes during the First Week of Postnatal Life

Our previous work showed that VEGF-dependent vasculature of the thymus transitions to a mature VEGF-independent vasculature during the first week of life (ie, by the end of the murine neonatal period) [13]. We therefore evaluated if the permissive environ- ment for thymic reconstitution post-HSCT also changes during the first week of life. Animals were transplanted without prior irradiation at 1, 4, 7, or 10 days after birth, and thymocyte numbers were ana- lyzed 3 weeks after transplantation. Age at time of transplantation did not affect the level of donor chime- rism in the bone marrow (Figure 2C). However, the ability of donor cells to reconstitute the thymus declined markedly during the first week of life (Figure 2D), a pattern coinciding with the previously reported temporal changes in vascular density and VEGF-dependence [13].

VEGF Inhibition Significantly Delays Thymic Reconstitution in Neonatal NSG Mice

In view of the parallel decline in thymic reconstitu- tion and VEGF-dependence of thymic vasculature, we administered VEGF-Trap (a VEGFR1/2 fusion recep- tor [18]) 24 hours before transplantation to determine if thymic reconstitution was VEGF-dependent. VEGF inhibition significantly delayed thymic reconstitution in nonirradiated neonatal mice, as shown by a significant reduction in donor thymopoiesis at 3 weeks post-BMT (Figure 3A; P \ .01). A similar trend was seen 3 weeks after transplantation of irradiated neonatal mice (Figure 3B). By 6 weeks posttransplantation, thymocyte numbers had increased to equivalent levels in control and VEGF-Trap-treated neonates (Figure 3A and B), demonstrating that

VEGF inhibition did not limit the ability of the thymus to recruit and support proliferation of precursors through the more typical mechanisms of reconstitution that occur after marrow engraftment is well-established. In contrast, thymic reconstitution of irradiated adults was not affected by pretransplantation VEGF inhibition (Figure 3C).

The age-specific effect of VEGF inhibition was also seen when examining the differentiation stages of donor-derived thymocytes. Treatment with VEGF- Trap resulted in a higher frequency of the immature CD42CD82 double negative (DN) fraction in both nonirradiated (Figure 3D) and irradiated newborn mice (Figure 3E; P \ .01) at 3 weeks post-BMT. The frequency of CD41CD81 DP thymocytes corre- spondingly dropped with VEGF inhibition in nonirra- diated (Figure 3G) and irradiated (Figure 3H; P \ .01) neonatal mice. However, by 6 weeks, VEGF inhibition had no effect on the frequencies of DN or DP thymo- cytes in the newborn mice (Figure 3D-H). VEGF inhi- bition had no effect on the frequency of DP or DN cells in adults (Figure 3F and I). Thus, VEGF inhibition in the neonate resulted in both lower numbers of total thymocytes and a more immature thymocyte profile at 3 weeks post-BMT, consistent with a delay in thymic reconstitution. The frequencies of single positive CD41 and CD81 cells in both newborn and adult mice were not affected by VEGF inhibition (data not shown), suggesting that VEGF is unlikely to be in- volved in the egress of mature thymocytes.

The effects of VEGF inhibition on thymic recon- stitution were confirmed by analysis of thymic size and histology. Three weeks posttransplantation, thymi from VEGF-Trap-treated neonates were smaller and lacked the medullary and cortical

structures of control mice, regardless of whether the mice were irradiated before transplantation. By 6 weeks, thymi from VEGF-Trap-treated mice showed similar thymic ar- chitecture and size compared with control mice, again demonstrating that VEGF inhibition did not perma- nently damage the thymus architecture or function (Figure 3J, K).

The size and histology of the thymi from irradiated adult NSG mice was not affected by VEGF inhibition (Figure 3L). Of note, at three weeks post-BMT, thymi from mice transplanted as adults were significantly smaller and less cellular than those transplanted as ne- onates, in most cases being too small to clearly identify. By six weeks post-BMT, even though thymi from adult recipients had developed distinct cortical and medul- lary structures (Figure 3L), they never achieved sizes equivalent to those from mice transplanted as neonates.

DISCUSSION

Our data demonstrate that the thymus of the new- born immune-deficient mouse provides a highly per- missive environment for rapid thymic reconstitution after BMT, and that VEGF-mediated mechanisms have a role in producing this unique environment. The thymic microenvironment changes during the first 7 days after birth, during which time the thymic vascu- lature matures and becomes VEGF-independent [13]. Neonatal thymic reconstitution is both rapid and robust, does not require pretransplantation condition- ing, and does not require a high level of BM chimerism.

During steady state, ingress of progenitors into the thymus occurs in waves in response to the availability of empty intra-thymic niches [19-21]. These waves of

recruitment and ‘‘settling’’ of marrow-derived progeni- tors in the adult murine thymus are thought to be medi- ated at least partly by interactions between the homing molecules P-selectin with PSGL-1 [22], and the chemo- kine receptors CCR7 and CCR9 with their ligands [23,24]. Zlotoff et al. [25] found that although long-term thymic reconstitution after BMT used the same mechanisms as seen in steady state, early (3 weeks post- BMT) thymic reconstitution occurred independently of CCR7 and CCR9 [25]. It is interesting to note that in our own study with neonatal animals, dependence on VEGF was also different between the 3-week and 6- week phases of reconstitution, irrespective of irradiation. Although the data from Zlotoff et al. [25] was generated in a different transplantation setting from our own (adult irradiated mice versus neonatal mice), the 2 studies share the concept that early and late thymic reconstitution may be mediated by different mechanisms.

We propose that high local VEGF specifically affects the early phase of thymic seeding in neonates, as VEGF inhibition reduces thymocyte numbers 3 weeks after BMT. By 6 weeks after BMT, when the delivery of thymic precursors is dependent on previ- ously described mechanisms of recruitment from the BM, the effect of VEGF inhibition on thymocyte numbers is not evident. This later production of marrow-derived thymocytes presumably overlaps and further adds to the thymopoiesis derived from the ini- tial phase of thymic seeding, thereby accounting for higher levels of thymocyte production in neonates even at later time points. Porritt et al. [6] found that at least 13 days (average .15 days) were required for cells entering the adult thymus to reach the outer cortex and begin to differen-

tiate into DP cells, and even by 3 weeks after transplan- tation, most donor cells had not passed the DN3 stage of differentiation. In our own studies, .95% of donor cells had reached the DP stage of thymocyte differen- tiation by 2 weeks after transplantation of neonatal an- imals. VEGF inhibition in the newborn mice skewed the thymocyte differentiation toward a more immature phenotype with a higher frequency of DN and rela- tively fewer DP thymocytes. We postulate that in new- born mice, VEGF-dependent vasculature permits rapid ingress of thymic progenitors (possibly even by direct seeding before marrow engraftment), which then undergo proliferation in an empty niche resulting in rapid and robust reconstitution of the thymus. It is also possible that local VEGF mediates rapid reconsti- tution of the thymus by augmenting differentiation of DN to DP thymocytes, and subsequent proliferation through mechanisms that are yet to be elucidated.

It is intriguing to speculate whether the processes described here in the murine setting may also contrib- ute to the robust thymopoiesis seen in clinical trans- plantations of infants, particularly in those with SCID who, without pretransplantation conditioning, can achieve rapid T cell reconstitution with little or no donor contribution to the myeloid and B cell lineages [26,27]. Our findings reveal previously unreported mechanisms that mediate efficient thymic reconstitution in neonates, and present novel pathways that might be targeted to improve post- BMT immune reconstitution in the adult.

Figure 1

Neonatal mice show rapid and robust thymic reconstitution after HSCT

Despite similar patterns of BM chimerism in both age groups, a profound difference was seen in the pattern of thymic reconstitution between neonatal and adult recipients. In parallel with BM chimerism, reconstitution of the thymus in adults was almost undetectable in non-irradiated recipients, and was significantly increased with irradiation (Figure 1B, $p < 0.001$)

Figure 2

Immature vascular architecture and robust thymic reconstitution are lost during the first week of postnatal life. (A) In vivo tomato lectin staining comparing vasculature between newborn (left panel) and adult (right panel) immune-competent (C57Bl/6) and immune-deficient (NOD/ SCID/b2m–/–) mice. (B) Vascular endothelial growth factor (VEGF)-Trap reduces vascular density of newborn thymi in immune-competent (C57Bl/ 6) and immune-deficient (NSG) mice. Control mice were treated with hFc. (C, D) Effect of host age on bone marrow (C) and thymic reconstitution (D). NSG neonatal mice were transplanted with CD45.21 bone marrow (BM) without irradiation at day 1, 4, 7, and 10 of life, (n 5 4, 7, 7, and 9 mice, respectively) and analyzed at 3 weeks post–bone marrow transplantation (BMT). All numbers are mean 6 SEM.

Figure 3

Vascular endothelial growth factor (VEGF) inhibition impairs early thymic engraftment of donor cells in mice transplanted as neonates, but not adults. (A) Number of thymocytes in nonirradiated neonates harvested at 3 weeks (hFc [black bars] n 5 9; VEGF-Trap [grey bars] n 5 11; *P \.01) and 6 weeks (hFc n 5 14; VEGF-Trap n 5 11; P 5.30). (B) Number of thymocytes in irradiated neonates harvested at 3 weeks (hFc n 5 6; VEGF-Trap n 5 5; P 5.14) and 6 weeks (hFc n 5 5; VEGF-Trap n 5 4; P 5.5). (C) Number of thymocytes in irradiated adults harvested at 3 weeks (hFc n 5 8; VEGF- Trap n 5 6; P 5.48) or 6 weeks (hFc n 5 7; VEGF-Trap n 5 6; P 5.84). P values were unchanged when thymocyte numbers were normalized to body weight, to account for the smaller size of the VEGF-Trap treated mice. (D-I) Percentage of CD42CD82; double-negative (DN) (D-F) and CD41CD81; double-positive (DP) (G-I) thymocytes from mice treated with hFc (black bars) and VEGF-Trap (grey bars) before transplantation. (D, G) Nonirradiated neonates harvested 3 weeks (hFc n 5 9; VEGF-Trap n 5 5) and 6 weeks (hFc n 5 8; VEGF-Trap n 5 6) posttransplantation. (E, H) Irradiated neonates harvested 3 weeks (hFc n 5 5; VEGF-Trap n 5 3, *P \.01) and 6 weeks (hFc n 5 5; VEGF-Trap n 5 4) posttransplantation. (F, I), Irradiated adults har- vested 3 weeks (hFc n 5 4; VEGF-Trap n 5 2) and 6 weeks (hFc n 5 6; VEGF-Trap n 5 6) posttransplantation. (J-L) H&E stains of thymi from NSG mice treated as described in (A-C) harvested at 3 and 6 weeks. All images shown are at original magnification 4. (J) Nonirradiated NSG mice transplanted as neonates. (K) Irradiated NSG mice transplanted as neonates. (L) Irradiated NSG mice transplanted as adults. In (L), the largest examples of tissue from the 3-week adult cohorts are shown because, in most cases, the thymus was not detected.

Acknowledgments

We would like to thank Gavin Thurston (Regeneron Pharmaceuticals, Tarrytown, NY) for generously providing hFc and VEGF-Trap; Lora Barsky and Ewa Zelinska (CHLA), and Jessica Scholes and Felicia Codrea (Broad Stem Cell Research Center flow cytometry core, UCLA) for assistance with flow cytometry; Chintan Parekh, Brile Chung, Erica Sloan and Katherine Monaghan for invaluable comments and feedback. This work was supported by a California Institute for Regenerative Medicine fellowship to A.R.C (CHLA), and grants from the National Institutes of Health (1P01AI072686) and California Institute of Regenerative Medicine grant (RM1-01707) to G.M.C.

Financial Disclosure: The authors have nothing to disclose

Author Contributions and Conflict of Interests

A.R.C., B.T.S. and G.M.C. designed research and wrote the paper. A.R.C., B.T.S., S.G., L.A.K., J.J. and J.A. performed research, collected, analyzed and interpreted data. X.W. performed statistical analysis. The authors declare no conflict of interest.

References

1. Parkman R, Weinberg KI. Immunological reconstitution following bone marrow transplantation. Immunol Rev. 1997;157:73–8. [PubMed]

2. Storek J, Geddes M, Khan F, Huard B, Helg C, Chalandon Y, et al. Reconstitution of the immune system after hematopoietic stem cell transplantation in humans. Semin Immunopathol. 2008;30(4):425–37. [PubMed]

3. Krenger W, Blazar BR, Hollander GA. Thymic T-cell development in allogeneic stem cell transplantation. Blood. 2011;117(25):6768–76. [PMC free article] [PubMed]

4. Ciurea SO, Mulanovich V, Jiang Y, Bassett R, Rondon G, McMannis J, et al. Lymphocyte recovery predicts outcomes in cord blood and T cell-depleted haploidentical stem cell transplantation. Biol Blood Marrow Transplant. 2011;17(8):1169–75. [PubMed]

5. Seggewiss R, Einsele H. Immune reconstitution after allogeneic transplantation and expanding options for immunomodulation: an update. Blood. 2010;115(19):3861–8. [PubMed]

6. Porritt HE, Gordon K, Petrie HT. Kinetics of Steady-state Differentiation and Mapping of Intrathymic-signaling Environments by Stem Cell Transplantation in Nonirradiated Mice. Journal of Experimental Medicine. 2003;198(6):957–962. [PMC free article] [PubMed]

7. Haynes BF, Markert ML, Sempowski GD, Patel DD, Hale LP. The role of the thymus in immune reconstitution in aging, bone marrow transplantation, and HIV-1 infection. Annu Rev Immunol. 2000;18:529–60. [PubMed]

8. Mackall CL, Fleisher TA, Brown MR, Andrich MP, Chen CC, Feuerstein IM, et al. Age, thymopoiesis, and CD4+ T-lymphocyte regeneration after intensive chemotherapy. N Engl J Med. 1995;332(3):143–9. [PubMed]

9. Hakim FT, Memon SA, Cepeda R, Jones EC, Chow CK, Kasten-Sportes C, et al. Age-dependent incidence, time course, and consequences of thymic renewal in adults. J Clin Invest. 2005;115(4):930–9. [PMC free article] [PubMed]

10. Eyrich M, Wollny G, Tzaribaschev N, Dietz K, Brugger D, Bader P, et al. Onset of thymic recovery and plateau of thymic output are differentially regulated after stem cell transplantation in children. Biol Blood Marrow Transplant. 2005;11(3):194–205. [PubMed]

11. Buckley RH. Molecular defects in human severe combined immunodeficiency and approaches to immune reconstitution. Annu Rev Immunol. 2004;22:625–55. [PubMed]

12. Myers LA. Hematopoietic stem cell transplantation for severe combined immunodeficiency in the neonatal period leads to superior thymic output and improved survival. Blood. 2002;99(3):872–878. [PubMed]

13. Cuddihy AR, Ge S, Zhu J, Jang J, Chidgey A, Thurston G, et al. VEGF-mediated crosstalk within the neonatal murine thymus. Blood. 2009;113(12):2723–31. [PMC free article] [PubMed]

14. Steinmann GG. Changes in the human thymus during aging. Curr Top Pathol. 1986;75:43–88. [PubMed]

15. Haynes BF, Sempowski GD, Wells AF, Hale LP. The human thymus during aging. Immunol Res. 2000;22(2–3):253–61. [PubMed]

16. Andrade J, Ge S, Symbatyan G, Rosol MS, Olch AJ, Crooks GM. Effects of sublethal irradiation on patterns of engraftment after murine bone marrow transplantation. Biol Blood Marrow Transplant. 2011;17(5):608–19. [PMC free article] [PubMed]

17. SAS I. SAS/GeneticsTM 9.1.3 User's Guide. SAS Institute Inc; Cary, NC: 2005.

18. Holash J, Davis S, Papadopoulos N, Croll SD, Ho L, Russell M, et al. VEGF-Trap: a VEGF blocker with potent antitumor effects. Proc Natl Acad Sci U S A. 2002;99(17):11393–8. [PMC free article] [PubMed]

19. Foss DL, Donskoy E, Goldschneider I. The importation of hematogenous precursors by the thymus is a gated phenomenon in normal adult mice. J Exp Med. 2001;193(3):365–74. [PMC free article] [PubMed]

20. Donskoy E, Foss D, Goldschneider I. Gated importation of prothymocytes by adult mouse thymus is coordinated with their periodic mobilization from bone marrow. J Immunol. 2003;171(7):3568–75. [PubMed]

21. Cyster JG. Settling the thymus: immigration requirements. J Exp Med. 2009;206(4):731–734. [PMC free article] [PubMed]

22. Rossi FM, Corbel SY, Merzaban JS, Carlow DA, Gossens K, Duenas J, et al. Recruitment of adult thymic progenitors is regulated by P-selectin and its ligand PSGL-1. Nat Immunol. 2005;6(6):626–34. [PubMed]

23. Ueno T, Saito F, Gray DH, Kuse S, Hieshima K, Nakano H, et al. CCR7 signals are essential for cortex-medulla migration of developing thymocytes. J Exp Med. 2004;200(4):493–505. [PMC free article] [PubMed]

24. Krueger A, Willenzon S, Lyszkiewicz M, Kremmer E, Forster R. CC chemokine receptor 7 and 9 double-deficient hematopoietic progenitors are severely impaired in seeding the adult thymus. Blood. 2010;115(10):1906–12. [PubMed]

25. Zlotoff DA, Zhang SL, De Obaldia ME, Hess PR, Todd SP, Logan TD, et al. Delivery of progenitors to the thymus limits T-lineage reconstitution after bone marrow transplantation. Blood. 2011;118(7):1962–70. [PMC free article] [PubMed]

26. Buckley RH, Schiff SE, Schiff RI, Roberts JL, Markert ML, Peters W, et al. Haploidentical bone marrow stem cell transplantation in human severe combined immunodeficiency. Semin Hematol. 1993;30(4 Suppl 4):92–101. discussion 102–4. [PubMed]

27. Buckley RH, Schiff SE, Schiff RI, Markert L, Williams LW, Roberts JL, et al. Hematopoietic stem-cell transplantation for the treatment of severe combined immunodeficiency. N Engl J Med. 1999;340(7):508–16. [PubMed]

Figure 1

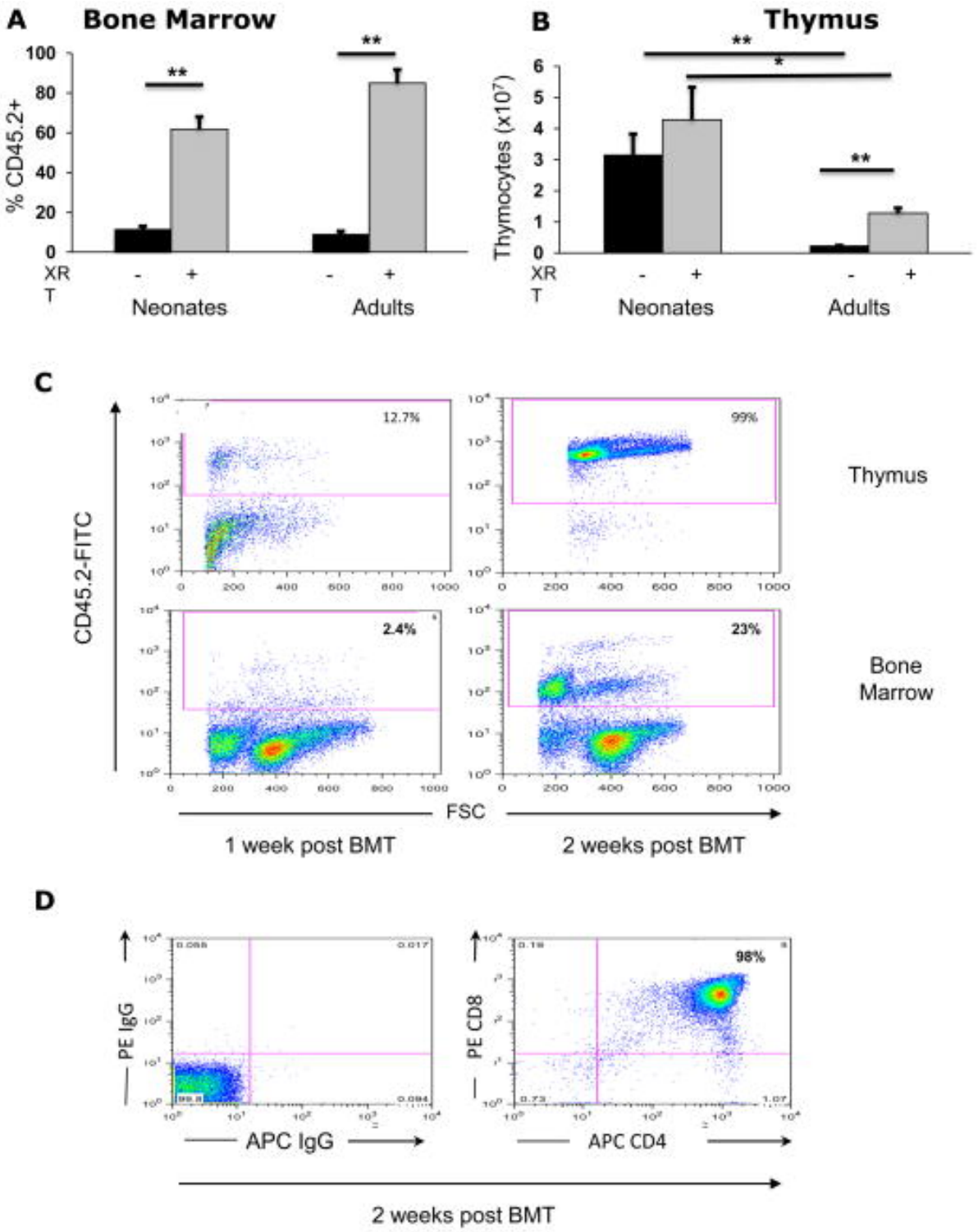
A
Bone Marrow
% CD45.2+
100
80
60
40
20
0
**
**
XR
T
-
+
-
+
Neonates
Adults
B
Thymus
Thymocytes (x10⁷)
6
5
4
3
2
1
0
**
*
**
XR
T
-
+
-
+
Neonates
Adults
C
CD45.2-FITC
12.7%
99%
2.4%
23%
Thymus
Bone Marrow
FSC
1 week post BMT
2 weeks post BMT
D
PE IgG
APC IgG
PE CD8
APC CD4
98%
2 weeks post BMT

Figure 2

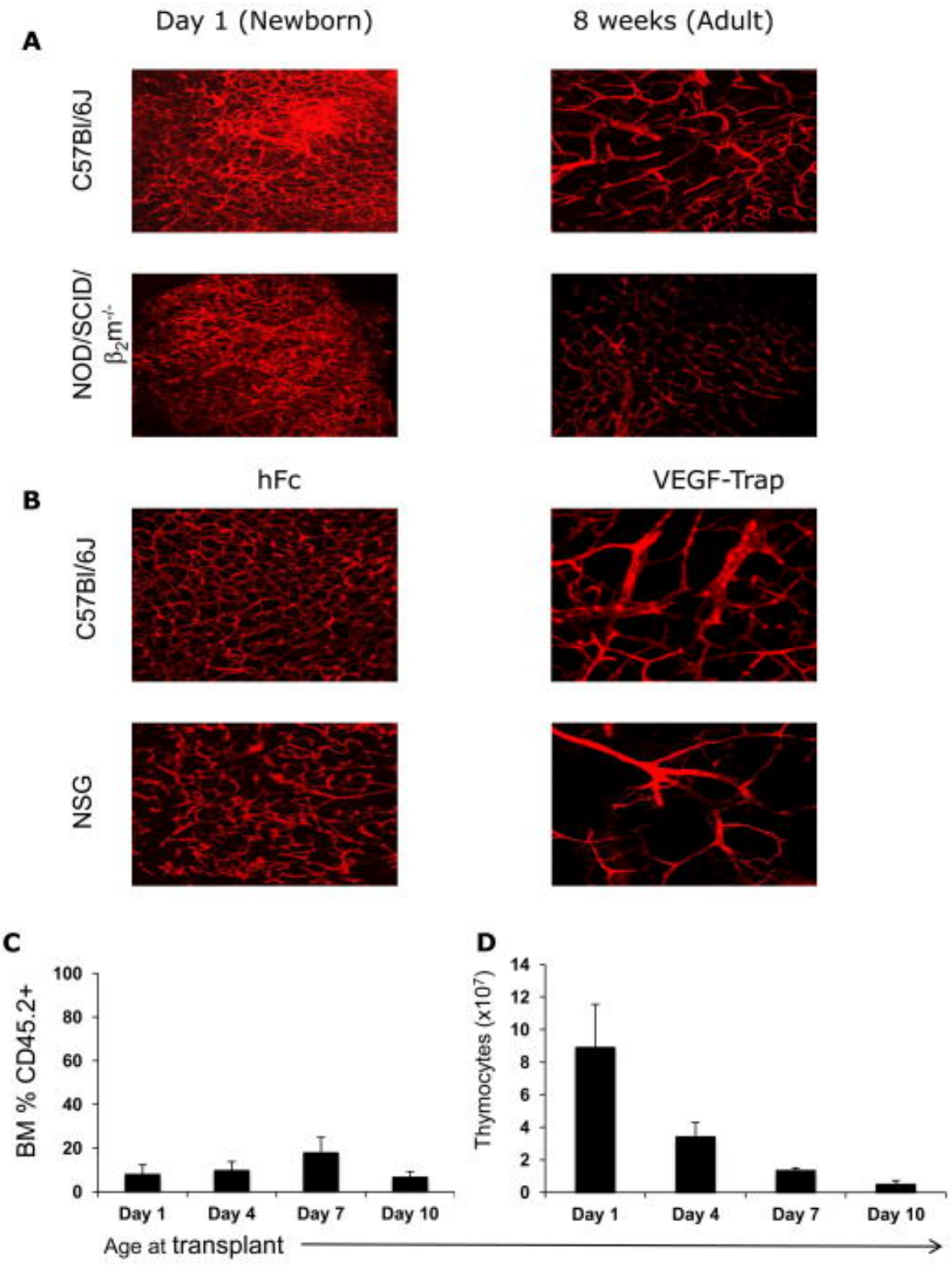
A
Day 1 (Newborn)
8 weeks (Adult)
C57Bl/6J
NOD/SCID/
$\beta_2m^{-/-}$
B
hFc
VEGF-Trap
C57Bl/6J
NSG
C
BM % CD45.2+
100
80
60
40
20
0
Day 1
Day 4
Day 7
Day 10
Age at transplant
D
Thymocytes (x10^7)
14
12
10
8
6
4
2
0
Day 1
Day 4
Day 7
Day 10

Figure 3

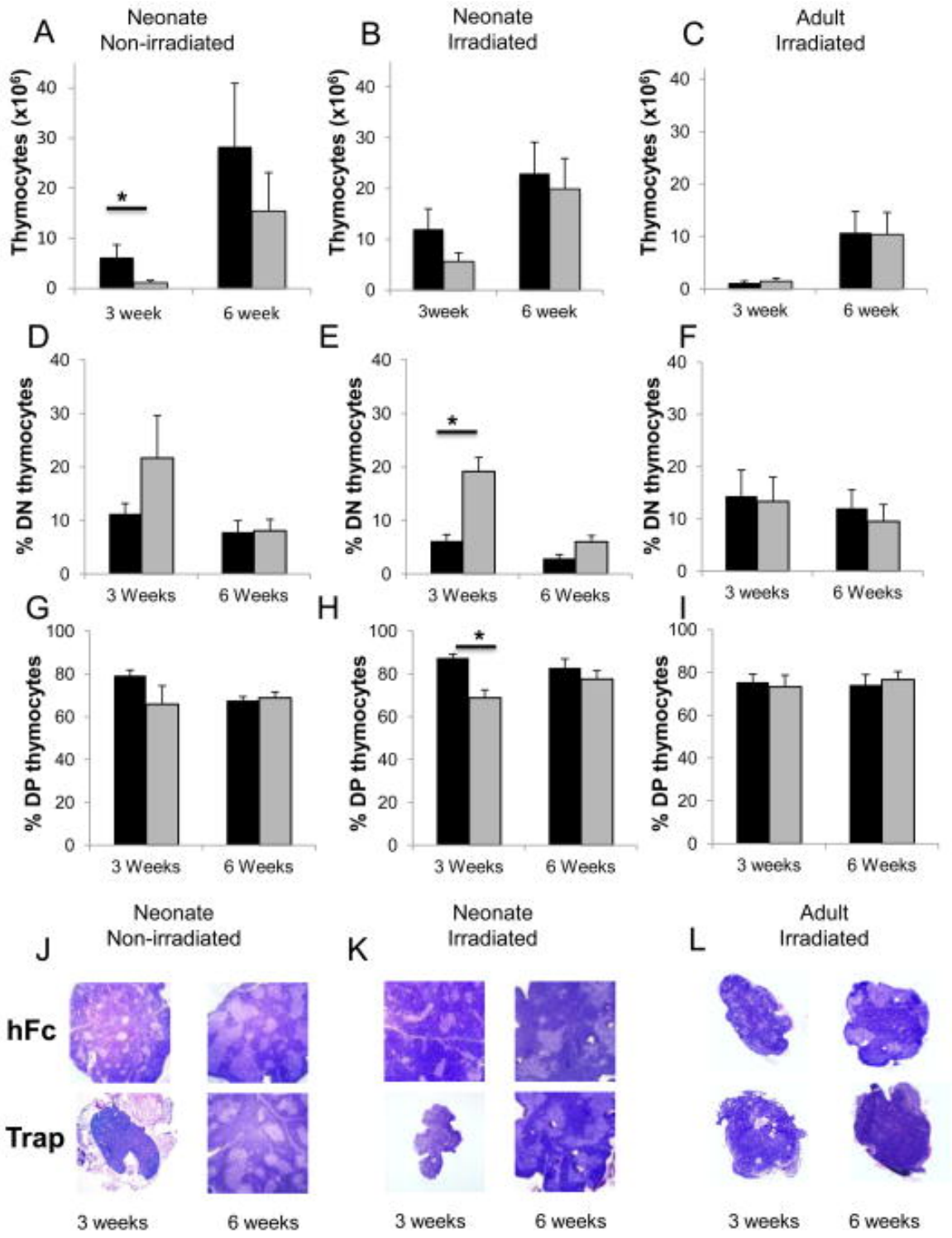
A
Neonate
Non-irradiated
B
Neonate
Irradiated
C
Adult
Irradiated
Thymocytes (x10⁶)
3 week
6 week
3week
D
E
F
% DN thymocytes
3 Weeks
6 Weeks
3 weeks
G
H
I
% DP thymocytes
J
K
L
hFc
Trap

Chapter 5

Conclusions

To summarize my findings, the majority of my research presented in this thesis focused on the identification of a functionally and molecularly distinct stage of early human hematopoietic commitment. This stage of commitment corresponds to the loss of erythroid and megakaryocytic potential while maintaining the capacity to generate all cells of the lymphoid lineage and the monocytic/macrophage cells of the myeloid lineage. These progenitors are distinctive from all previously identified human BM lymphoid-committed progenitors, in that this population lacks the cell surface antigen CD10 and therefore does not have a bias toward B cell potential and minimal T and NK cell potential. These cells are functionally analogous to a population of cells described in mouse, the Lymphoid-primed Multi-Potent Progenitor (LMPP), and both the mouse LMPP and our novel human LMPP are strong candidates to be thymic seeding cells.

From this work, our future directions are to investigate the transcriptional regulatory network that guides loss of self-renewal capacity and loss of lineage potential through a thorough evaluation of changes amongst HSC, LMPPs, CLPs and Pre-B cells. After examining these populations in bulk, we will focus on profiling transcription factors in individual cells. Profiling individual cells will provide insight into functionally significant variations in individual cell's regulatory network, rather than average expression data for all of the cells examined. These examinations may provide insight into new categories of molecular diversity of cells with similar surface protein expression.

The concepts of identifying a functionally distinct stage of early human lympho-myeloid commitment can be useful to several clinically relevant questions. In HSCT, the $CD34^+$ content of a graft has significant impact on clinical outcome, including time to

neutrophil and platelet recovery, severity of graft vs host disease, and overall survival. However, there is no marker that can be used to quantitate grafts specifically for lymphoid content, analogous to overall $CD34^+$ content. A clinical study could quantitate the percent of primitive, lymphoid primed population phenotype in BM grafts to determine if there is a link between of percentage of LMPP cells and time to lymphoid cell recovery and overall transplant outcome.

Mobilized Peripheral Blood (MPB) is a major source of cells for HSCT and tumor immunotherapy. However, little is known about the function or phenotype of MPB progenitors with strong lymphoid capacity. Using similar techniques to our investigations in BM, we could examine MPB for to discover similarly primitive, lymphoid primed cells.

The data presented in Chapter 3 underscores the importance of studying disordered human lymphopoiesis alongside investigations of murine differentiation despite the technical and logistical difficulties of acquiring and studying human tissue. We applied the identification of the human LMPP progenitor population in normal BM to the clinically relevant question how the lack of IL2RG signaling affects the regulation of the lymphoid commitment. The in-progress studies demonstrate that the earliest stages of B lymphoid development are unaffected by defects in IL2RG signaling in these human patients.

The results of these studies highlight the critical differences between lymphopoiesis in mice and humans, and the importance of overcoming experimental hurdles in order to directly investigate human lymphoid commitment.

Appendix

The human bone marrow samples originate from UCLA (waste cells from filters of healthy allogeneic BM collections) and Commercial Sources (AllCells), which supplies only fully de-identified human samples. The memorandum entitled "Determination That IRB Review is Not Required" from the UCLA Office For Protection of Human Research Subjects states because that "the samples provided by these sources will include no information by means of which you can identify donors, the activities included in the above noted submission do NOT involve "human subjects" and therefore do NOT require UCLA IRB review or certification or exemption from IRB review." Therefore, although this work uses human samples, these are not human subjects, as the samples are de-identified.